Structural health monitoring
Signal-based data analysis

Nejra Beganovic, Dorra Baccar, Dirk Söffker
Website: www.srs.uni-due.de

UNIVERSITÄT DUISBURG ESSEN

Chair of Dynamics and Control
University of Duisburg-Essen

Outline

- Structural health monitoring (SHM)
- Signal-based approaches
- Structural health monitoring of metallic structures
  - Classification of system states based on Acoustic Emission (AE) signal
  - Damage acumulation calculation

Structural health monitoring I

Diagnosis

- Failure detection/localization
- Failure classification and quantification

Prognosis

- Description of stochastic nature of deterioration processes

SHM advantages

- Avoidance of premature breakdowns
- Reduction of operating and maintenance costs

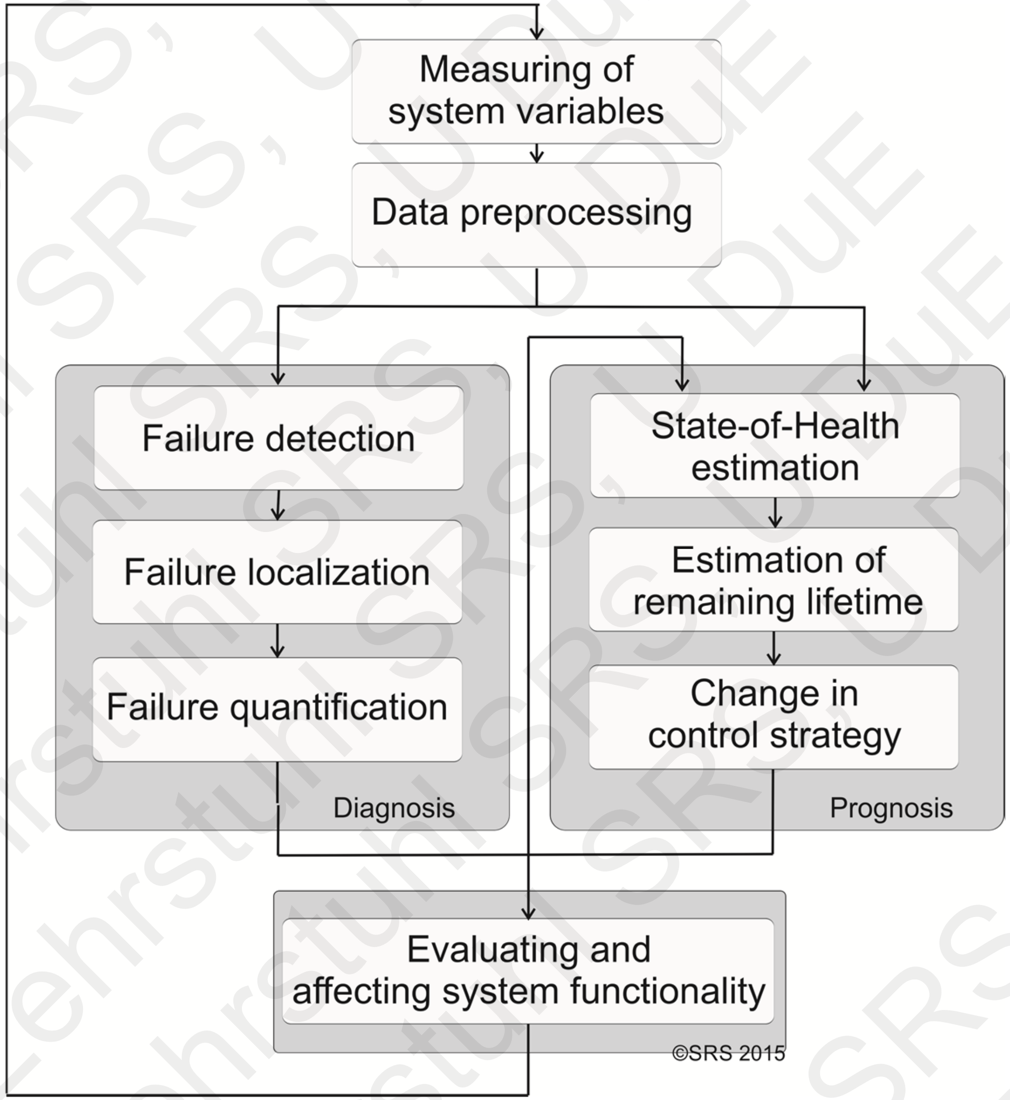

Structural health monitoring II

Challenges

- Differentiation of various events
- Automated classification of events
- Improvement of events detectability

Data analysis and processing

- Data size reduction
- Noise reduction
- Separation of redundant and irrelevant information
- Feature extraction and representation in a suitable way

Structural health monitoring III

Model-based approaches

- Mathematical description of physical processes

Signal-based approaches

- Signal analysis in time domain (Threshold exceedance)
- Analysis of signal frequency spectrum (FFT/DFT, Autoccorrelation/Crosscorrelation)
- Analysis of time-frequency spectrum (STFT, CWT/DWT)

	FFT/DWT	STFT	CWT/DWT	Auto-/ Crosscorrelation
Presentation	Energy-Frequency	Energy-Time-Frequency	Energy-Time-Frequency	Energy-Querfrequency
Complexity of algorithm	Feasible	High	High	High
Resolution		Limited	Variable	Limited
Feature extraction	Nein	Ja	Ja	Ja

Signal-based data analysis I

Fast Fourier Transform (FFT)

$$y = 10 \cdot sin(2 \cdot \pi \cdot 50 \cdot t) + 5 \cdot cos(2 \cdot \pi \cdot 20 \cdot t)$$

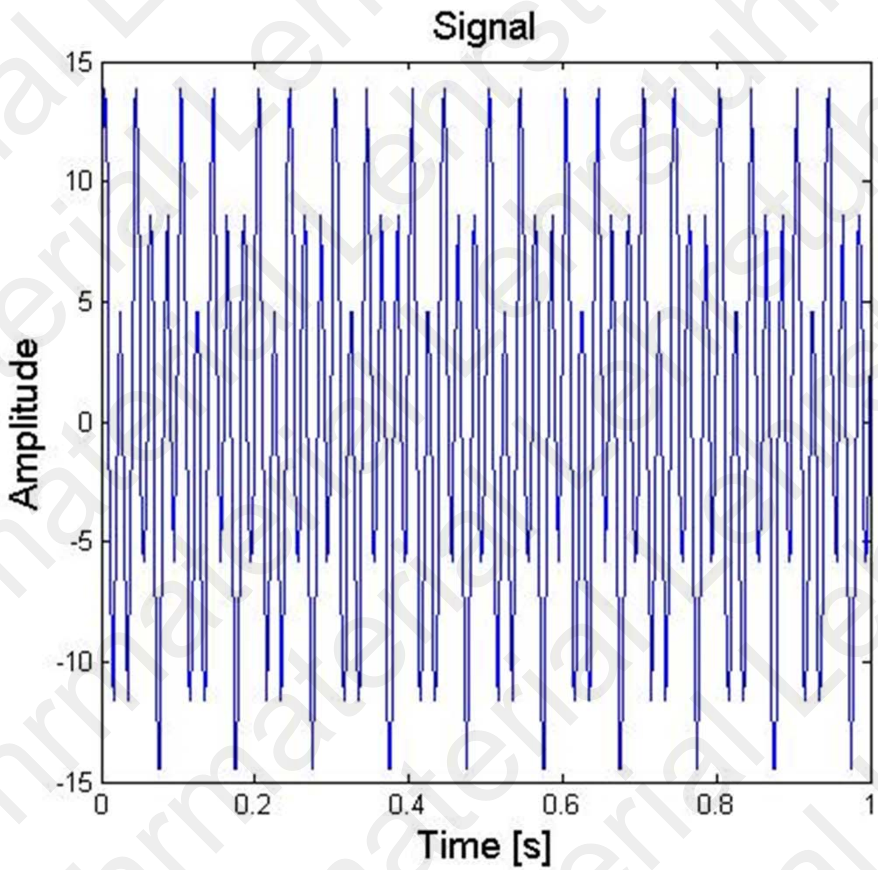

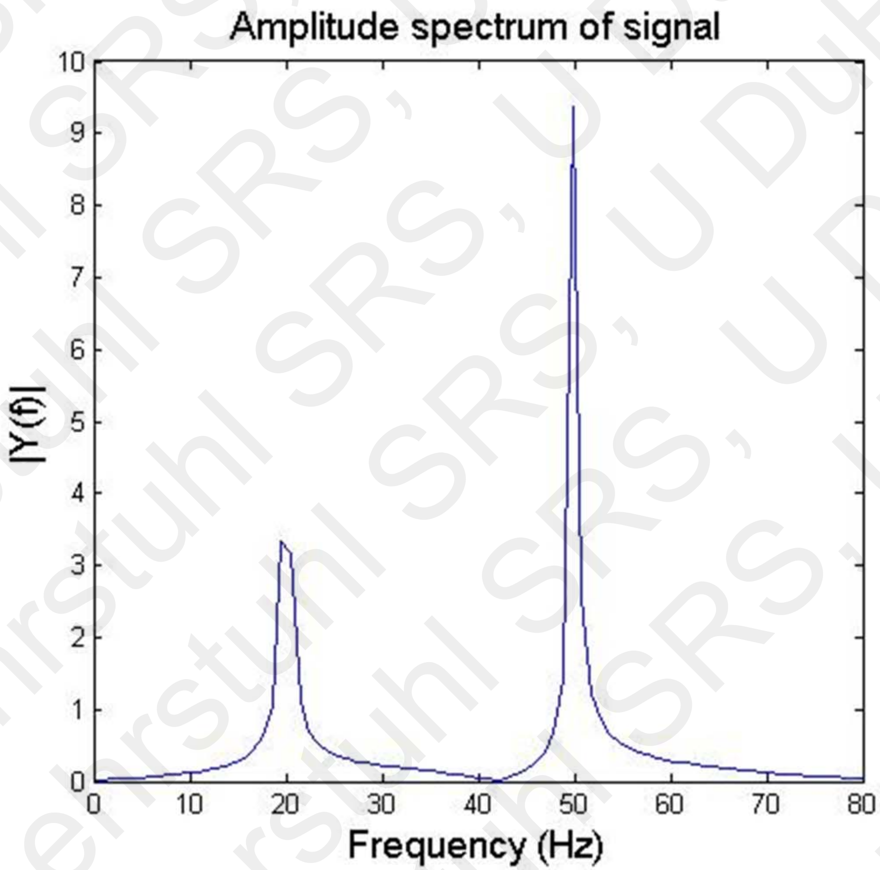

- Signal contains two different frequencies (20 Hz, 50 Hz).
- Frequency spectrum can be identified.
- It is not possible to allocate frequencies in time.

Signal-based data analysis I

Fast Fourier Transform (FFT)

$$y1 = 10 \cdot sin(2 \cdot \pi \cdot 50 \cdot t)(t <= 0.5)\ \&\ y1 = 5 \cdot cos(2 \cdot \pi \cdot 20 \cdot t)(t > 0.5)$$

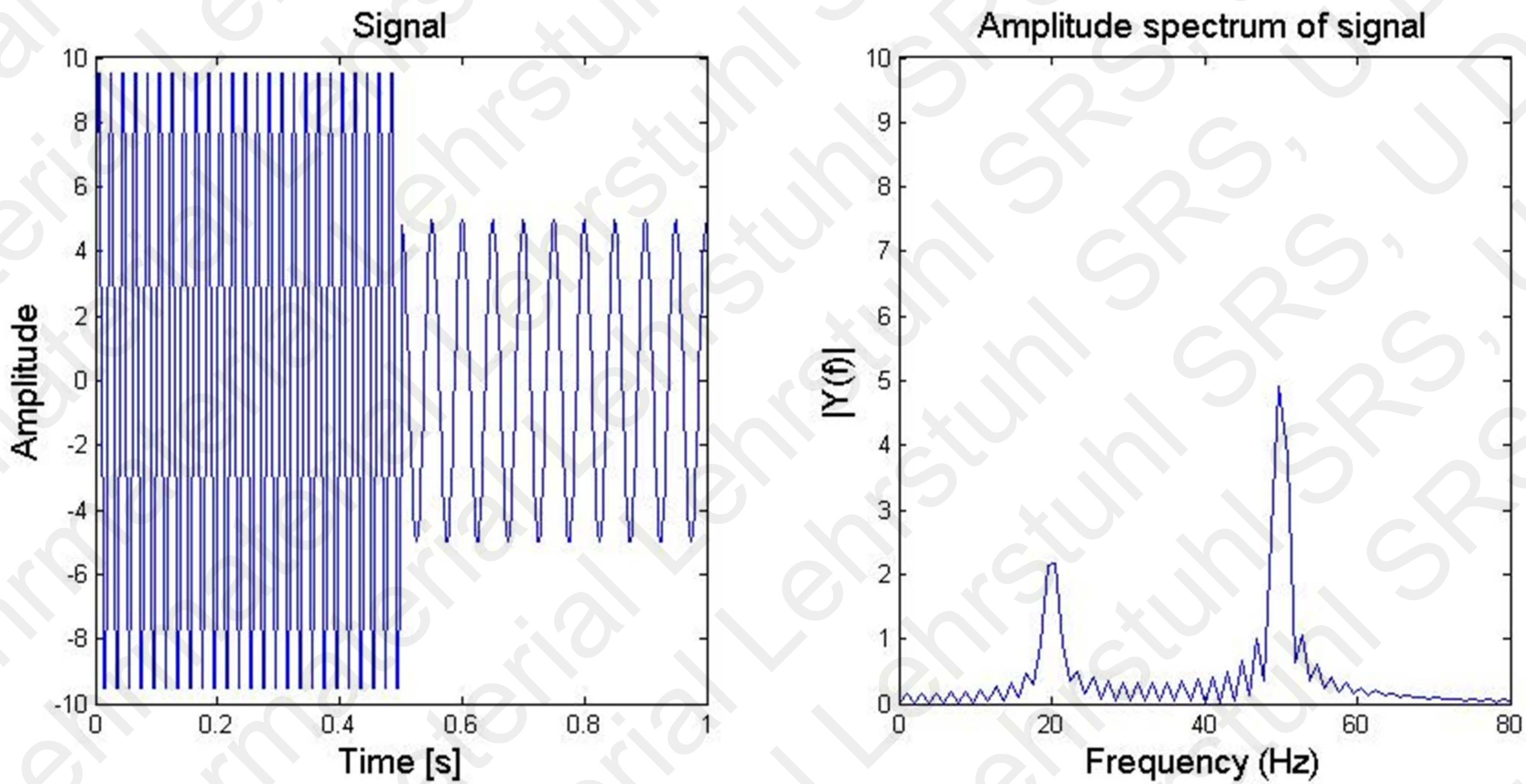

- It is not possible to allocate frequencies in time.

Signal-based data analysis II

Short-time Fourier Transform (STFT)

$$y = 10 \cdot sin(2 \cdot \pi \cdot 50 \cdot t) + 5 \cdot cos(2 \cdot \pi \cdot 20 \cdot t)$$

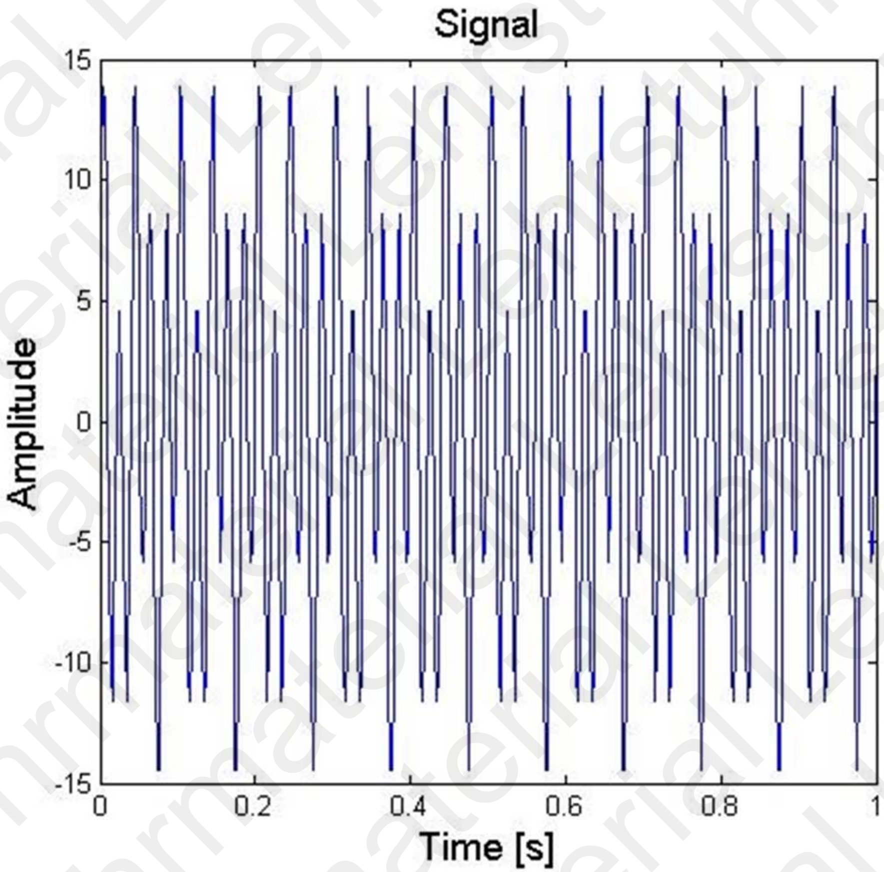

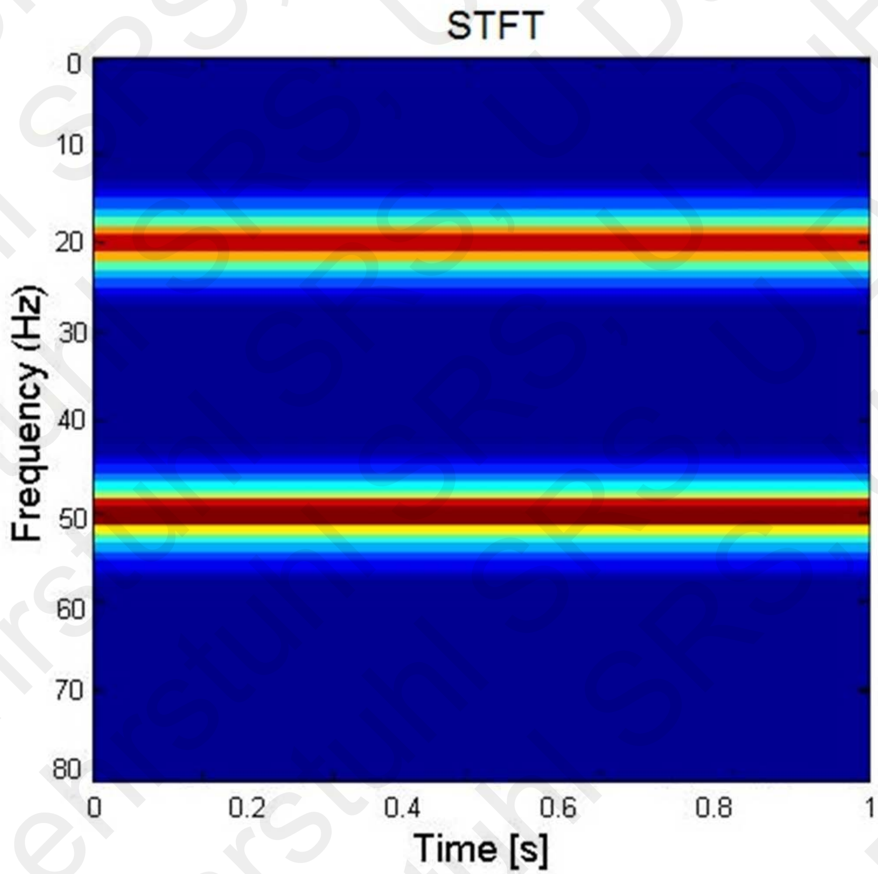

- Transformation of signal as a function of time and frequency
- Frequency spectrum identified, as well as allocated in time
- Better frequency resolution, worse time resolution (and vice versa)

Signal-based data analysis III

Continuous Wavelet Transform (CWT)

$$y = 10 \cdot sin(2 \cdot \pi \cdot 50 \cdot t) + 5 \cdot cos(2 \cdot \pi \cdot 20 \cdot t)$$

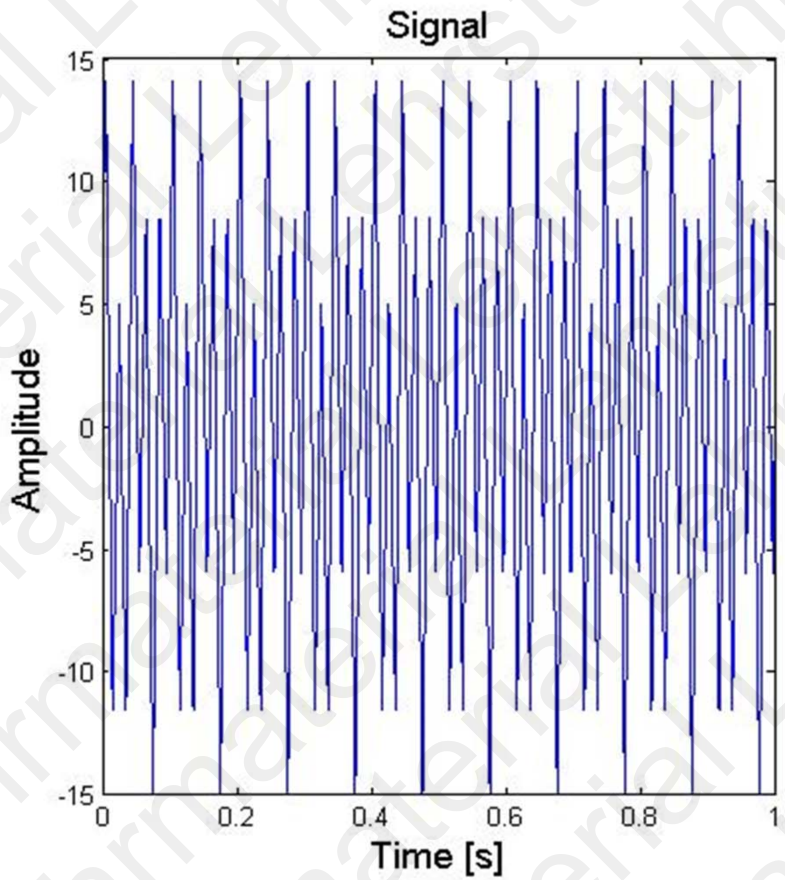

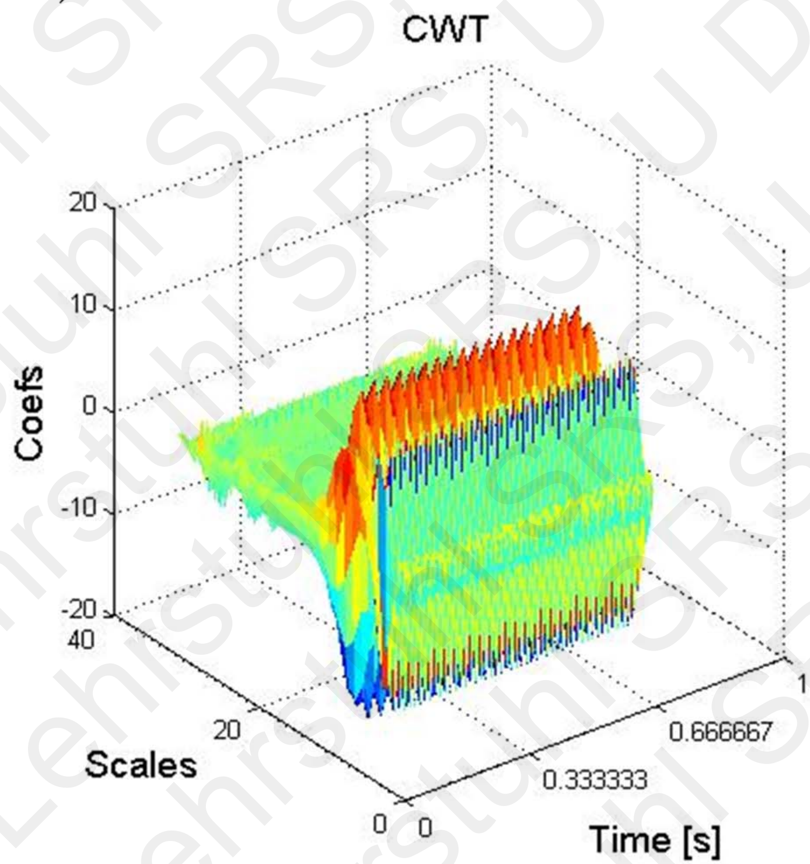

- Transformation of signal as a function of time, scale (frequency) and amplitude
- Different wavelet scales as well as wavelet functions
- High frequency and time resolution: Suitable for non-stationary or transient signals

Signal-based data analysis III

Continuous Wavelet Transform (CWT)

$$y = 10 \cdot sin(2 \cdot \pi \cdot 50 \cdot t) + 5 \cdot cos(2 \cdot \pi \cdot 20 \cdot t)$$

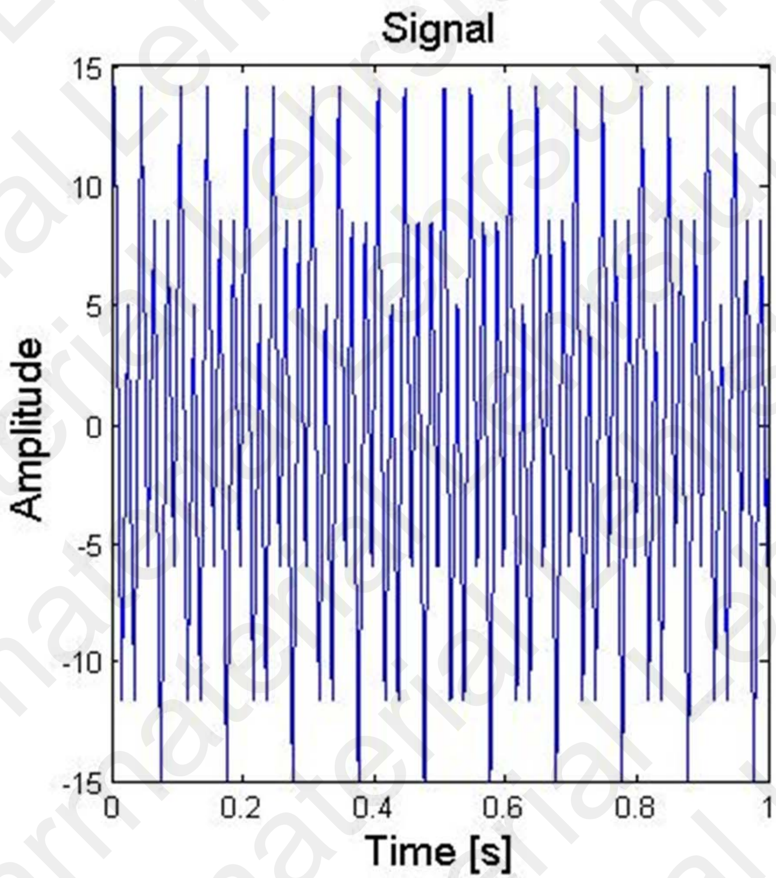

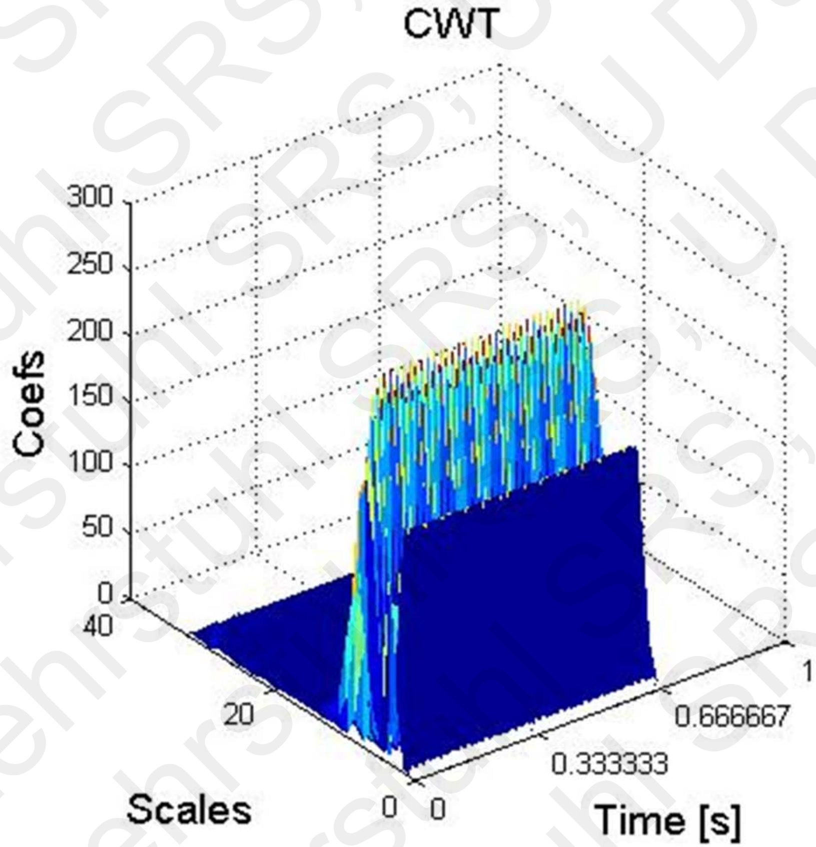

- Transformation of signal as a function of time, scale (frequency) and amplitude
- Different wavelet scales as well as wavelet functions
- High frequency and time resolution: Suitable for non-stationary or transient signals

Signal-based data analysis IV

Discrete Wavelet Transform (DWT)

$$y = 10 \cdot sin(2 \cdot \pi \cdot 50 \cdot t) + 5 \cdot cos(2 \cdot \pi \cdot 20 \cdot t)$$

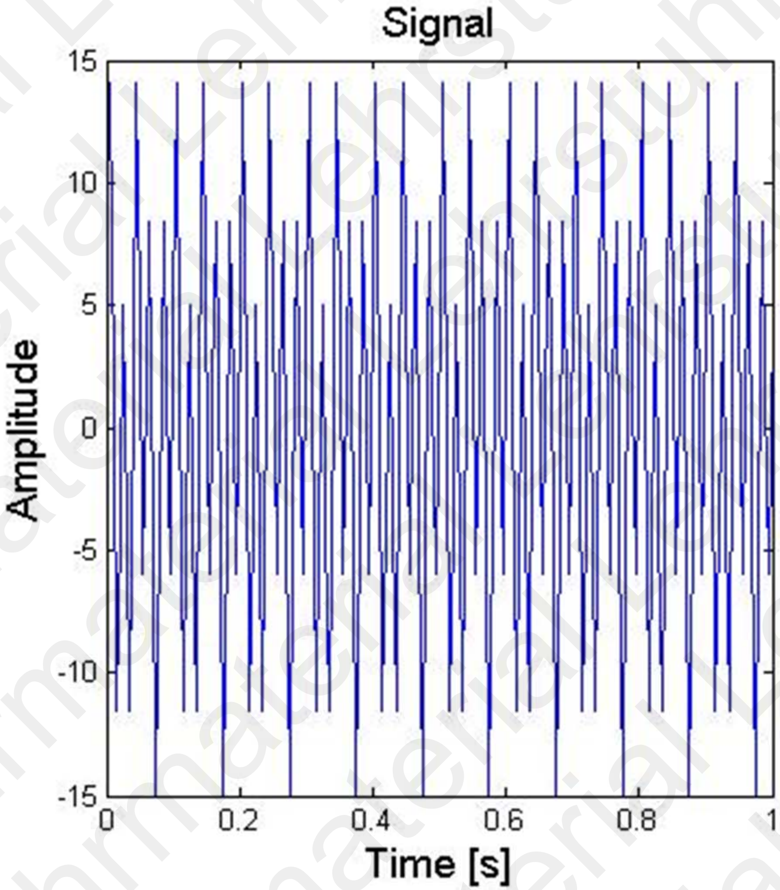

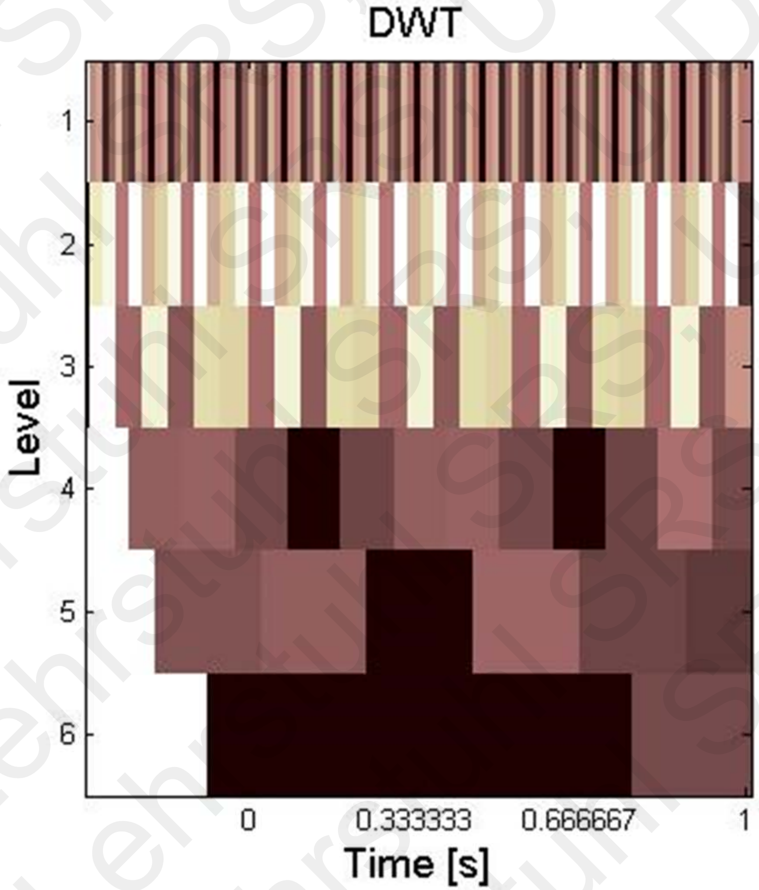

- Transformation of signal as a function of time, level and amplitude
- Clear distincion of frequencies (contrary to CWT)
- Suitable for signal denoising and frequency identification

Signal-based data analysis V

Discrete Wavelet Transform (DWT)

$$y = 10 \cdot sin(2 \cdot \pi \cdot 50 \cdot t) + 5 \cdot cos(2 \cdot \pi \cdot 20 \cdot t)$$

- Iterative high- and low-pass filtering with further decreasing resolution
- Details cD: coefficients of high-pass filtered signal
- Details cA: coefficients of low-pass filtered signal

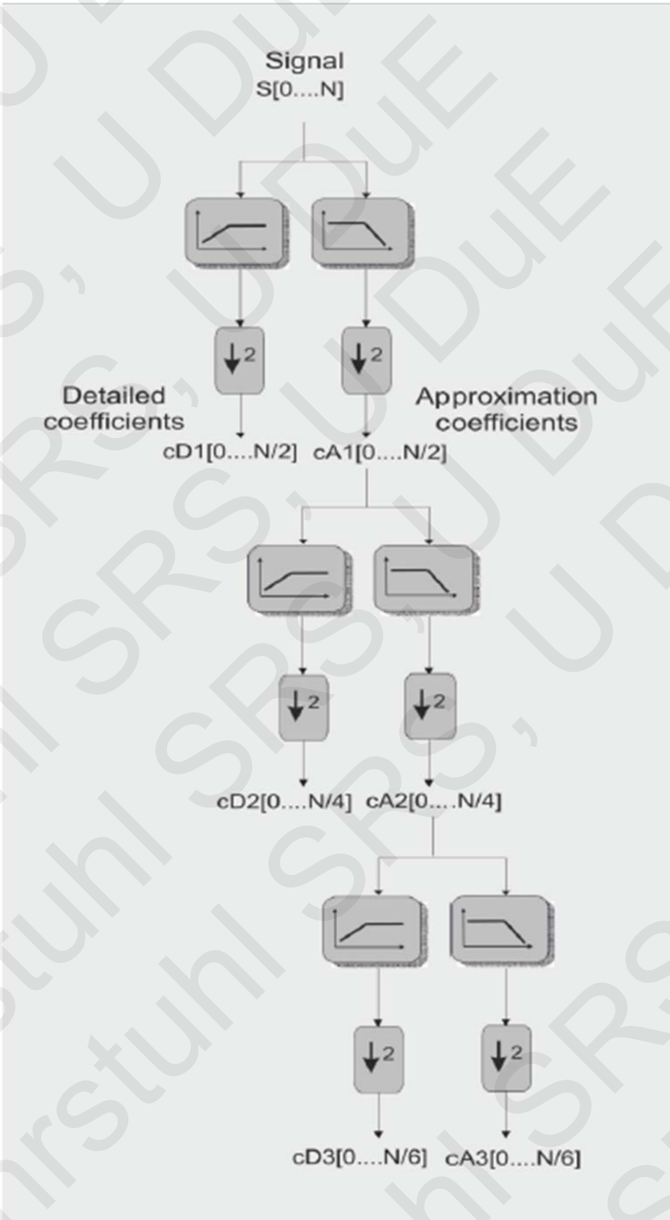

Signal-based data analysis VI

Discrete Wavelet Transform (DWT)

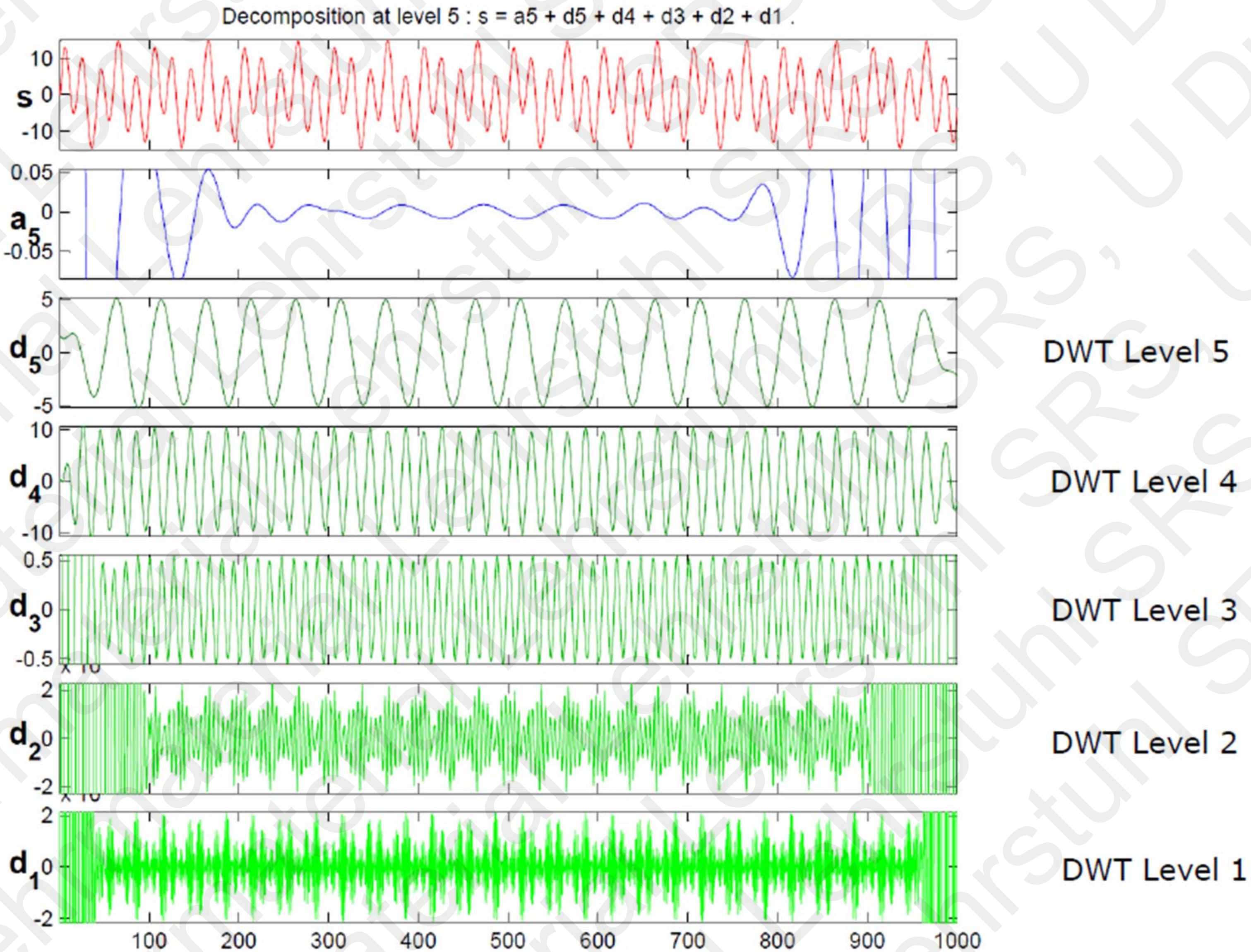

Condition monitoring of metallic structures I

Classification and prediction of wear state based on measured signals

- Tribological system under sliding wear conditions
- Effect of operating conditions on wear propagation
- Main wear effects induced by deficient lubrication
  - Welding
  - Cracks close to the surface
  - Particles …
- Damage accumulated in the system

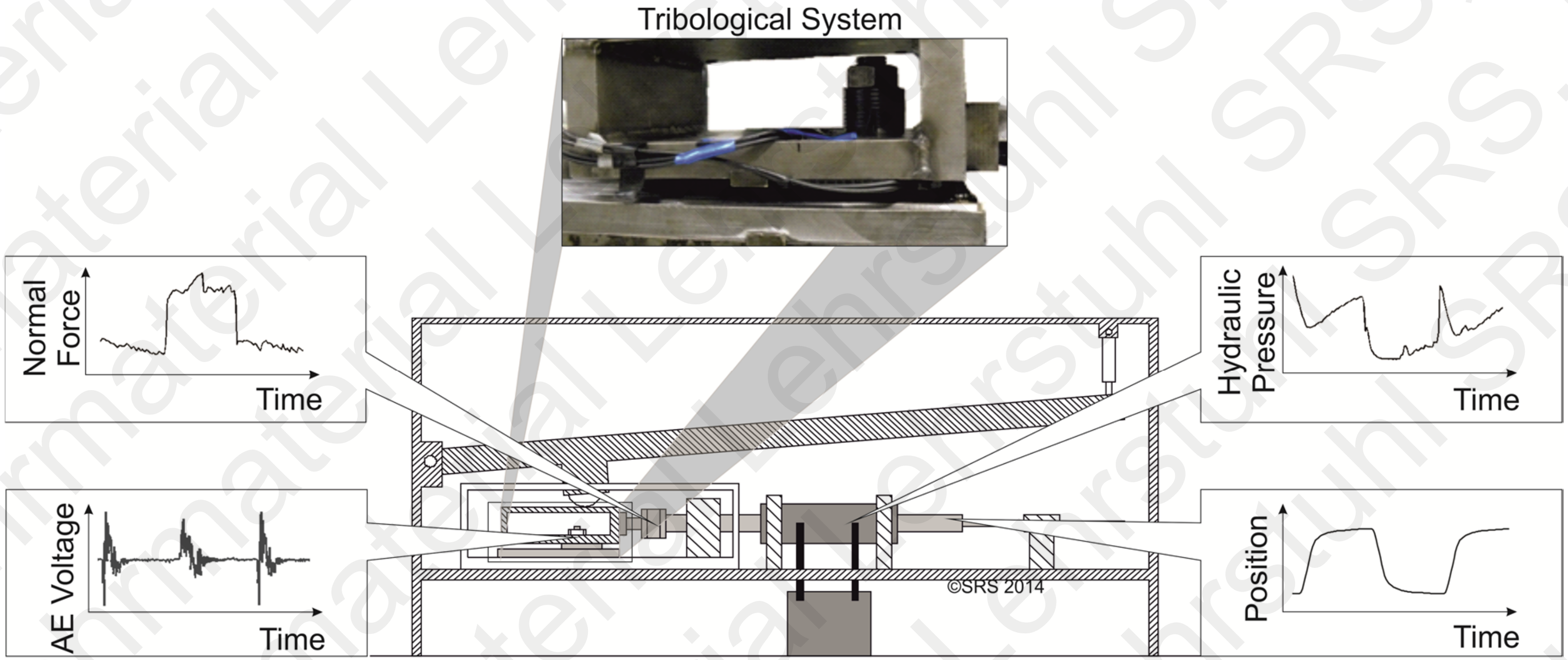

Condition monitoring of metallic structures II

Acoustic emission signals

- Transient elastic waves of high-frequency
- Induced by material removal
- Acoustic emission used as wear indicator
- Non-destructive monitoring technique
  - Application during loading
  - Surface mountable
  - Suitable for microstructural characterization and monitoring of damage processes
  - Low costs

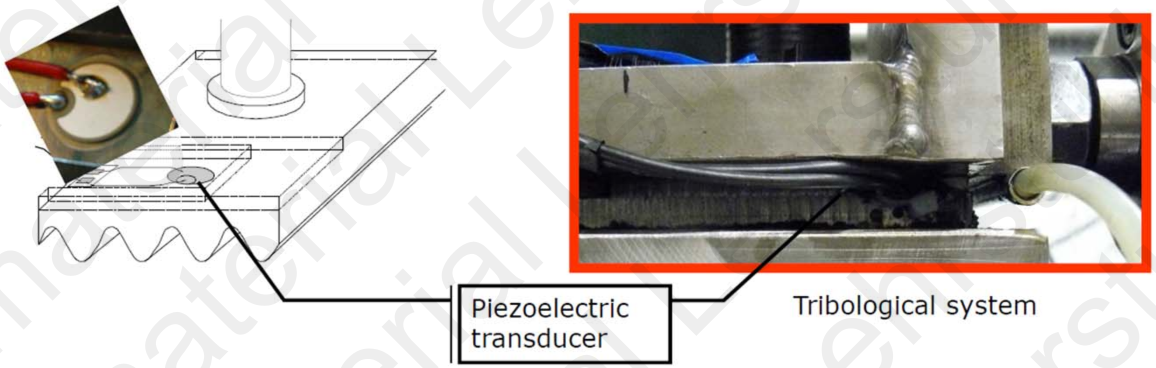

→ Application of different signal processing techniques to acoustic emission signal

→ Correlation of measured AE signals to wear/damage propagation

Condition monitoring of metallic structures III

Acoustic emission energy distribution over system usage

- Application of STFT to AE signal
- Structure deterioration

a) Run-in phase
- Early failure region

b) Permanent wear phase
- Constant failure rate

c) Wear-out phase
- System failure

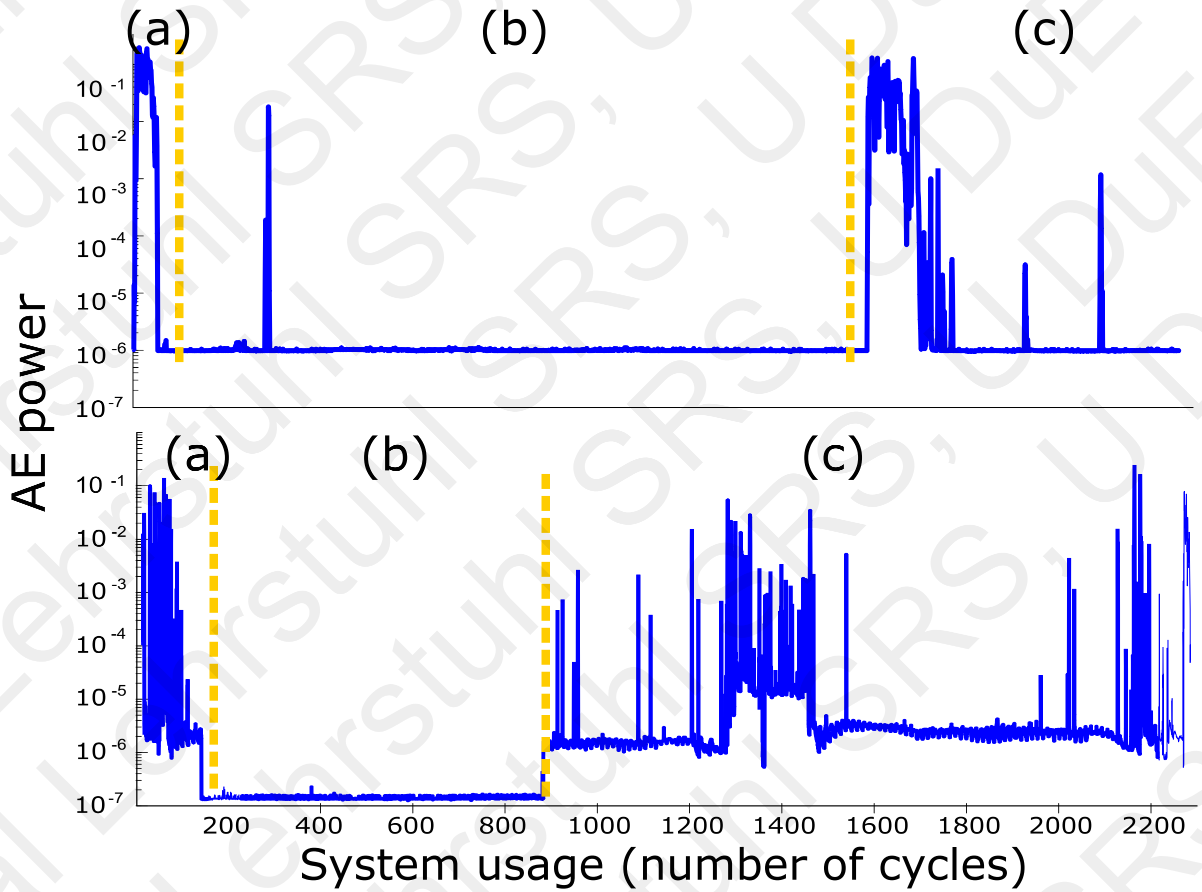

➔ Identification of wear state based on AE signals possible

➔ Calculation of damage accumulation in the system possible

Condition monitoring of metallic structures IV

Frequency examination of acoustic emission signal

- Identification of transient events
- Distincion of three wear phases based on frequency based signal analysis
- Application of STFT on AE signal

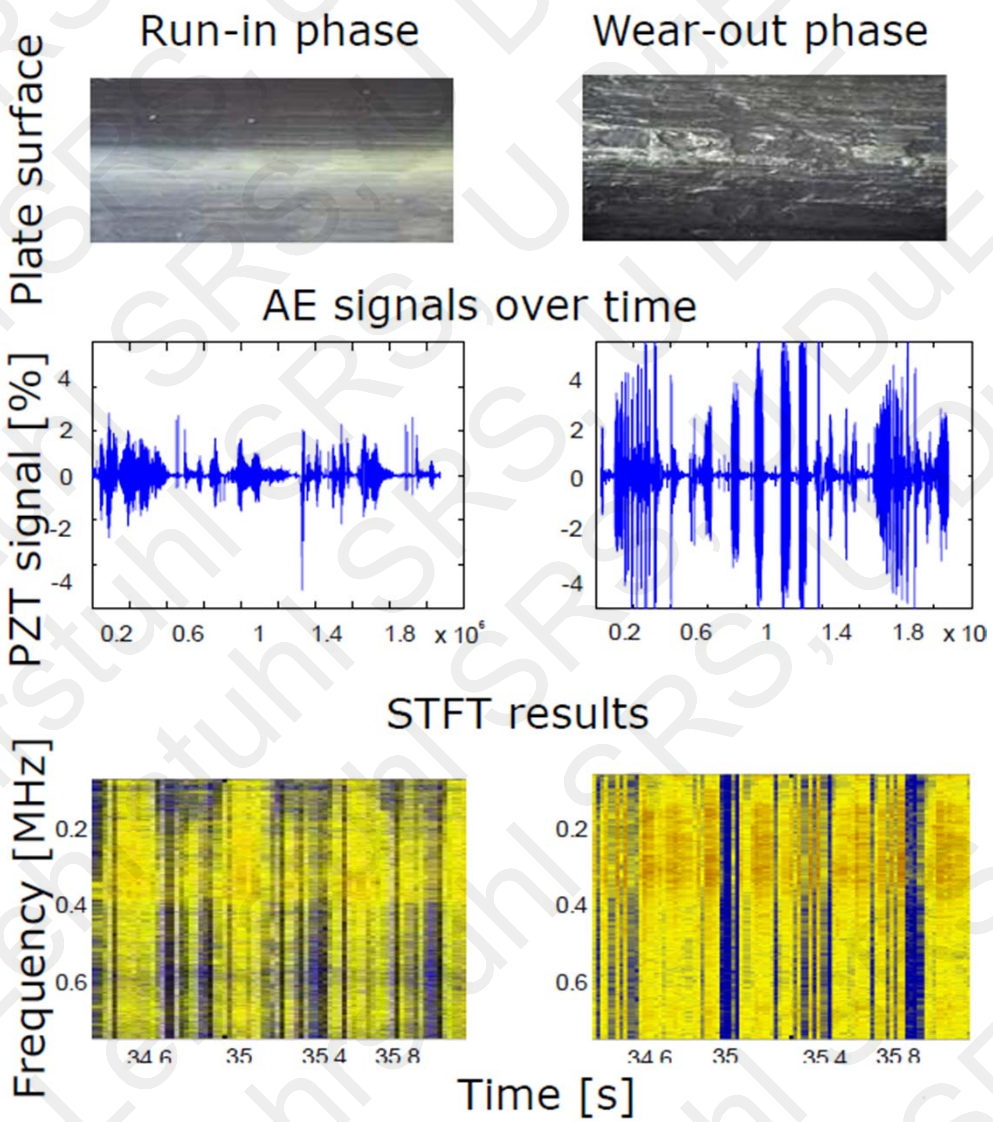

➔ STFT transformed AE signals during run-in and wear-out phase nearly identical

Frequency examination of acoustic emission signal

- Application of CWT on AE signal

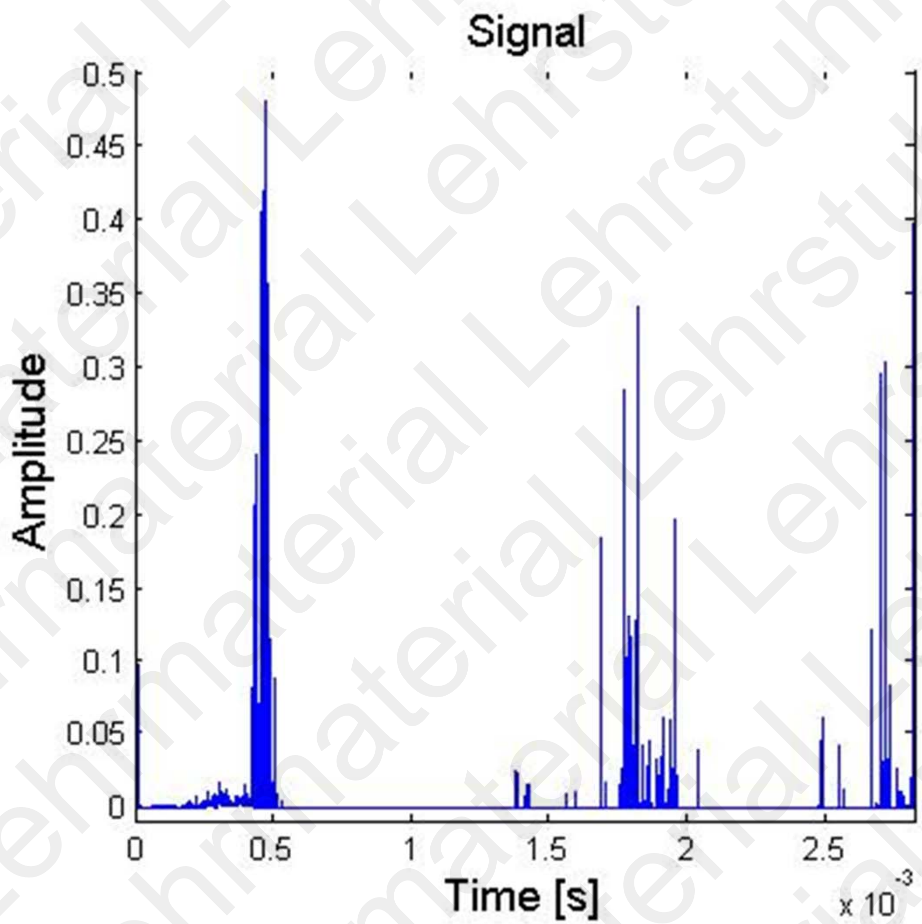

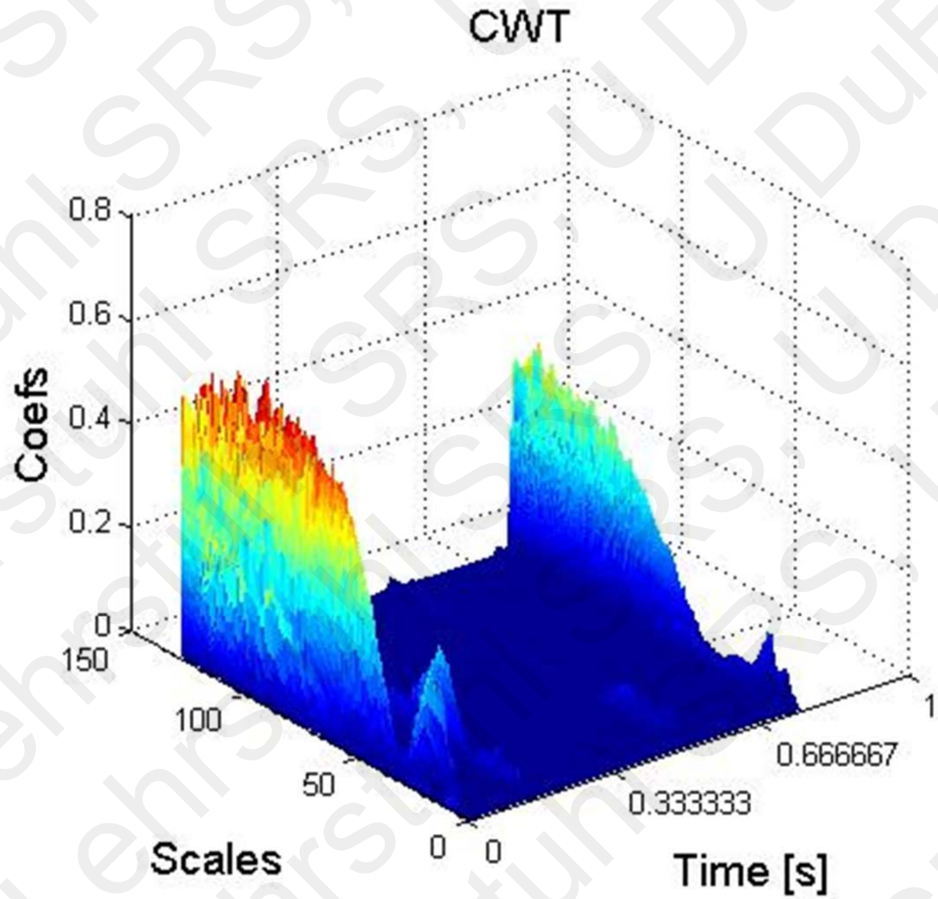

➔ Better representation of wear state using CWT transformed AE signal in comparison with STFT

Conclusion

- Classification of wear states using
  appropriate measured signals possible
- Frequency based signal analysis successfully applied in classification of wear states
- Signal-based processing methods requiring higher computational effort
  in general give better results concerning signal analysis = trade off have to be found
- Damage accumulated in the system can be revealed
  using information about acoustic emission energy

Comparison of Three – Easy to Apply and Innovative – Signal-based Approaches for Diagnosis of a Technical System with Wear

Dirk Söffker and Sandra Rothe
Web: www.srs.uni-due.de

UNIVERSITÄT DUISBURG ESSEN

Chair of Dynamics and Control (SRS)
University of Duisburg-Essen

Outline

- Motivation
- Wear-oriented monitoring
- Three innovative approaches
  - Acoustic Emission-based analysis
  - Diagnosis-oriented data filtering
  - Data-based classification approach
- Comparison of results
- Condition lights for brief evaluation of system state
- Summary and outlook

Motivation I

Monitoring of critical components
Here:
Mechanical system with periodic load

Wear process
- Stochastically occuring wear
- Dependence on operating conditions

Loss of functionality due to surface destruction

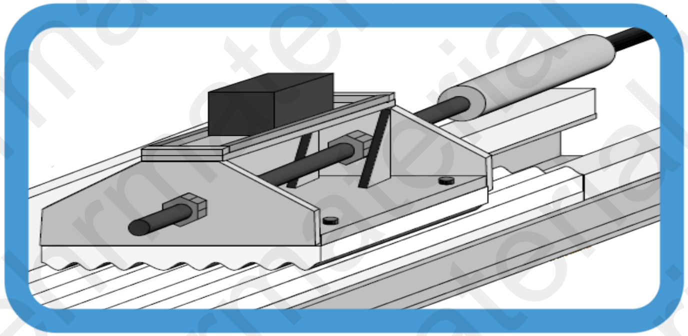

Tribological system

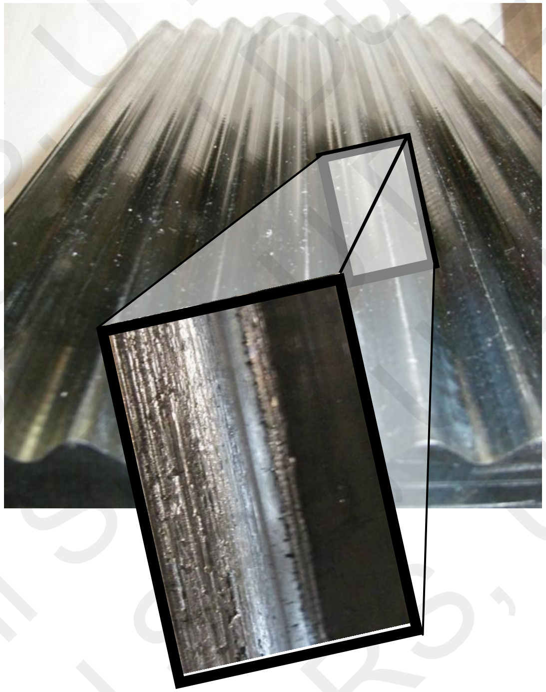

Material surface

➔ Goal: Establishment of a continuous, non-destructive state assessment

Motivation II

Development and use of monitoring approaches for continuous monitoring of components and systems

- Fault diagnosis
  - Error detection: Detection of deviations and non-normal behavior
  - Damage diagnosis: Assignment of deviation cause

➔ Here: Real-time determination of the degree of wear

- Prediction:
  - Determine the end of life-time
  - Optimal use of remaining life-time

➔ Upcoming goal: Wear-oriented operation

Wear-oriented monitoring I: Goals

Wear classification

- Specific distinctions
  - Adhesive wear
  - Surface distress
- Typical investigation methods
  - Wear energy recording
  - Measurement of geometrical changes
  - Technical analysis of the material

Automation goals

- Real-time determination and recording of wear characterizing parameters
- Wear-oriented operation

Method-oriented goals

- Knowledge required for design and use of models

Wear-oriented monitoring II: Experiment

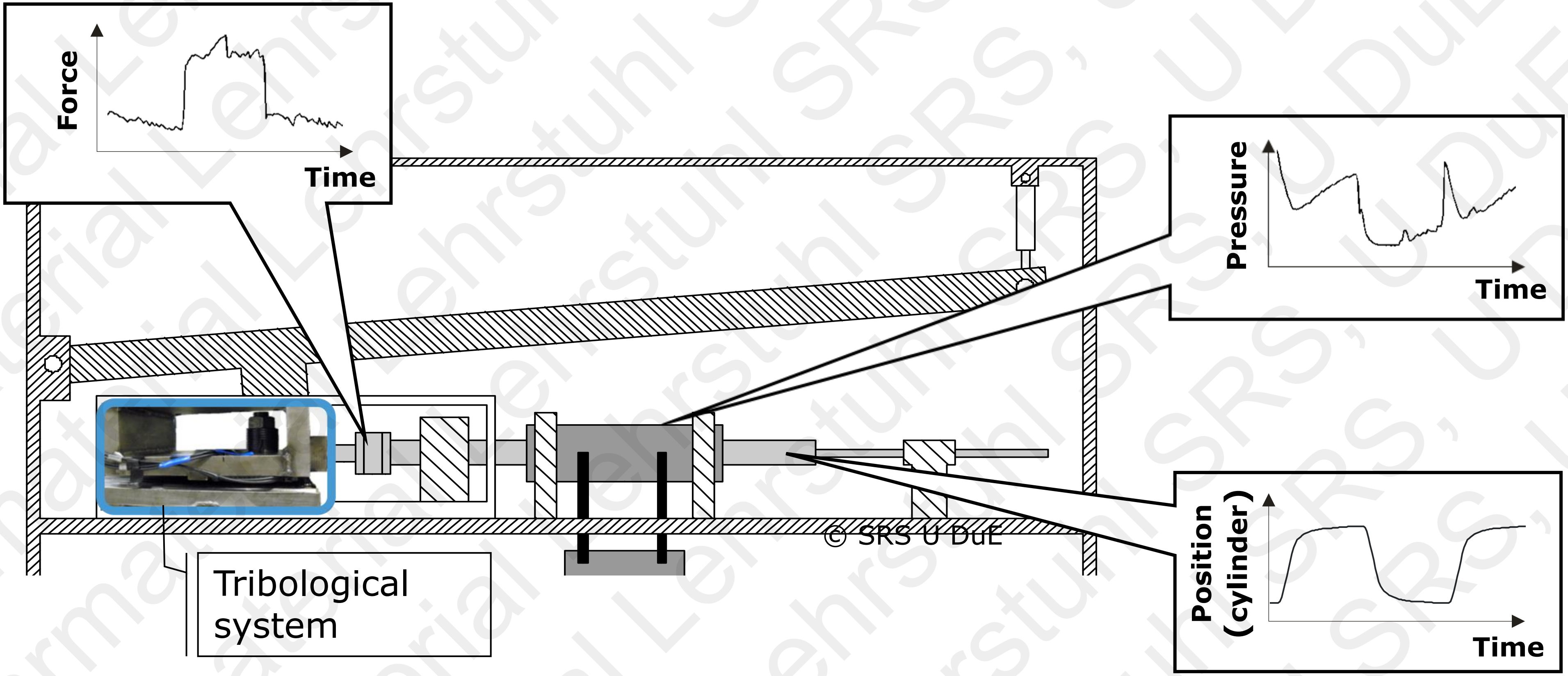

Features of tribological system test rig

- Programmable trajectory of the wear plates
- Variable normal force (by lever arm)
- Variable lubrication

Wear-oriented monitoring III: Experiment

Measurement chain

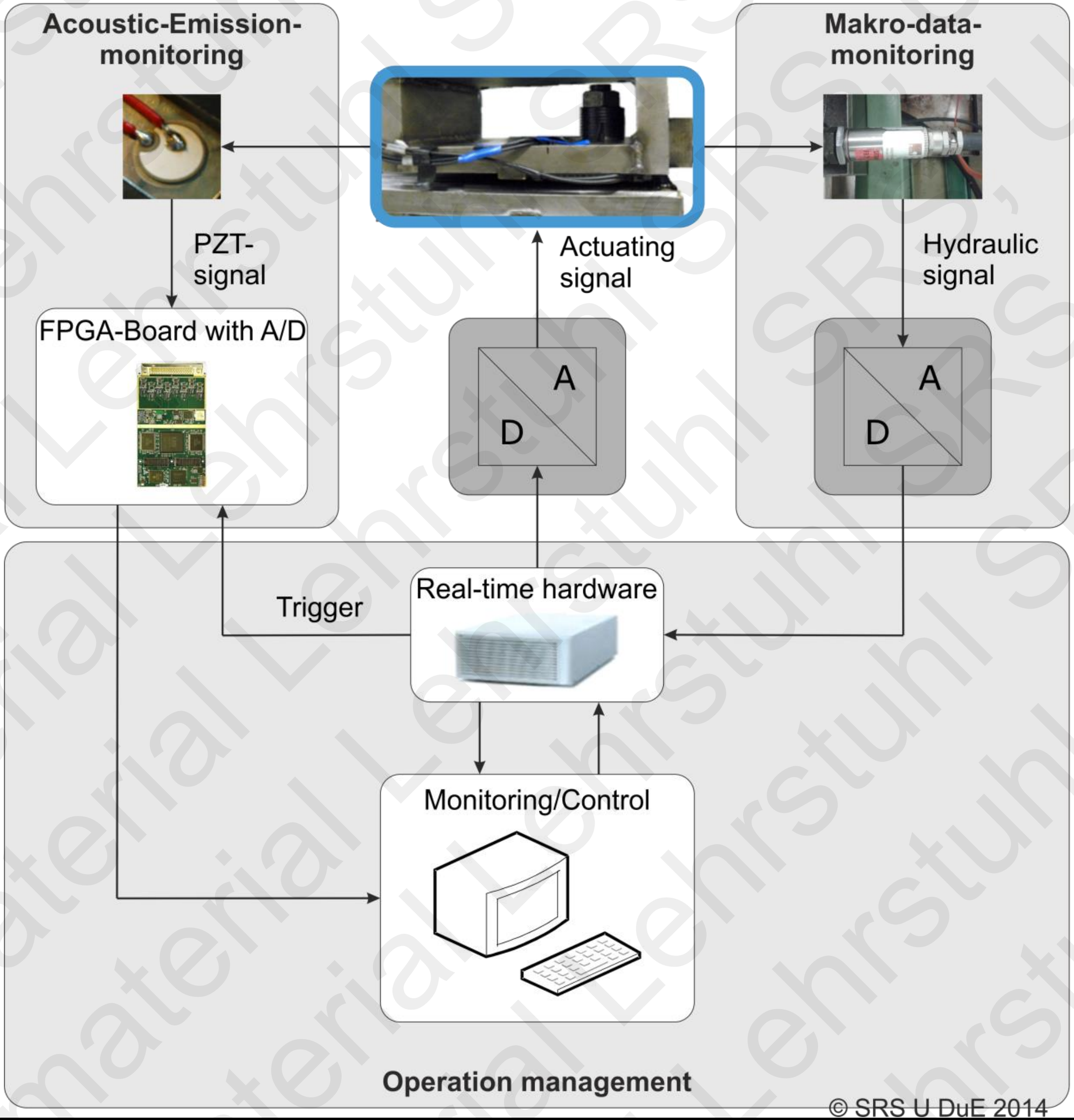

AE-based analysis I

Wear progression of the tribo-system

- Local insufficient lubrication: Metal-to-metal contact
- Cold shuts/surface crack
- Particle creation/discharge
- Fatigue of surface = Change of material

➔ Acoustic Emission (AE): Short-term, transient event whereby elastic energy is generated by loading and crack extension.

Advantages of the AE-analysis

- Inexpensive
- Easy to integrate
- Ability for online use
- Adaptability for high frequency range

➔ Possible application for non-destructive monitoring of damage processes

AE-based analysis II

FPGA-based filtering and analysis of sensor data [Baccar, Söffker, 2011f]

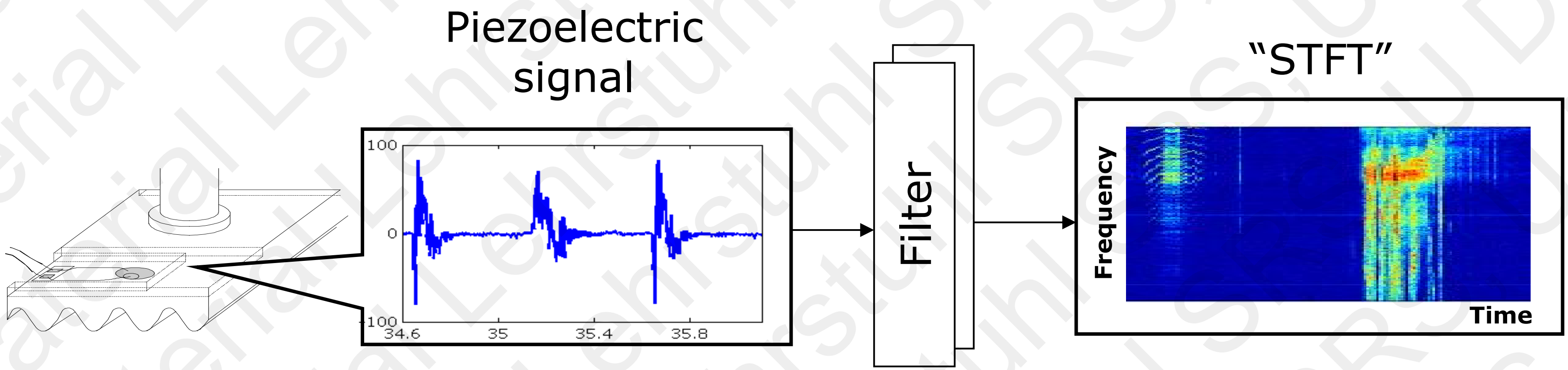

➔ Correlation with time-dependent process information

➔ Establishment of the relationship
between material change and system damage

AE-based analysis III

Frequency analysis of the AE-signals [Baccar, Söffker, 2011f]

- Change of the surface condition correlates to signal change
- Determination of the three main phases
  (Run-in phase, permanent wear phase, and wear-out phase)
- Temporal allocation of
  – Wear
  – Degree of wear

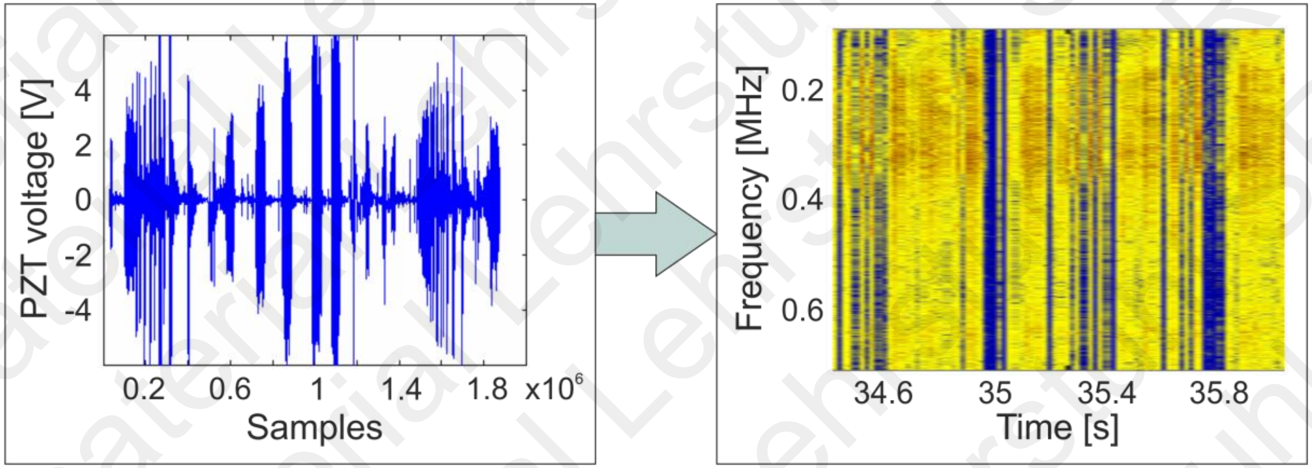

Task

Detection of suitable features to distinguish the effects

AE-based analysis IV

Frequency examinations of AE-signal
[Baccar, Söffker, 2011f]

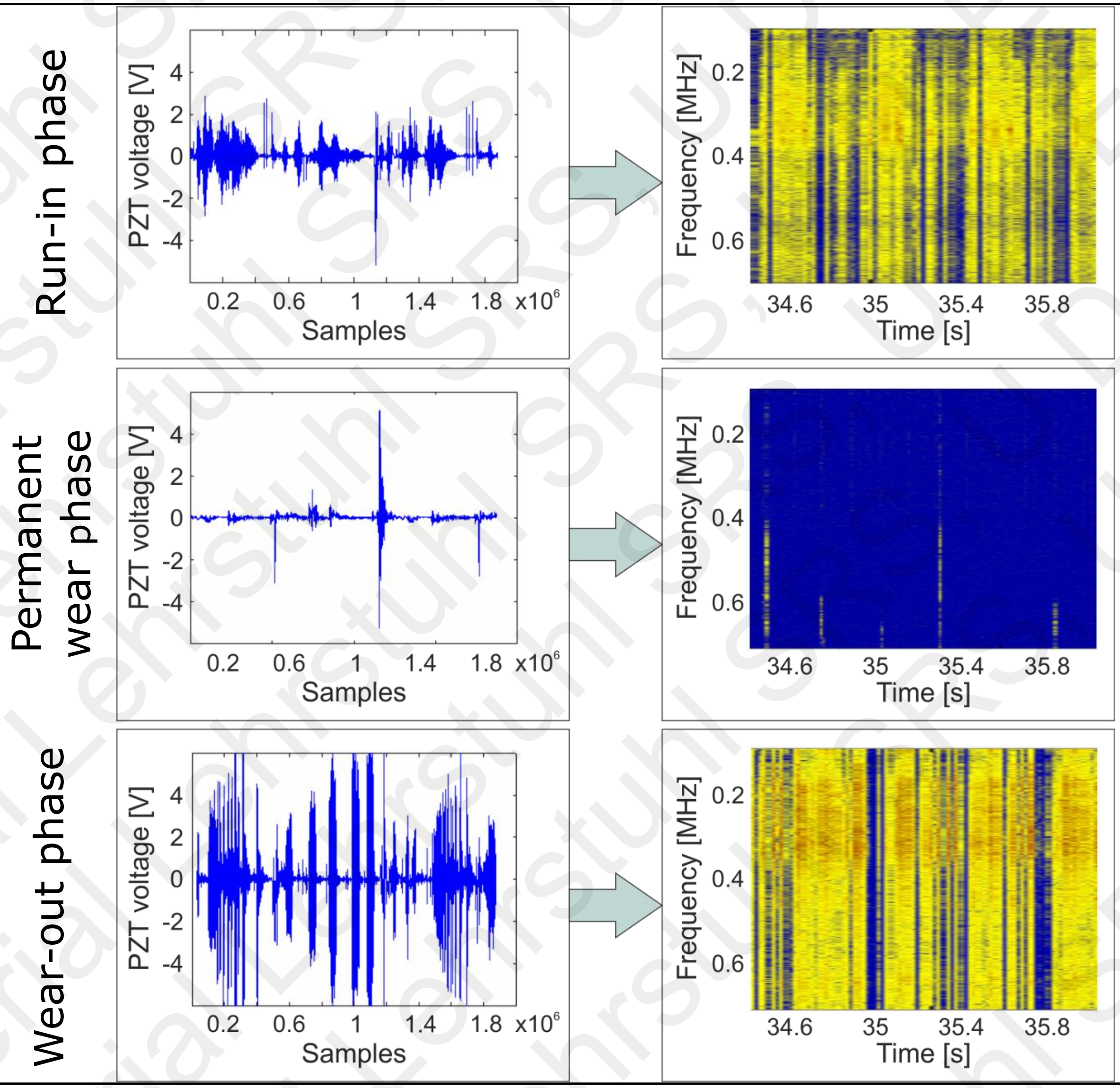

- ➔ Distinction between three major phases of system failure
- ➔ Correlation of AE-signals to identify phases
- ➔ Identification of typical patterns and wear inherent frequencies
- ➔ Conclusion of state-of-wear from recorded AE-signals

Diagnosis-oriented data-filtering I

Generation of characteristic value for one load-cycle

- Consideration of the last 20 s of measured pressure
- Sliding window
  - Size: 1 s
  - Arithmetic mean of each window
- Arithmetic mean of all windows

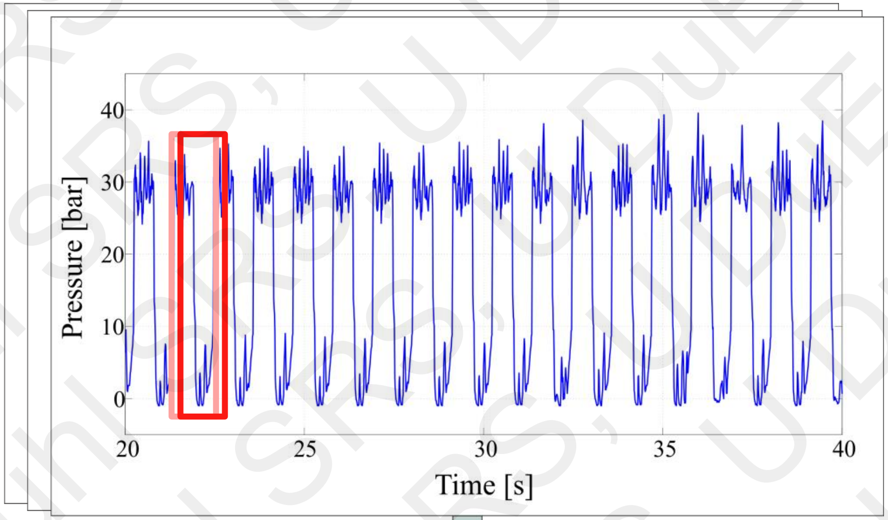

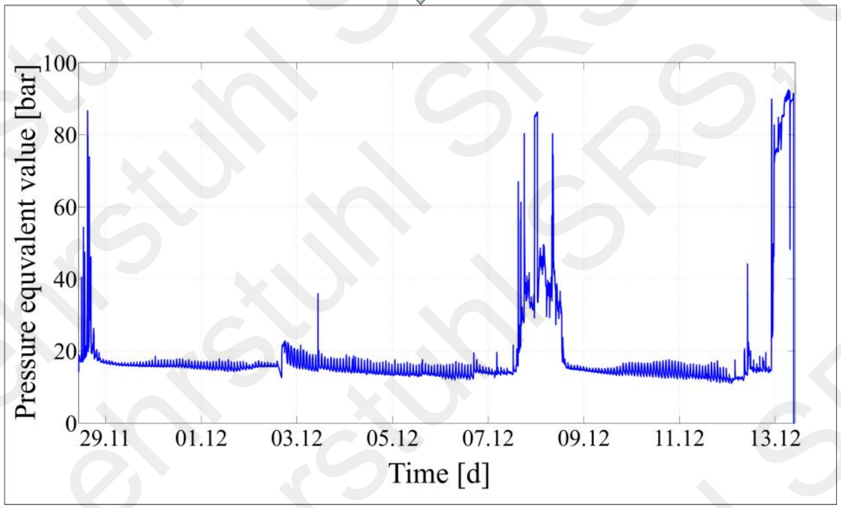

➔ Time-behavior of pressure equivalent characteristic values

Diagnosis-oriented data-filtering II

Further generation of characteristics I

- Calculation of damage increments

$$S(i) = \frac{|\bar{x}(i) - \bar{x}(i-1)|}{|t(i) - t(i-1)|}$$

$\bar{x}$: pressure equivalent value
t : time
i : actual number of load-cycle

- Accumulation of damage increments (AS)

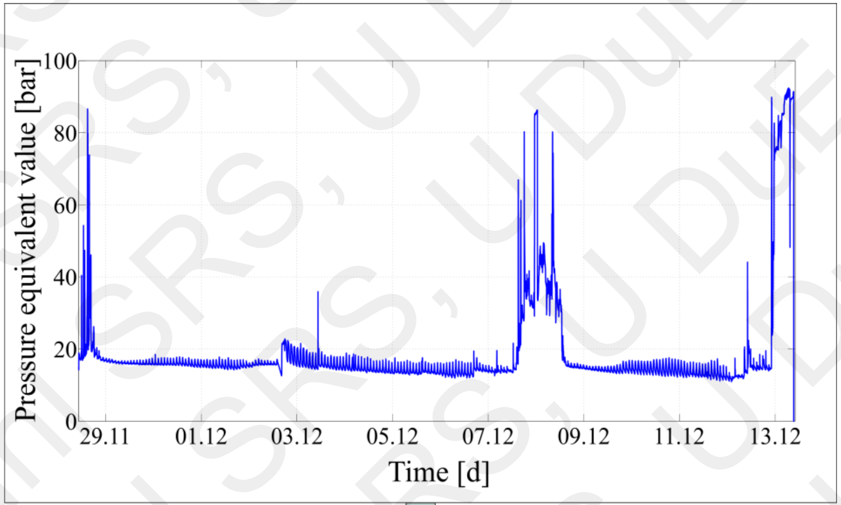

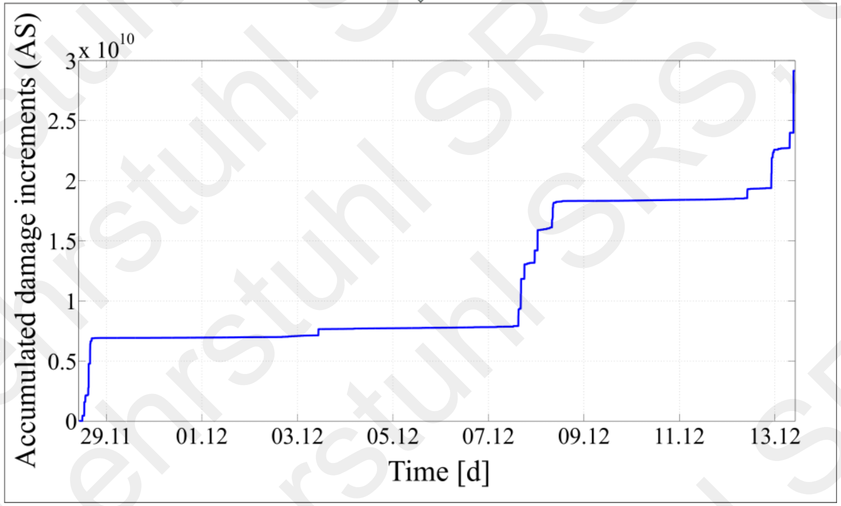

Diagnosis-oriented data-filtering III

Further generation of characteristics II

- Calculation of gradient of AS-curve
- Smoothing by using
  centered moving average:
  Using a specific number of values
  before and after the actual value

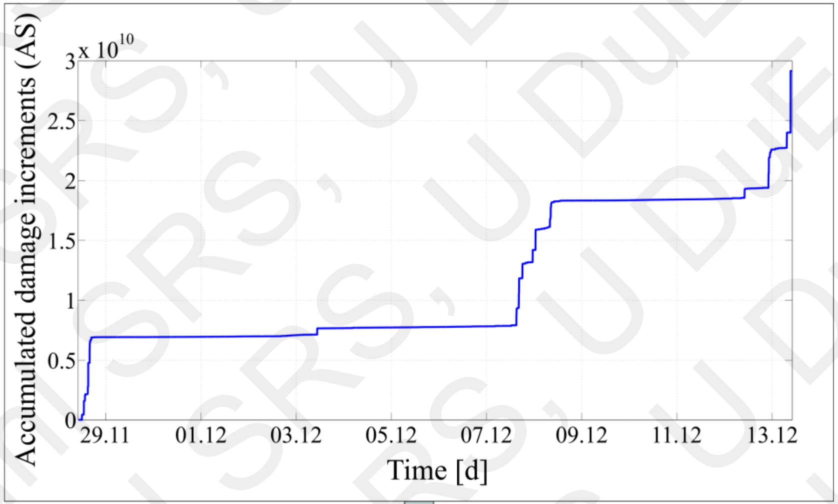

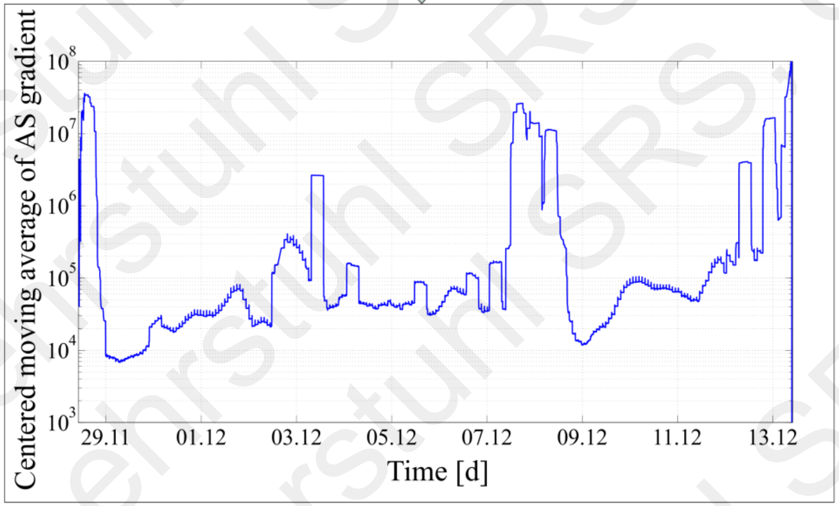

➔ Surface condition temporarily
generates very large friction.

Diagnosis-oriented data-filtering IV

Accumulated damage increments and gradients for three set-ups

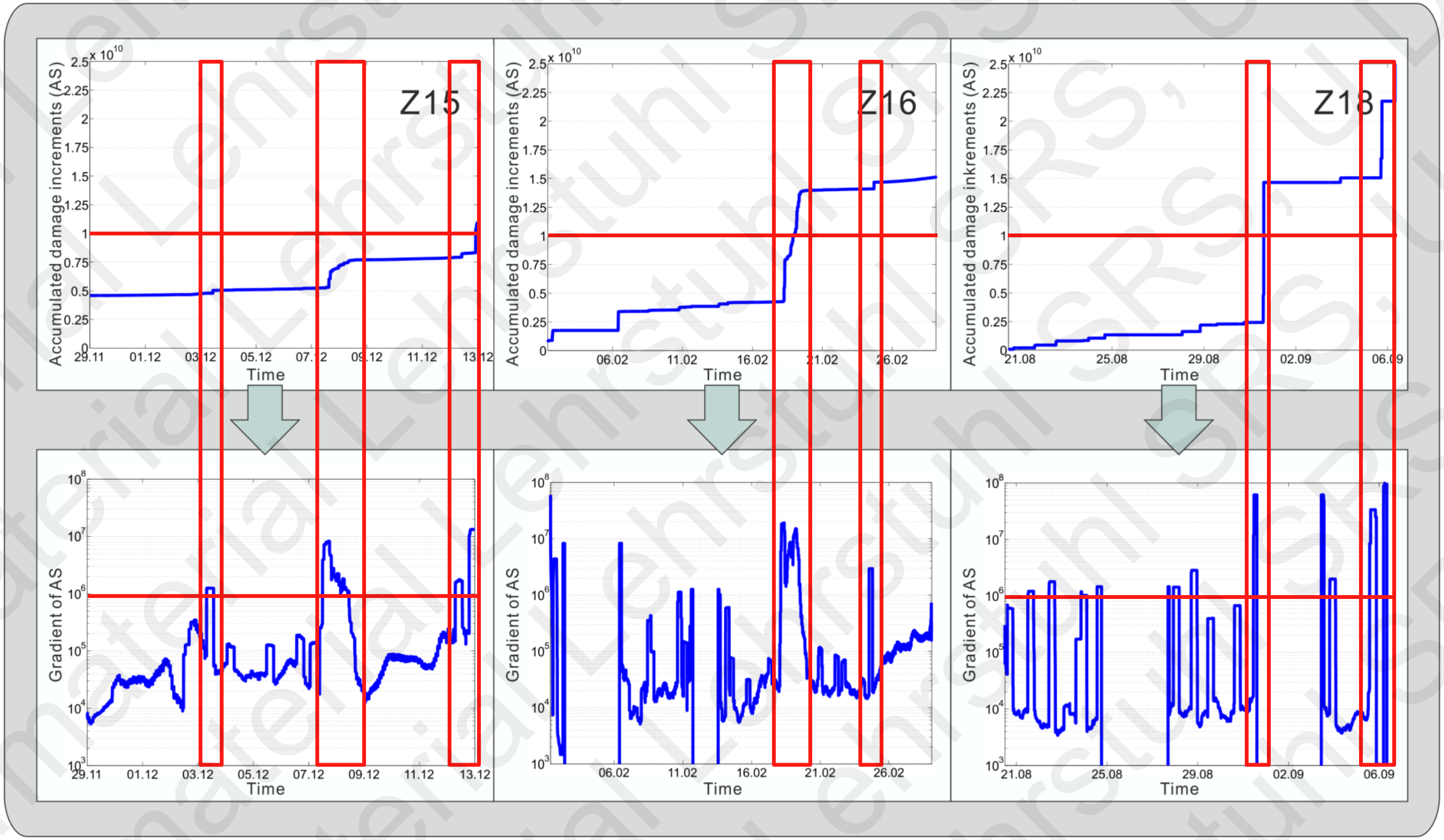

➔ Correlations between degree of wear and waveform changes

➔ Strong correlations of experimental results

Data-based classification approach I

Sliding window feature extraction

- Scan of training data
- Variation of size of scanning matrix

Calculation of statistical features

- Mean value
- Standard deviation
- …

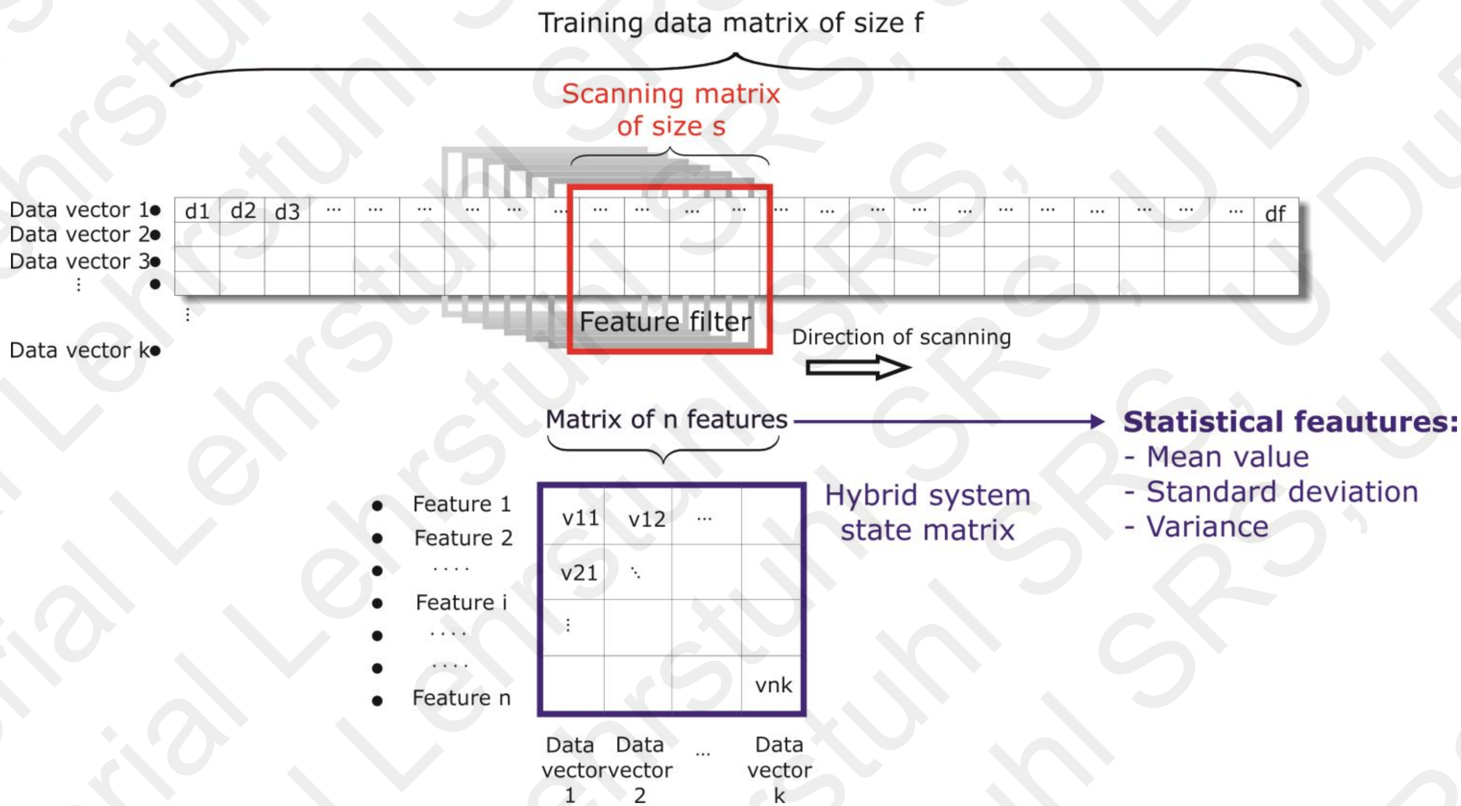

[Aljoumaa, Söffker, 2011]

Data-based classification approach II

Fuzzy classifier

- Use of features bounds
  and features from training data
- Fuzzyfication using
  triangular membership function μ(xi)
- Determination of state
  for each feature Mi
- Determination of final state
  using decision unit

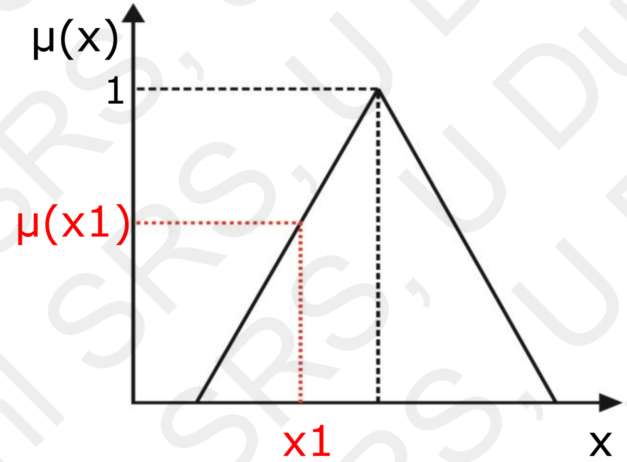

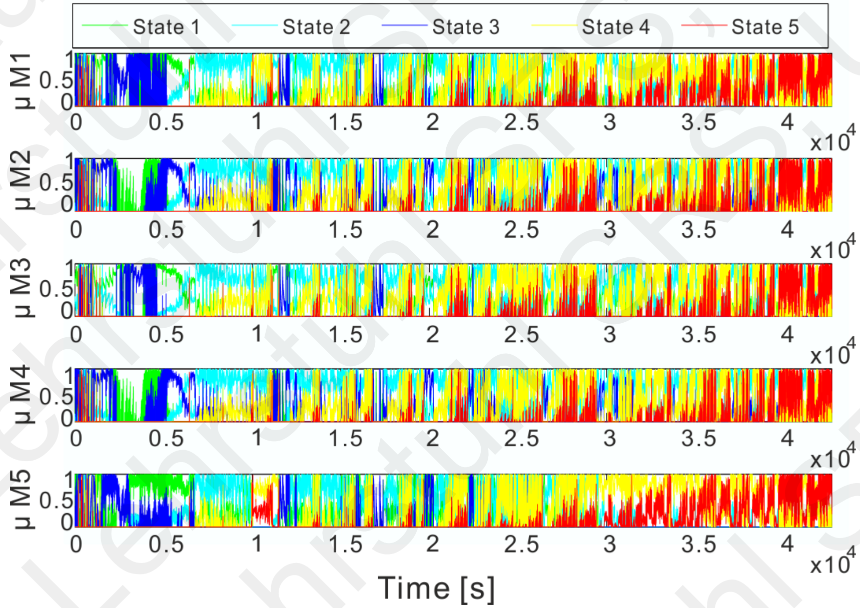

➔ Application to complex test data
➔ Automated detection, differentiation,
and classification of data

Söffker, D.; Rothe, S.:
Comparison of Three – Easy to Apply and Innovative –
Signal-based Approaches for Diagnosis of a Technical System with Wear

Comparison of results I

Comparison of the three methods using identical test data

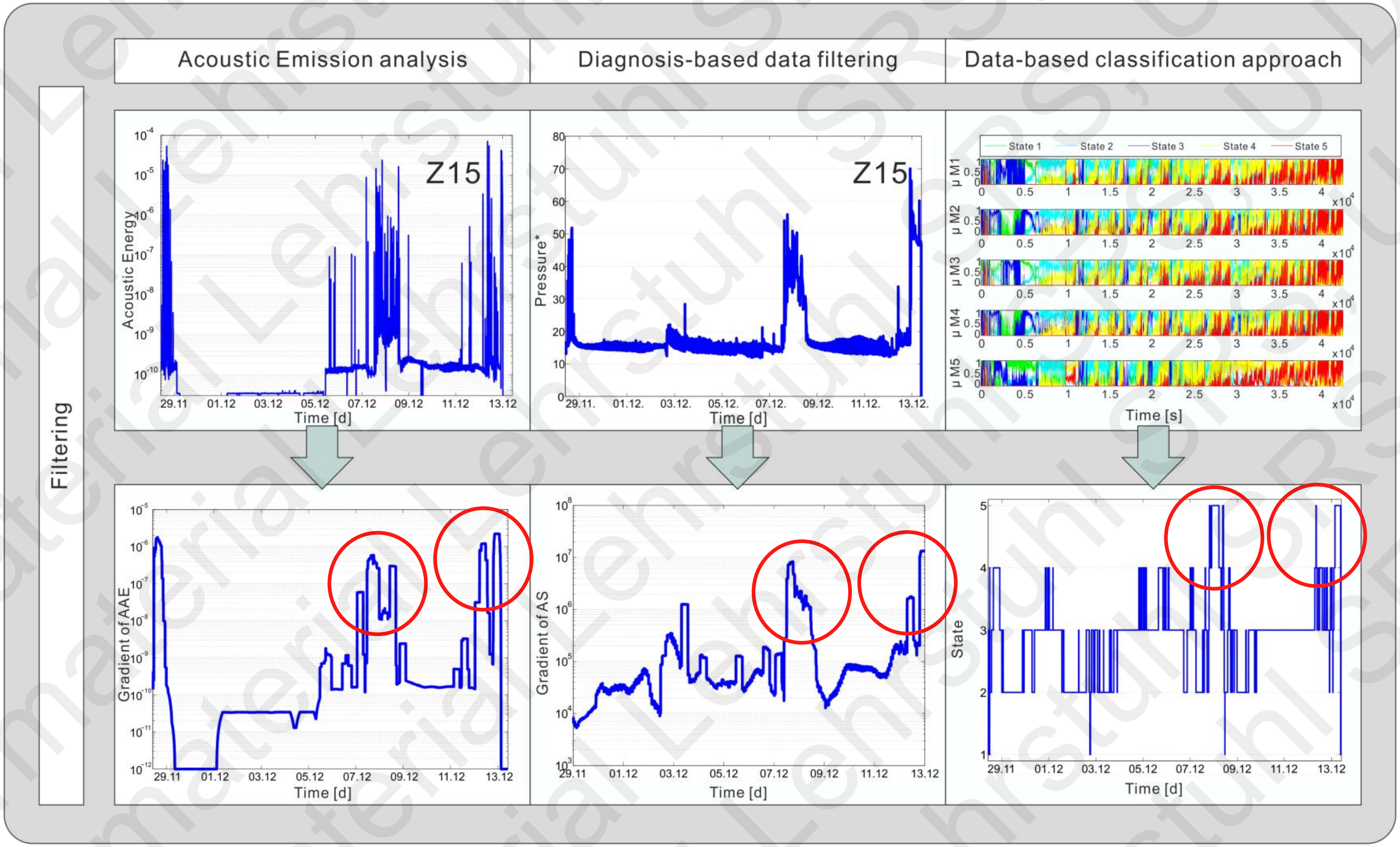

➔ Three different methods show same results

Comparison of results II

Method / Characteristic	Acoustic Emission (AE) [Baccar, Dettmann, Söffker]	Diagnosis-based Data Filtering [Dettmann, Söffker]	Fuzzy-based Classification (with Macro-data) [Aljoumaa, Söffker]
Effort of Sensor Application	+	+ +	+ +
Effort of Data Analysis	- -	0	+ +
Device-related Effort	- -	+ +	+ +
Real-time Capability	-	+	+
Complexity for Users	- -	0	+ +
Complexity for Developers	0	+ +	- -
Capability for Error Detection	+ +	+	+
Simple Diagnosis/ State-classification	+ +	+ +	+ +
Complex Diagnosis	+ +	- -	- -

Condition lights for brief evaluation of system state

State-related evaluation for diagnosis-oriented data filtering approach

- Two main aspects
  - Actual level of wear (y-axis)
  - Actual changes of the last step (x-axis)
- Combination of both aspects: sensitivity matrix
- Heuristic definition of three states (green, yellow, and red)

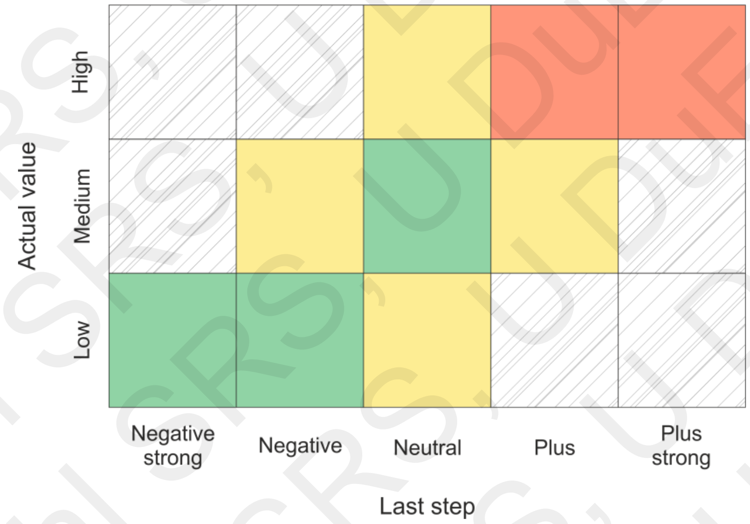

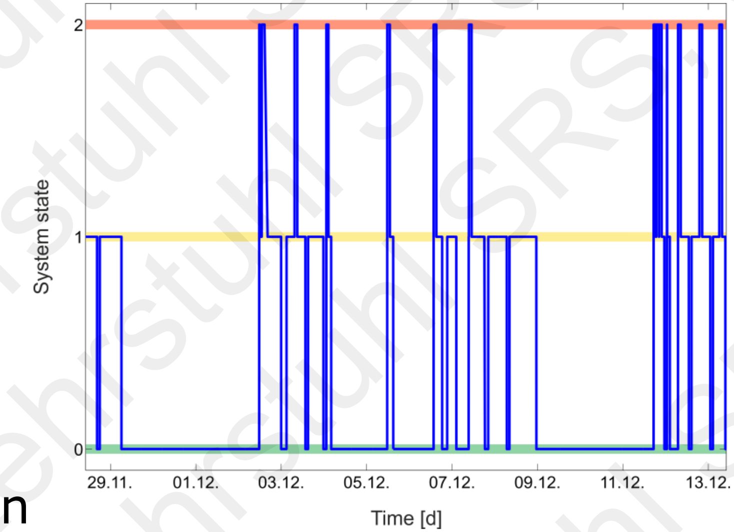

➔ Derivation of the system state for whole test-run

Summary and outlook

Summary

Representation of three signal-based data analysis methods

- AE-based analysis
  - Wear characteristic sound signals (PZT, STFT)
  - Close to physical effects
- Diagnosis-oriented data filtering
  - Evaluation of surface state by generation of characteristic values
  - Calculation of actual damage level
- Data-based classification approach
  - Fuzzy-based model to characterize classification state
  - Automated state classification

➔ Automatic classification of occured wear phases

➔ Different detailed insights using the three approaches

Outlook

- Implementation of failure rate calculation and life-time control strategies

Thank you for your attention!

Comparison of Three – Easy to Apply and Innovative – Signal-based Approaches for Diagnosis of a Technical System with Wear

Univ.-Prof. Dr.-Ing. Dirk Söffker

University of Duisburg-Essen
Chair of Dynamics and Control (SRS)

Lotharstr. 1-21, 47048 Duisburg, GERMANY

E-mail: soeffker@uni-due.de
Web: www.srs.uni-due.de

Any questions?

Multi-Klassifikatorfusion basierend auf der Zuverlässigkeit individueller Klassifikatoren

Sandra Rothe

Betreuer:
Univ.-Prof. Dr.-Ing. Dirk Söffker
Lou'i Al-Shrouf, M.Sc.

24. April 2012

Motivation

RWE Power AG Kohleförderung

- Problem: Schäden durch geförderte Steine
- Lösung: Steinerkennungssystem
  - Beschleunigungssensoren und Laserscanner
  - Filterung und Klassifikation
- Ziele der Steinerkennung:
  - Erkennungsquote größer als 90%
  - Geringe Anzahl an Fehlauslösungen

[Quelle: Privat, November 2011]

Motivation

Komplexes System

Keine zuverlässige Gesamtentscheidung
auf Grund der einzelnen Sensorinformationen

Fusion der individuellen Entscheidungen zu einer Schlussentscheidung

- Entwicklung von neuen Fusionsmethoden
  - » Möglichkeit der Realisierung von Gewichtungsfaktoren
- Vergleich der neuen Methoden mit vorhandenen Methoden

Gliederung

- Methoden der Fusion
- Erweiterung der Dempster-Shafer Theorie
- Vergleich anhand einiger Beispiele
- Diskussion der Ergebnisse anhand von Testdaten
- Zusammenfassung und Ausblick

Background: Fusion techniques

Definition:

"The process of fusing information from several individual data sources after each data source undergone a preliminary classification" [Fauvel, et al. 2006].

Types of sensor fusion

- Observation fusion
- Feature fusion
- Decision fusion

Observation fusion (direct fusion)

- Raw data combination of multiple sensors of the same type
- Accurate synchronization of raw data required

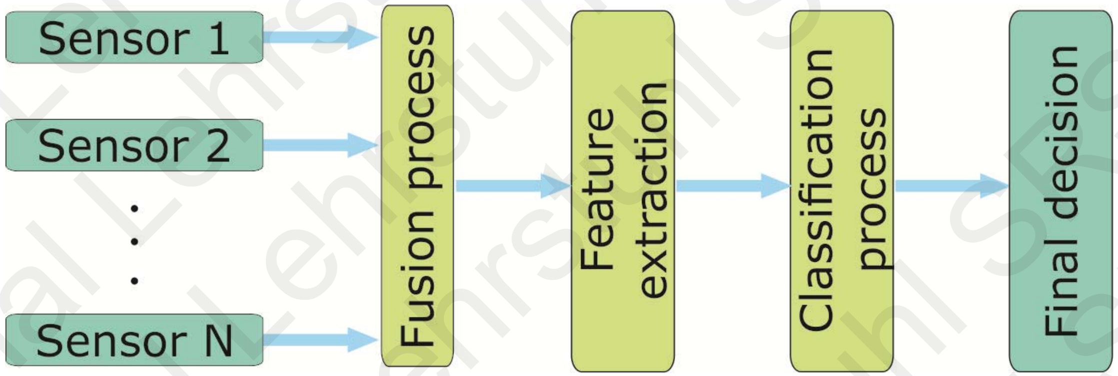

Background: Fusion techniques

Feature fusion

- Individual feature extraction of sensor signals
- Fusing extracted features
- Appropriate for combination sensor signals of different types

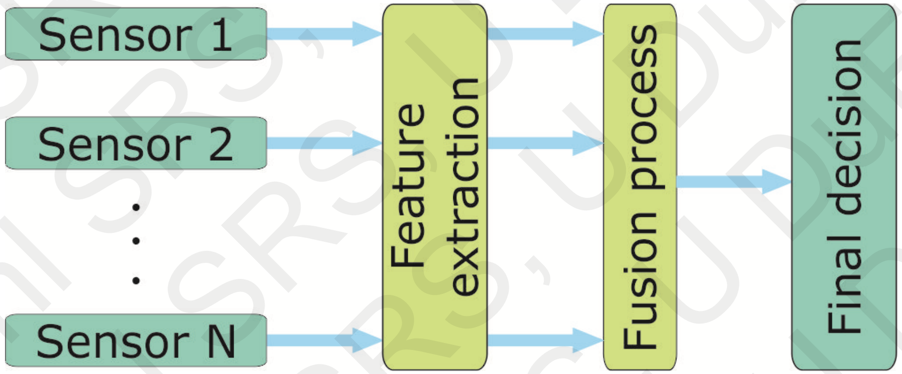

Decision fusion

- Individual feature extraction and classification of sensor signals
- Appropriate for combination sensor signals of different types

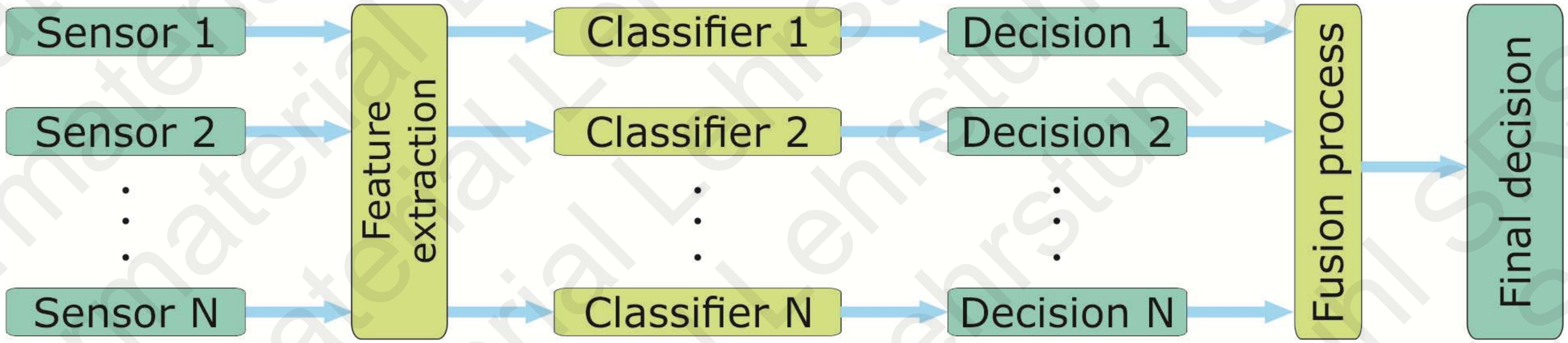

Methoden der Fusion I

Zwei Arten der Fusion

- Konkurrenz-Methoden

  Entscheidung für die Aussage eines Klassifikators

  - Rangordnung
  - Mehrheitswahl
  - Gewichtete Wahl

- Kooperative Methoden

  Kombination der Aussagen zu einer neuen Aussage

  - Bayes'sche Kombinationsregel
  - Dempster-Shafer Theorie

Background: Bayesian Combination Rule (BCR)

Basic concept

- The performance of the individual classifiers is obtained based on a training data set.
- A confusion matrix CM^k for each classifier is constructed based on the training data set.
- Confusion matrix CM^k indicates the performance of the related classifier.

$$CM^k = \begin{bmatrix} n^k{}_{11} & n^k{}_{12} & \dots & n^k{}_{1M} & n^k{}_{1(M+1)} \\ n^k{}_{21} & n^k{}_{22} & \dots & n^k{}_{2M} & n^k{}_{2(M+1)} \\ \vdots & \vdots & \vdots & \vdots & \vdots \\ n^k{}_{M1} & n^k{}_{M2} & \dots & n^k{}_{MM} & n^k{}_{M(M+1)} \end{bmatrix}$$

- Element n_{ij} denotes the number of samples with actual class i that is assigned class j when $j \leq M$. When $j = M + 1$, it represents the number of rejected samples.

Background: Bayesian Combination Rule (BCR)

Basic concept

Conditional probability that a sample X actually belongs to class i, given that classifier cl^k assigns it to class j is

$$P(x \in C_i / cl^k(x) = j) = \frac{n^k{}_{ij}}{\sum_{i=1}^{M} n^k{}_{ij}}.$$

Degree of belief that x belongs to class i by K classifiers, given that $cl_k = j_k$ for $1 \le k \le K$ is

$$bel(i) = P(x \in C_i / cl^k(x) = j_1, \ldots, cl^k(x) = j_K).$$

Degree of belief $bel(i)$ for independent decisions can be approximated using Bayes formula as

$$bel(i) \approx \frac{\prod_{k=1}^{K} P(x \in C_i / cl^k(x) = j_k)}{\sum_{i=1}^{M} \prod_{k=1}^{K} P(x \in C_i / cl^k(x) = j_k)}.$$

Methoden der Fusion III

Dempster-Shafer Theorie (DST) [Dempster, A. P., Shafer, G., 1976] I

– Betrachtungsrahmen bestehend aus drei Aussagen:

$$\Omega = \{h_1, h_2, h_3\}$$
$$\equiv \{\text{Ereignis tritt auf, Unsichere Aussage, Ereignis tritt nicht auf}\}$$

– Basis-Wahrscheinlichkeiten des Klassifikators X bezüglich der Aussagen h_1, h_2 und h_3: $m(X_1)$, $m(X_2)$ und $m(X_3)$

– Kombinationstabelle für zwei Klassifikatoren [Erweiterung von Rakowsky, U.K., 2007]:

AND	A_1	A_2	A_3
B_1	h_1	h_2	h_3
B_2	h_2	h_2	h_3
B_3	h_3	h_3	h_3

OR	A_1	A_2	A_3
B_1	h_1	h_1	h_1
B_2	h_1	h_2	h_2
B_3	h_1	h_2	h_3

Methoden der Fusion IV

Dempster-Shafer Theorie (DST) II

Berechnung der Glaubenswerte

– Dempster-Shafer Theorie mit AND-Gate

$$
\begin{aligned}
m(Z_1) &= m(A_1)m(B_1) \\
m(Z_2) &= m(A_1)m(B_2)+m(A_2)m(B_1)+m(A_2)m(B_2) \\
m(Z_3) &= m(A_1)m(B_3)+m(A_2)m(B_3)+m(A_3)m(B_1) \\
&\quad +m(A_3)m(B_2)+m(A_3)m(B_3)
\end{aligned}
$$

– Dempster-Shafer Theorie mit OR-Gate

$$
\begin{aligned}
m(Z_1) &= m(A_1)m(B_1)+m(A_1)m(B_2)+m(A_1)m(B_3) \\
&\quad +m(A_2)m(B_1)+m(A_3)m(B_1) \\
m(Z_2) &= m(A_2)m(B_2)+m(A_2)m(B_3)+m(A_3)m(B_2) \\
m(Z_3) &= m(A_3)m(B_3)
\end{aligned}
$$

Erweiterung der Dempster-Shafer Theorie I

Mittels Mehrheitswahl I

Annahme: Ereignis „unsicher" wird als Entscheidung der Klassifikatoren nicht betrachtet

$m(X_2)=0$

Kombinationstabelle:

- Anzahl positive Entscheidungen > Anzahl negative Entscheidungen => Zwischenentscheidung positiv (h_1)
- Anzahl positive Entscheidungen < Anzahl negative Entscheidungen => Zwischenentscheidung negativ (h_3)
- Anzahl positive Entscheidungen = Anzahl negative Entscheidungen => Zwischenentscheidung unsicher (h_2)

Erweiterung der Dempster-Shafer Theorie II

Mittels Mehrheitswahl II

Kombinationstabelle für drei Klassifikatoren

	A_1		A_3	
	C_1	C_3	C_1	C_3
B_1	h_1	h_1	h_1	h_3
B_3	h_1	h_3	h_3	h_3

Glaubenswerte

$$m(Z_1) = m(A_1)m(B_1)m(C_1) + m(A_1)m(B_1)m(C_3) + m(A_1)m(B_3)m(C_1) + m(A_3)m(B_1)m(C_1)$$

$$m(Z_2) = 0$$

$$m(Z_3) = 1 - m(Z_1)$$

Erweiterung der Dempster-Shafer Theorie III

Mittels Mehrheitswahl III

Kombinationstabelle für vier Klassifikatoren

		A_1		A_3	
		C_1	C_3	C_1	C_3
B_1	D_1	h_1	h_1	h_1	h_2
	D_3	h_1	h_2	h_2	h_3
B_3	D_1	h_1	h_2	h_2	h_3
	D_3	h_2	h_3	h_3	h_3

Glaubenswerte

$$
\begin{aligned}
m(Z_1) = {} & m(A_1)m(B_1)m(C_1)m(D_1) \\
& + m(A_1)m(B_1)m(C_1)m(D_3) \\
& + m(A_1)m(B_1)m(C_3)m(D_1) \\
& + m(A_1)m(B_3)m(C_1)m(D_1) \\
& + m(A_3)m(B_1)m(C_1)m(D_1)
\end{aligned}
$$

$$
\begin{aligned}
m(Z_2) = {} & m(A_3)m(B_3)m(C_1)m(D_1) \\
& + m(A_3)m(B_1)m(C_3)m(D_1) \\
& + m(A_3)m(B_1)m(C_1)m(D_3) \\
& + m(A_1)m(B_3)m(C_3)m(D_1) \\
& + m(A_1)m(B_3)m(C_1)m(D_3) \\
& + m(A_1)m(B_1)m(C_3)m(D_3)
\end{aligned}
$$

$$m(Z_3) = 1 - m(Z_1) - m(Z_2)$$

Erweiterung der Dempster-Shafer Theorie IV

Mittels Mehrheitswahl IV

Keine Berücksichtigung des Ereignisses h_2 in der Gesamtentscheidung

$m(Z_2)$ wird zur Hälfte auf $m(Z_1)$ und $m(Z_3)$ aufgeteilt

$$m(Z_1)^* = m(Z_1) + \frac{1}{2} m(Z_2)$$

$$m(Z_3)^* = m(Z_3) + \frac{1}{2} m(Z_2)$$

Erweiterung der Dempster-Shafer Theorie V

Mittels gewichteter Wahl

Zuweisung einer Anzahl an Stimmen für jede Entscheidung

Hier: Anzahl Stimmen = Basis-Wahrscheinlichkeiten

Kombinationstabelle:

- Berechnung der Summe der Basis-Wahrscheinlichkeiten für jede Entscheidung
- Relative Mehrheit für eine Entscheidung
  => Zwischenentscheidung entsprechend Mehrheit

Berechnung der Glaubenswerte entsprechend der Tabelle

Erweiterung der Dempster-Shafer Theorie VI

Möglichkeit der Realisierung von Gewichtungsfaktoren

Gewichtungsfaktor $g(X_i)$ für jede Einzelentscheidung

- Multiplikation der Basis-Wahrscheinlichkeiten mit den Gewichtungsfaktoren

$$\tilde{m}(X_i) = g(X_i)\, m(X_i)$$

- Ersetzen der Basis-Wahrscheinlichkeiten durch Gewichtungsfaktoren

$$\tilde{m}(X_i) = g(X_i)$$

Vergleich anhand einiger Beispiele – Beispiel Ia

Fusion von zwei Klassifikatoren I

- $m(A_1)$ und $m(B_1)$ sind variabel
- Zusammenhang für bestimmte Werte von $m(Z_1)$

  Bayes'sche Kombinationsregel

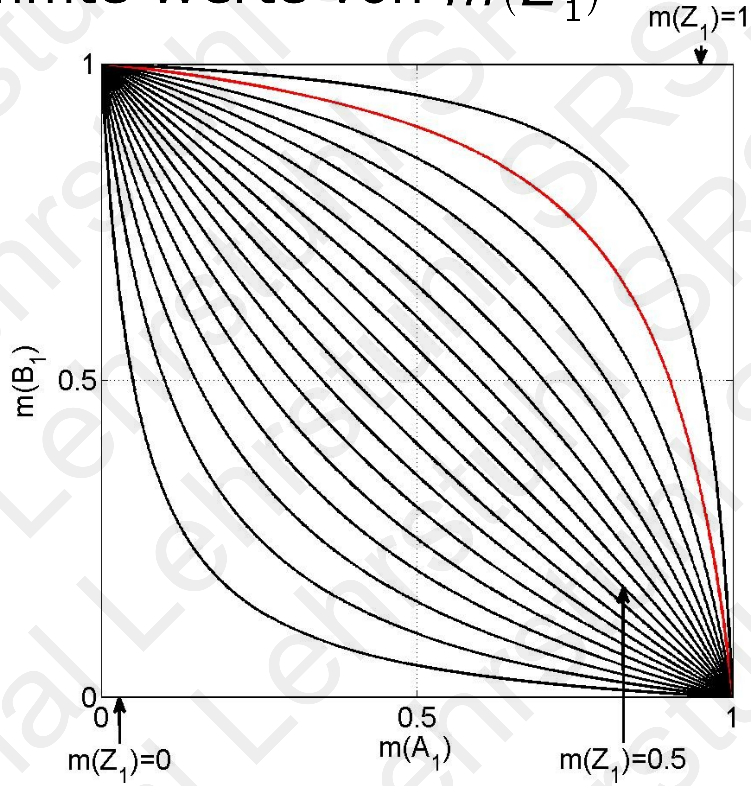

» Sehr variable Zuverlässigkeiten der individuellen Klassifikatoren

Vergleich anhand einiger Beispiele - Beispiel Ib

Fusion von zwei Klassifikatoren II

Dempster-Shafer Theorie (DST):

Mit AND-Gate

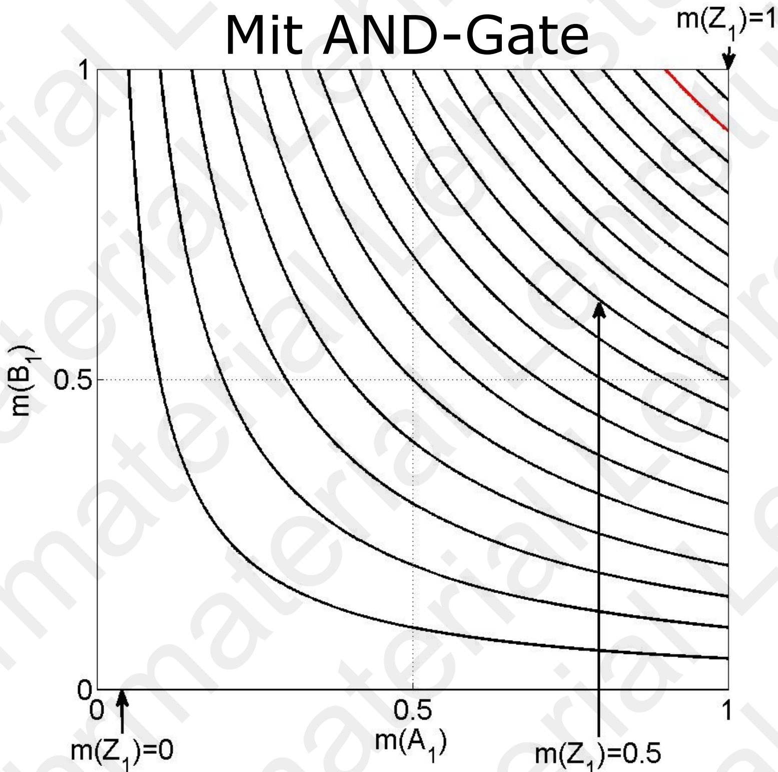

Mit OR-Gate

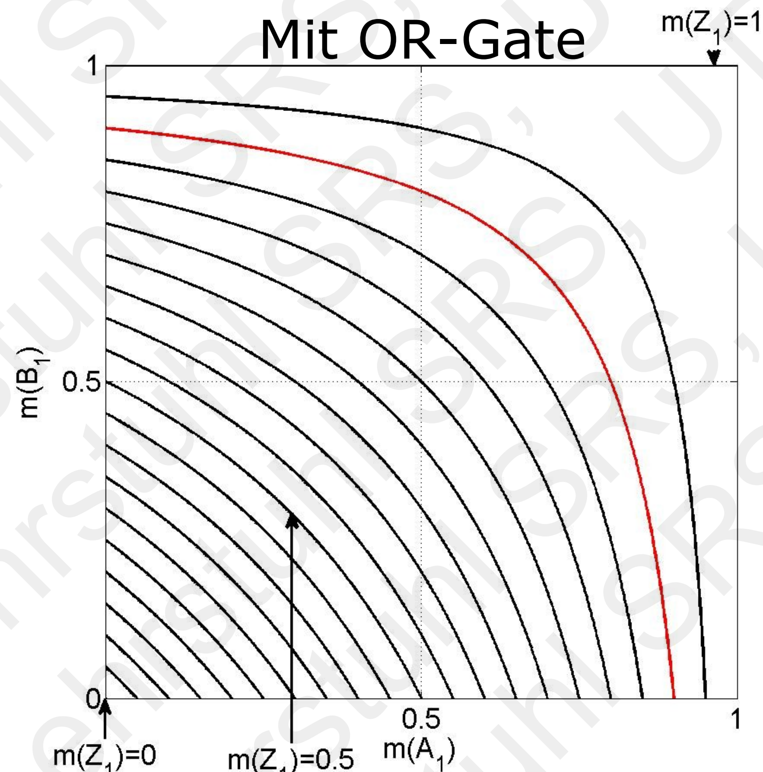

» AND: Zuverlässigkeiten der Klassifikatoren ≥ Gesamtzuverlässigkeit

» OR: Zuverlässigkeiten der Klassifikatoren ≤ Gesamtzuverlässigkeit

Vergleich anhand einiger Beispiele – Beispiel Ic

Fusion von zwei Klassifikatoren III

Erweiterung der Dempster-Shafer Theorie:

Mehrheitswahl

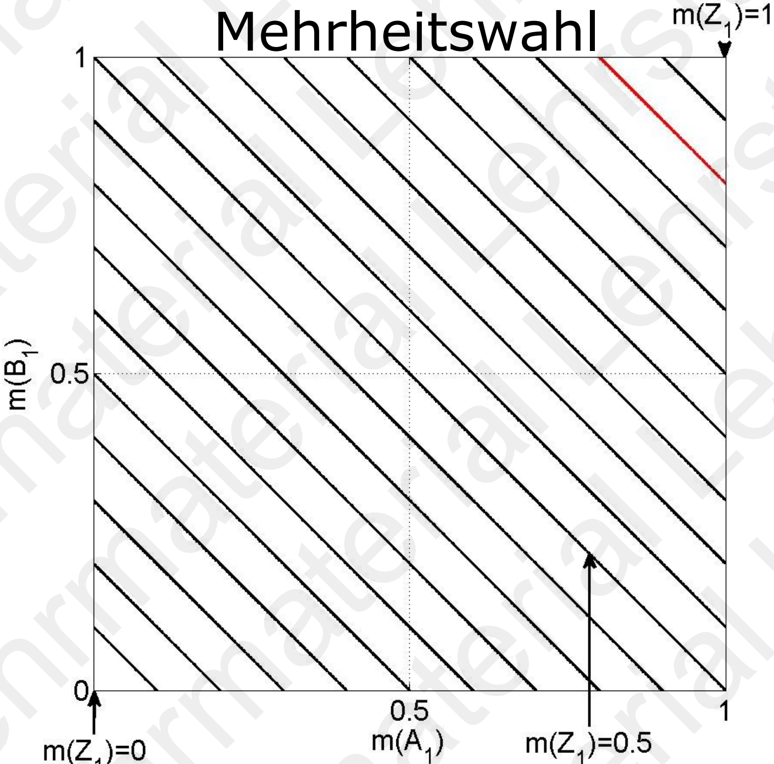

Gewichtete Wahl

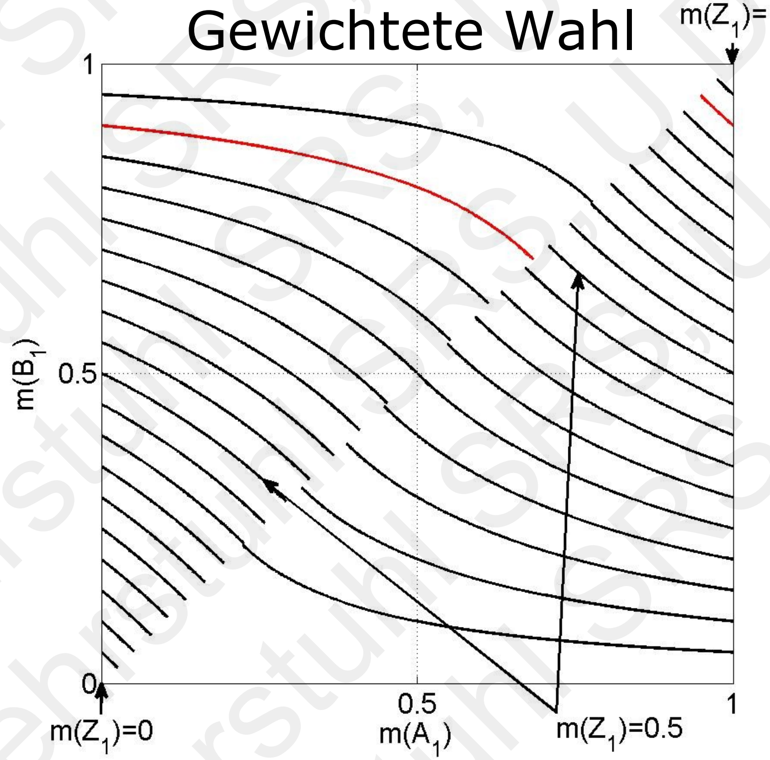

» Mehrheit: Linearer Zusammenhang der Zuverlässigkeiten

» Gewichtung: Unterteilung $m(A_1) < \text{oder} > 1-m(B_1)=m(B_2)$

Vergleich anhand einiger Beispiele – Beispiel II

Zuverlässigkeiten der Klassifikatoren A, B, C und D

Klassifikator	Pos. [%]	Neg. [%]
A	80	90
B	90	95
C	70	85
D	80	80

Berechnung der Basis-Wahrscheinlichkeiten aus Tabelle

- Klassifikator A

  Entscheidung positiv: $m(A_1)=0{,}8$ $m(A_2)=0{,}2$

  Entscheidung negativ: $m(A_1)=0{,}1$ $m(A_1)=0{,}9$

- Für Klassifikator B, C und D entsprechend

Comparison of BBF and BCR using theoretical example

Theoretical example: multiclassifier system

- Number of independent classifiers: four (A, B, D, E)
- Classifiers statements:
  - Positive (Pos.): a specific event exists, or
  - Negative (Neg.): no specific event
- Training data set: 400 samples (including 180 specific event)
- Confusion matrix CM^k:

$$CM^A = \begin{bmatrix} 160 & 20 & 0 \\ 40 & 180 & 0 \end{bmatrix}$$

$$CM^B = \begin{bmatrix} 180 & 10 & 0 \\ 20 & 190 & 0 \end{bmatrix}$$

$$CM^D = \begin{bmatrix} 140 & 30 & 0 \\ 60 & 170 & 0 \end{bmatrix}$$

$$CM^E = \begin{bmatrix} 160 & 160 & 0 \\ 40 & 40 & 0 \end{bmatrix}$$

$$P(x \in C_{pos.} / cl^A(x) = Pos.) = m(A_1) = 80\%$$

$$P(x \in C_{Neg.} / cl^A(x) = Pos.) = m(A_2) = 20\%$$

$$P(x \in C_{pos.} / cl^A(x) = Neg.) = m(A_1) = 10\%$$

$$P(x \in C_{Neg.} / cl^A(x) = Neg.) = m(A_1) = 90\%$$

Comparison of BBF and BCR using artificial example

Fusion results of first three classifiers using BBF and BCR

Classifier	Degree of accuracy	
	Pos. [%]	Neg. [%]
A	80	90
B	90	95
D	70	85
E	80	80

Case	A	B	D	$bel(Pos.)$ [%]	$bel(Pos.)$ [%]
1	Pos.	Pos.	Pos.	90.20	98.82
2	Neg.	Pos.	Pos.	66.40	70.00
3	Pos.	Neg.	Pos.	57.90	32.94
4	Pos.	Pos.	Neg.	75.90	86.40
5	Neg.	Neg.	Pos.	10.30	1.35
6	Neg.	Pos.	Neg.	21.30	15.00
7	Pos.	Neg.	Neg.	15.60	3.58
8	Neg.	Neg.	Neg.	2.00	0.10

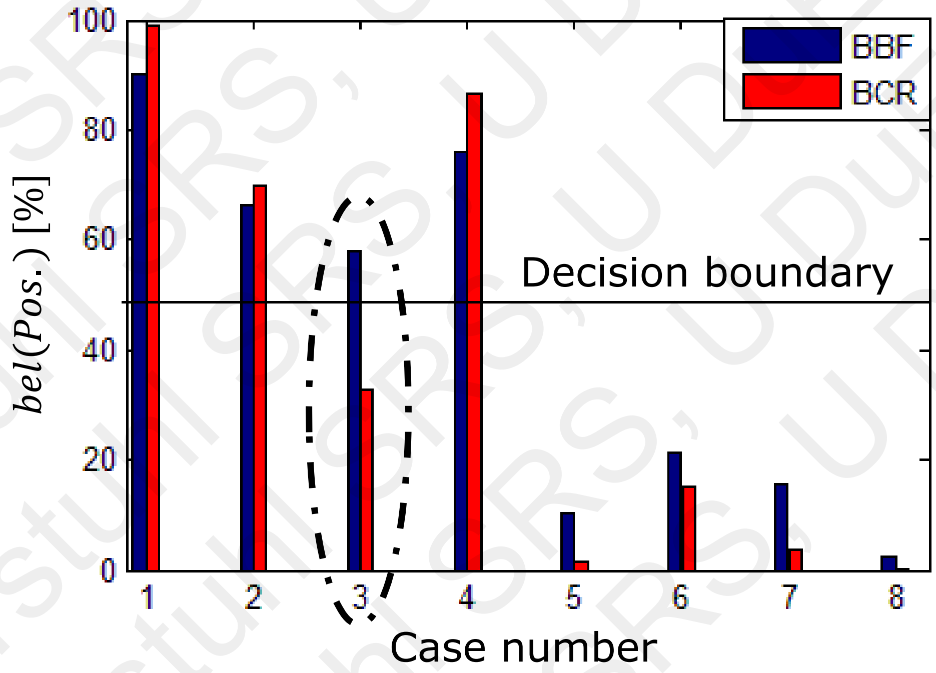

- ➔ The BBF led to plausible final decision for all scenarios.
- ➔ The plausibility of BBF is ensured by the comparison with BCR.
- ➔ Fusion results of BBF in case 3 seems to be more plausible than of BCR.

Comparison of BBF and BCR using theoretical example

Fusion results of the four classifiers using BBF and BCR

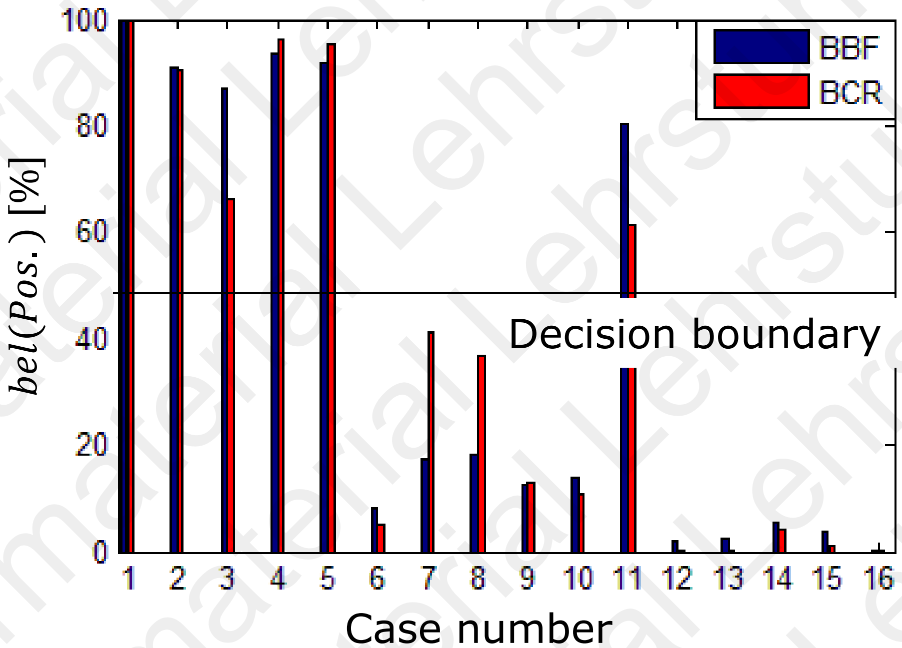

Case	A	B	C	D
1	Pos.	Pos.	Pos.	Pos.
2	Neg.	Pos.	Pos.	Pos.
3	Pos.	Neg.	Pos.	Pos.
4	Pos.	Pos.	Neg.	Pos.
5	Pos.	Pos.	Pos.	Neg.
6	Neg.	Neg.	Pos.	Pos.
7	Neg.	Pos.	Neg.	Pos.
8	Pos.	Neg.	Neg.	Neg.
9	Pos.	Neg.	Neg.	Pos.
10	Pos.	Neg.	Pos.	Neg.
11	Pos.	Pos.	Neg.	Neg.
12	Neg.	Neg.	Neg.	Pos.
13	Neg.	Neg.	Pos.	Neg.
14	Neg.	Pos.	Neg.	Neg.
15	Pos.	Neg.	Neg.	Neg.
16	Neg.	Neg.	Neg.	Neg.

➔ The BBF led to plausible final decisions for all scenarios.

➔ The difference of the final degree of belief between BBF and BCR is up to 23%.

➔ Both methods led to similar final decisions.

Vergleich anhand einiger Beispiele – Beispiel IIa

Fusion von drei Klassifikatoren

				Bayes	AND	OR	Mehrheit	Gewichtung
Case	A ([%])	B ([%])	C ([%])	bel(p) [%]	m(Z_1) [%]	m(Z_1) [%]	m(Z_1) [%]	m(Z_1) [%]
1	Pos. (80)	Pos. (90)	Pos. (70)	98,82	50,40	99,40	90,20	90,40
2	Neg. (90)	Pos. (90)	Pos. (70)	70,00	6,30	97,30	66,40	66,40
3	Pos. (80)	Neg. (95)	Pos. (70)	32,94	2,80	94,30	57,90	57,90
4	Pos. (80)	Pos. (90)	Neg. (85)	86,40	10,80	98,30	75,90	75,90
5	Neg. (90)	Neg. (95)	Pos. (70)	1,35	0,35	74,35	10,3	0,35
6	Neg. (90)	Pos. (90)	Neg. (85)	15,00	1,35	92,35	21,30	21,30
7	Pos. (80)	Neg. (95)	Neg. (85)	3,58	0,60	83,85	15,55	15,48
8	Neg. (90)	Neg. (95)	Neg. (85)	0,10	0,08	27,32	2,60	0,08

» Keine plausiblen Ergebnisse mit DST mit OR- und AND-Gate

» Ähnliche Ergebnisse mit BK,
Erweiterung mit Mehrheitswahl und Erweiterung mit gewichteter Wahl

Ausnahme Case 3
BK berücksichtigt Komponenten
mit hoher Zuverlässigkeit stärker

Vergleich anhand einiger Beispiele – Beispiel IIb

Fusion von vier Klassifikatoren

					Bayes	AND	OR	Mehrheit	Gewichtung
Case	A ([%])	B ([%])	C ([%])	D ([%])	bel(p) [%]	m(Z_1) [%]	m(Z_1) [%]	m(Z_1) [%]	m(Z_1) [%]
1	Pos. (80)	Pos. (90)	Pos. (70)	Pos. (80)	99,70	40,32	99,88	89,90	99,88
6	Neg. (90)	Neg. (95)	Pos. (70)	Pos. (80)	5,18	0,28	94,87	34,92	8,31
7	Neg. (90)	Pos. (90)	Neg. (85)	Pos. (80)	41,38	1,08	98,47	47,73	17,31
8	Neg. (90)	Pos. (90)	Pos. (70)	Neg. (80)	36,84	1,26	97,84	45,45	18,32
9	Pos. (80)	Neg. (95)	Neg. (85)	Pos. (80)	12,94	0,48	96,77	41,38	12,56
10	Pos. (80)	Neg. (90)	Pos. (70)	Neg. (80)	10,94	0,56	95,44	39,50	13,82
11	Pos. (80)	Pos. (90)	Neg. (85)	Neg. (85)	61,36	2,16	98,64	52,10	80,38
16	Neg. (90)	Neg. (95)	Neg. (85)	Neg. (80)	0,03	0,02	41,86	4,06	0,58

» Keine plausiblen Ergebnisse mit DST mit OR- und AND-Gate

» Gleiche Gesamtentscheidung mit BK,
Erweiterung der DST mit Mehrheitswahl und gewichteter Wahl
=> Korrektheit der neuen Methoden

» Eindeutige Entscheidungen bei Erweiterung
mit gewichteter Wahl (z. B. Case 7)

Diskussion der Ergebnisse anhand von Testdaten I

- Testdaten: Datensatz mit 40 manuell klassifizierten Objekten (Steine)
- Signale der Sensoren => Filter, Klassifikator => Entscheidungsvektor
- Berechnung der Quoten:

$$TPQ = \frac{\text{Anzahl der richtigen positiven Entscheidungen}}{\text{Anzahl aller positiven Entscheidungen}}$$

$$TNQ = \frac{\text{Anzahl der richtigen negativen Entscheidungen}}{\text{Anzahl aller negativen Entscheidungen}}$$

$$EQ = \frac{\text{Anzahl der richtig erkannten Steine}}{\text{Anzahl aller existierenden Steine}}$$

$$FQ = \frac{\text{Anzahl der Fehlauslösungen}}{\text{Anzahl aller Entscheidungen}}$$

Diskussion der Ergebnisse anhand von Testdaten II

Quoten der Beschleunigungssensoren und des Laserscanners

	Sensor 1	Sensor 2	Sensor 3	Sensor 5	Sensor 6	Laser-scanner
TPQ [%]	70,97	60,61	62,50	78,26	92,86	94,74
TNQ [%]	63,27	57,45	58,33	61,40	59,09	90,48
EQ [%]	55,00	50,00	50,00	45,00	32,50	90,00
FQ [%]	11,25	16,25	15,00	6,25	1,25	2,50

» Laserscanner ist die Komponente mit den höchsten Korrektheits- und Erkennungsquoten

» Drei mögliche Vorgehensweisen zur Fusion

- Fusion der Beschleunigungssensoren
- Fusion aller Sensoren gleichwertig
- Fusion der Beschleunigungssensoren mit dem Laserscanner

Diskussion der Ergebnisse anhand von Testdaten III

Ergebnisse:

- Nur positive Entscheidungen mit DST mit OR-Gate
- Nur negative Entscheidungen mit DST mit AND-Gate
- Ähnliche Ergebnisse bei mehreren Methoden

» Entscheidung für eine Methode schwierig

		EQ [%]	FQ [%]	Nr.
Fusion der Beschleunigungs-sensoren	Bayes	50	5	1
	OR	100	50	2
	AND	0	0	3
	Mehrheit	50	5	4
	Gewichtung	50	5	5
Fusion aller Sensoren	Bayes	92,5	4	6
	OR	100	50	7
	AND	0	0	8
	Mehrheit	65	1,25	9
	Gewichtung	65	1,25	10
Fusion der Beschleunigungs-sensoren mit dem Laserscanner	Bayes	90	2,5	11
	OR	92,5	6,25	12
	AND	47,5	1,25	13
	Mehrheit	90	2,5	14
	Gewichtung	90	2,5	15

Diskussion der Ergebnisse anhand von Testdaten IV

- Gütefunktion

$$G = \sqrt{(1-FQ)^2 + EQ^2}$$

- Optimum: *EQ=1, FQ=0*

$$G = \sqrt{2}$$

- Die Fusionierung entsprechend den Nr. 6, 11, 12, 14 und 15 weisen eine ähnliche Güte auf.

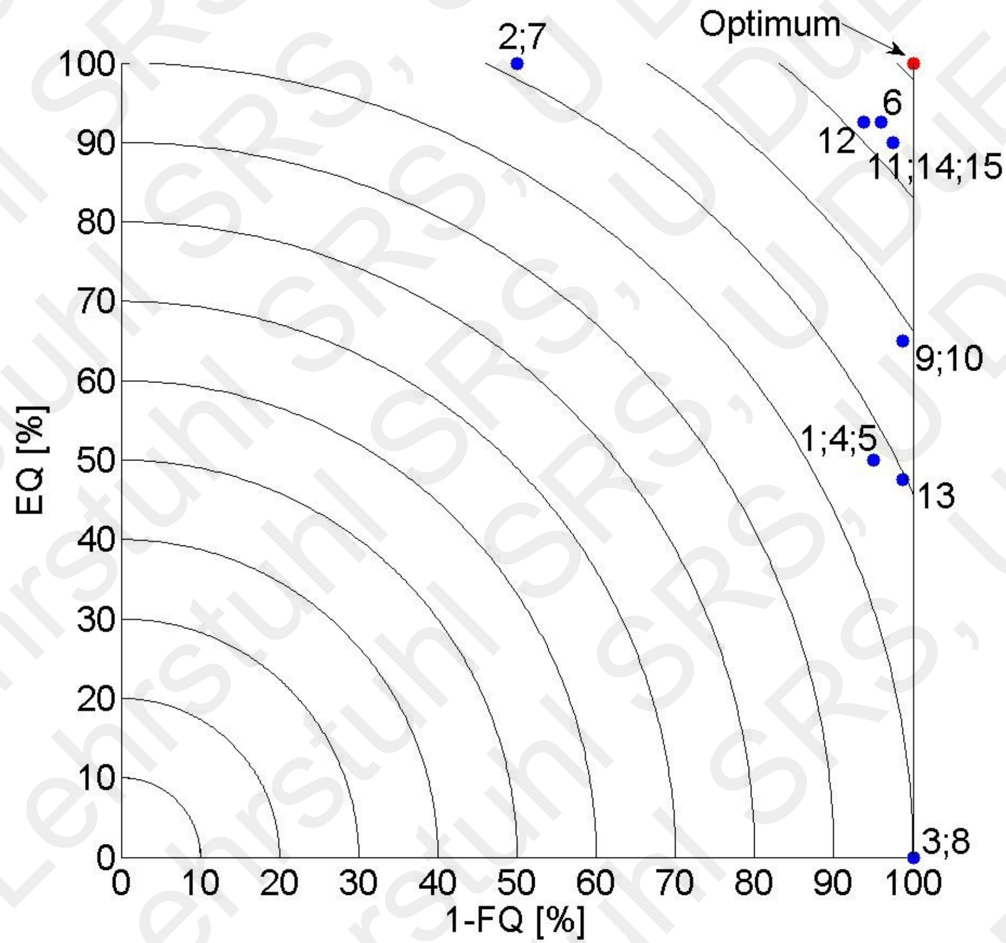

» Beste Güte bei der Fusion aller Sensoren mit Bayes'scher Kombinationsregel (Nr. 6)

Diskussion der Ergebnisse anhand von Testdaten V

- Dempster-Shafer Theorie nicht für Fusion von mehr als zwei Klassifikatoren geeignet
- Wichtigste Komponente zur Steinerkennung: Laserscanner
- Fusion aller Sensoren:
  - Bayes'sche Kombinationsregel: höchste Erkennungsquote, da Komponenten mit hohen Korrektheitsquoten stärker berücksichtigt werden
- Fusion der Entscheidungen der Beschleunigungssensoren mit der des Laserscanners: gleiche Ergebnisse mit
  - Bayes'sche Kombinationsregel
  - Erweiterung der Dempster-Shafer Theorie mit Mehrheitswahl
  - Erweiterung mit gewichteter Wahl

Diskussion der Ergebnisse anhand von Testdaten VI

Zielvorgabe: EQ >= 90%, Minimierung der FQ

- Alle Sensoren mit BK (Nr. 6)
- Beschleunigungssensoren mit Laserscanner
  - DST mit OR-Gate (Nr. 12)
  - BK (Nr. 11)
  - Erweiterung mittels Mehrheitswahl (Nr. 14)
  - Erweiterung mittels gewichteter Wahl (Nr. 15)

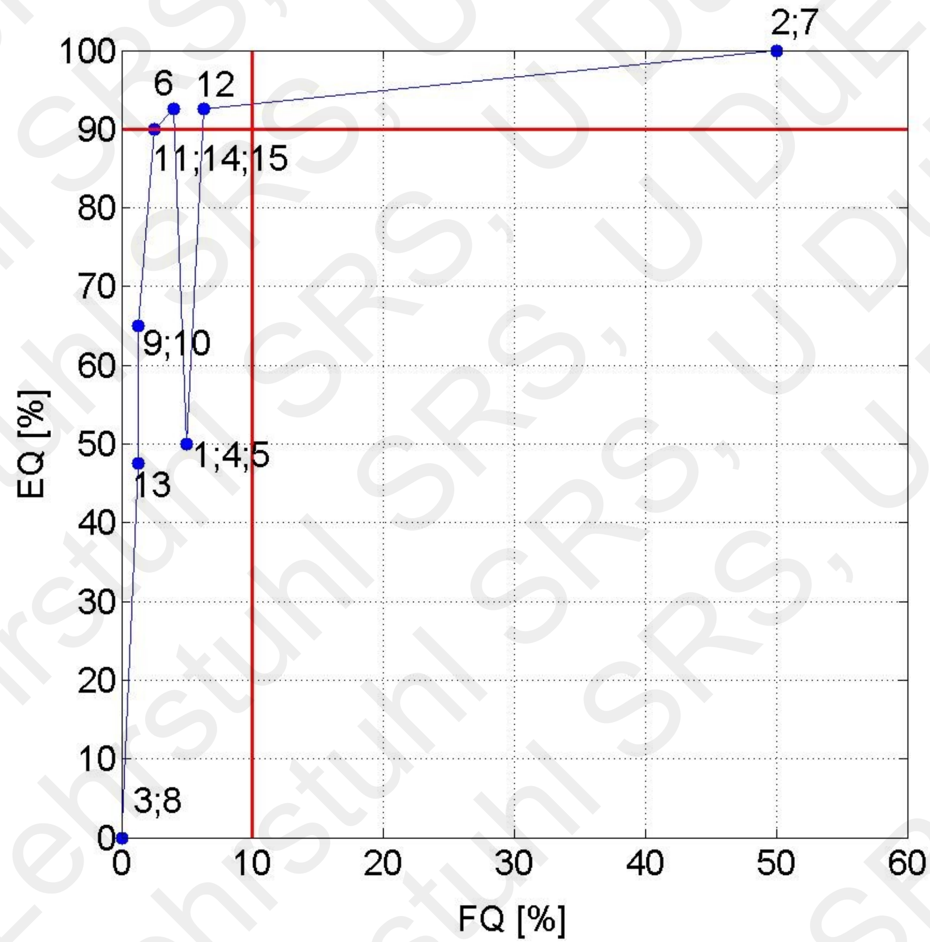

» Fünf Methoden erfüllen das Ziel des Steinerkennungssystems.

Zusammenfassung und Ausblick I

- Entwicklung von zwei neuen Fusionsmethoden
- Erweiterung der Dempster-Schafer Theorie
  - Mit Mehrheitswahl: Plausible Ergebnisse
  - Mit gewichteter Wahl: eindeutige Entscheidungen bei gerader Anzahl an Klassifikatoren
  - Möglichkeit der Realisierung von Gewichtungsfaktoren
- Vergleich der neuen Methoden mit vorhandenen Fusionsmethoden
  - Ähnliche Ergebnisse wie bei Bayes'scher Kombinationsregel => Korrektheit der neuen Fusionsmethoden
- Ausblick: Bestimmung von Gewichtungsfaktoren, Optimierung der Filterung der Beschleunigungssensordaten, Bestätigung der Ergebnisse durch Auswertung weiterer Testdaten

Vielen Dank für Ihre Aufmerksamkeit.

From data-driven NDT of systems to BIG DATA-based modeling

Dirk Söffker
www.srs.uni-due.de

(based on common work with
Dr. Dorra Baccar, Prof. Dr. Nejra Beganovic, Rosmawati Jihin, Sandra Rothe,
Dr. Mahmud-Sami Saadawia, Dr. Chunsheng Wei, Sebastian Wirtz)

UNIVERSITÄT DUISBURG ESSEN

Chair of Dynamics and Control (SRS)
University of Duisburg-Essen

SRS

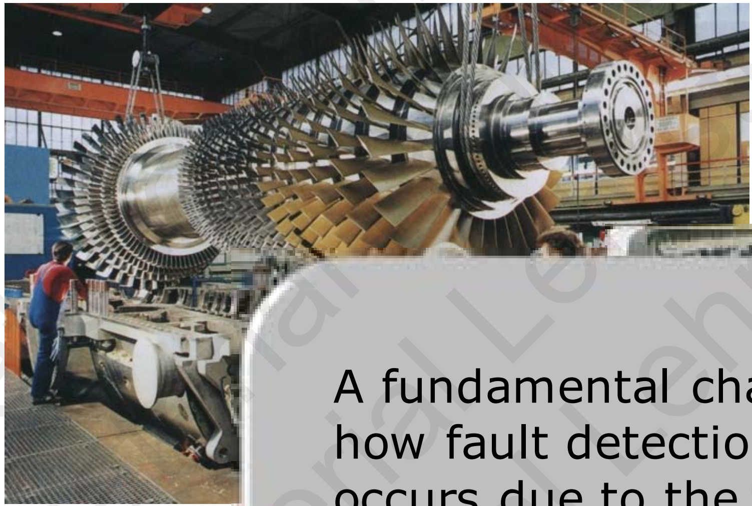

(Siemens, KWU)

A fundamental change in understanding
how fault detection and fault diagnosis is realized,
occurs due to the use of modern information science-based approaches.
Relevant terms are changing, methods are changing:

> Vibration Monitoring
  > Fault Detection and Isolation
    > Structural Health Monitoring (SHM), Prognostic …. (PHM)
      > BIG DATA
        > ?

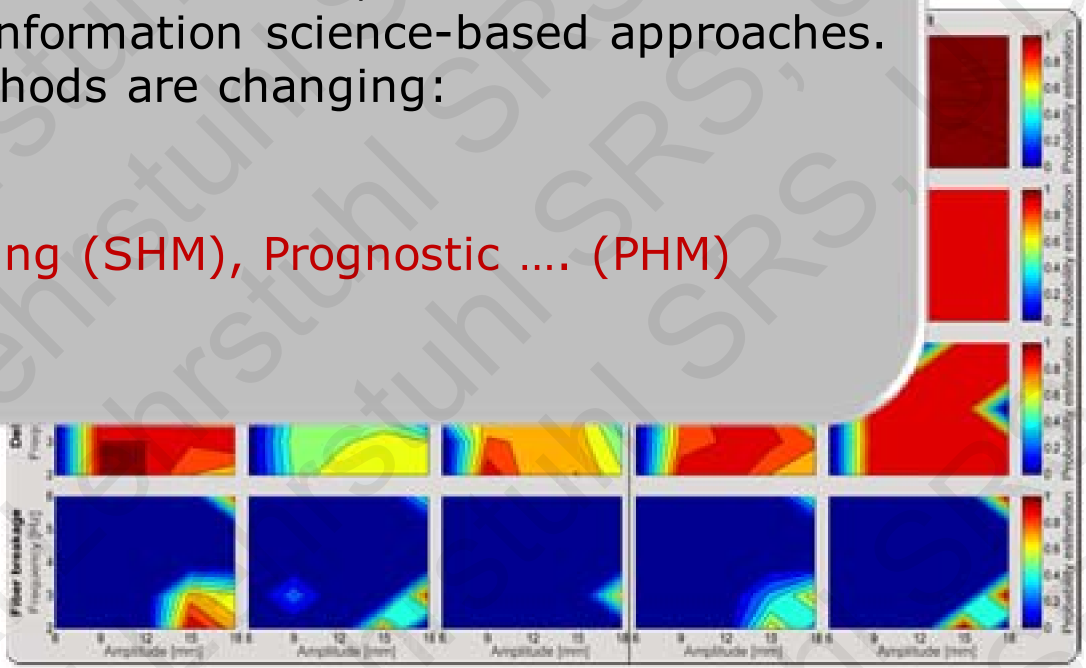

Motivation II

Reality

- Supervision and monitoring of systems are becoming more and more popular.
- Related approaches should use existing information and sensor data.
- Information and knowledge can be established
  using this kind of extensive data usage (> modeling, BIG DATA-based …)

Ideas and goals of this presentation

- Demonstrate the change from signal- to model-based to data-driven approaches
- Illustrate the effect of suitable sensor filtering in combination with data-driven approaches
- Introduce to AI/Machine learning approaches (ideas)
- Show how this can be realized (realized by SRS)
- Illustrate the change vom 1st-order principle thinking and modeling
  to data-driven approaches

➔ Here: focus to existing research results of the Chair of Dynamics and Control, U DuE

Outline

- Motivation
- I How FDI (NDT for vibrational systems) was realized years ago: crack detection
  - From the modeling of errors, faults, changes, and effects to
  - the analysis of effects (Fault detection and isolation)
  - Signal- and model-based FDI
  - Example: crack detection of rotors (198x-199x)
- II Looking for unique features: using AE leading to data-driven FDI (SHM) today
  - How to understand complex behaviors/changes?
  - How to use and how to find unique characteristics?
  - Example 1: Wear analysis and damage distinction (metal)
  - Example 2: Damage distinction (CFRP)
- III Using AI/Machine learning
  - Principles and how they can be used?
  - Example: Remaining useful lifetime calculation using trained/optimized state machine model
- IV Next step: BIG DATA-based modeling and analysis
  - What are the changes and the key tools in this ‚new world'?
  - What is possible, what can be obtained, what do we lose?
- Summary and outlook

I How FDI (NDT applied to vibrational systems) was realized years ago?

Diagnosis to realize safe operation and perfect functionality

Detecting faults like

- contacts
- **cracks**
- **delamination**
- unbalance
- ...

Problem solution I
Estimation of unknown inputs
(using observers etc.)

Problem solution II
Analyzing the output
(using trained filters)

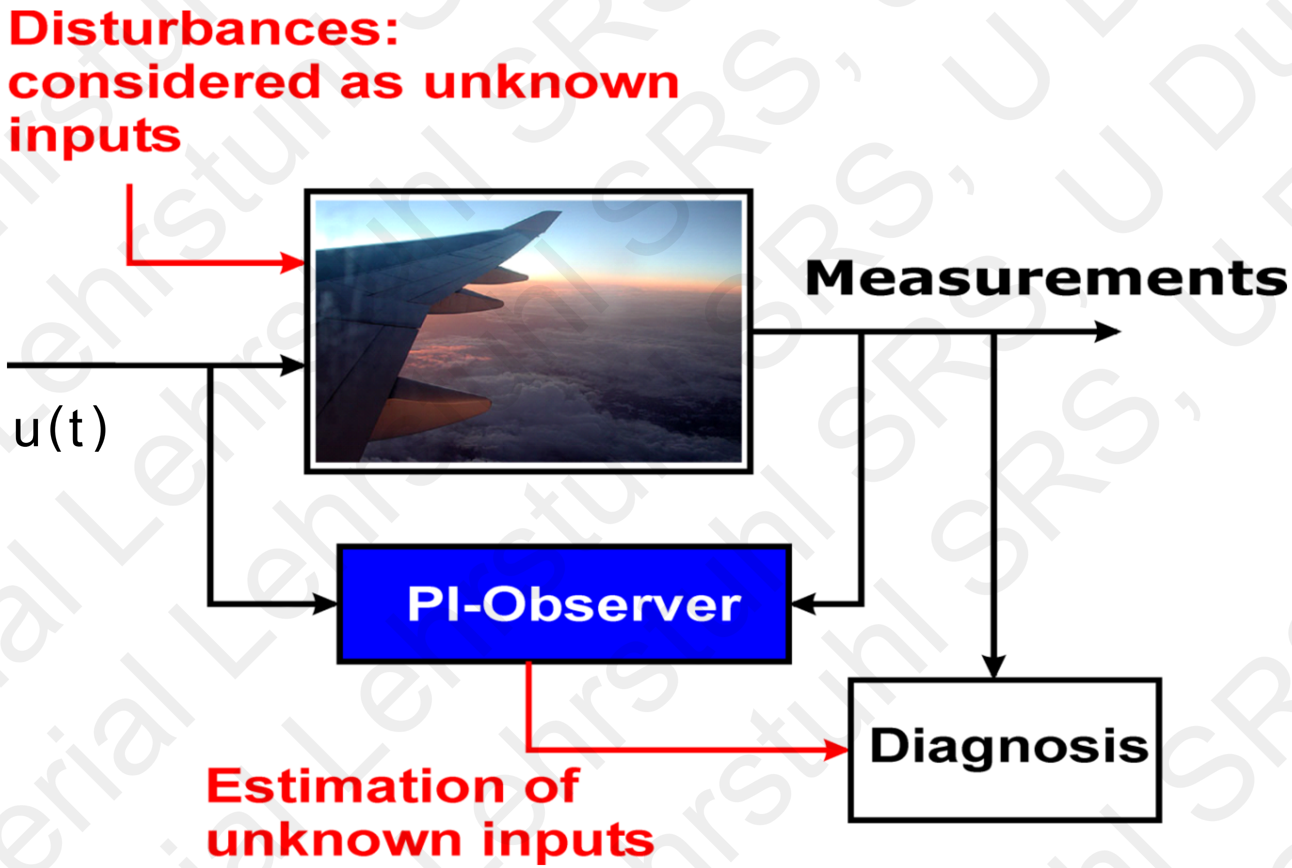

System parameters
Length: 4.2 m
Radius: 0.14 m
Damping: 9e3 Ns/m
Stiffness: 3e7 N/m

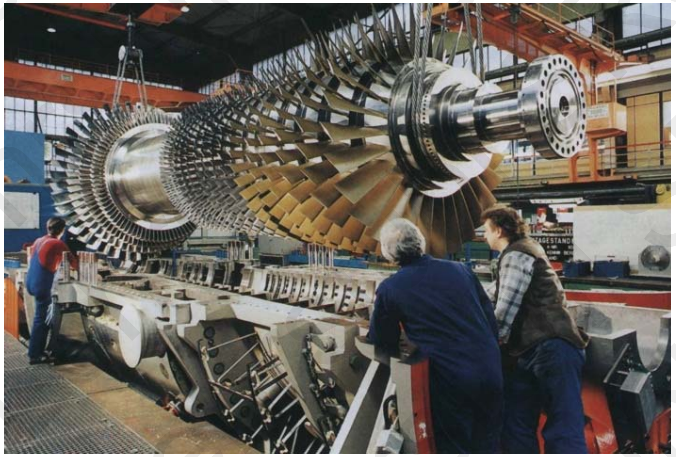
(Siemens, KWU)

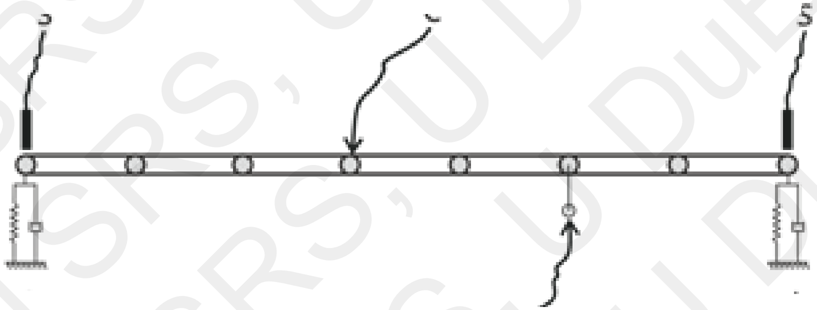

State-space model

$$\dot{x} = Ax + Bu$$
$$y = Cx$$

$$A = \begin{bmatrix} 0 & I \\ -M^{-1}K & -M^{-1}(D+\Omega G) \end{bmatrix} \qquad B = \begin{bmatrix} 0 \\ M^{-1}F \end{bmatrix}$$

$$C = \begin{bmatrix} C & 0 \end{bmatrix}, \quad \text{and} \qquad y = y$$

A: System matrix
C: Output matrix
u: Input vector
M: Mass matrix
K: Stiffness matrix

B: Input matrix
x: State vector
y: Output vector
D: Damping matrix
G: Gyroscopic matrix

➔ State-space model (based on FE approach) be used as **analytical reference**

I Modeling of the considered rotor system: mode shapes

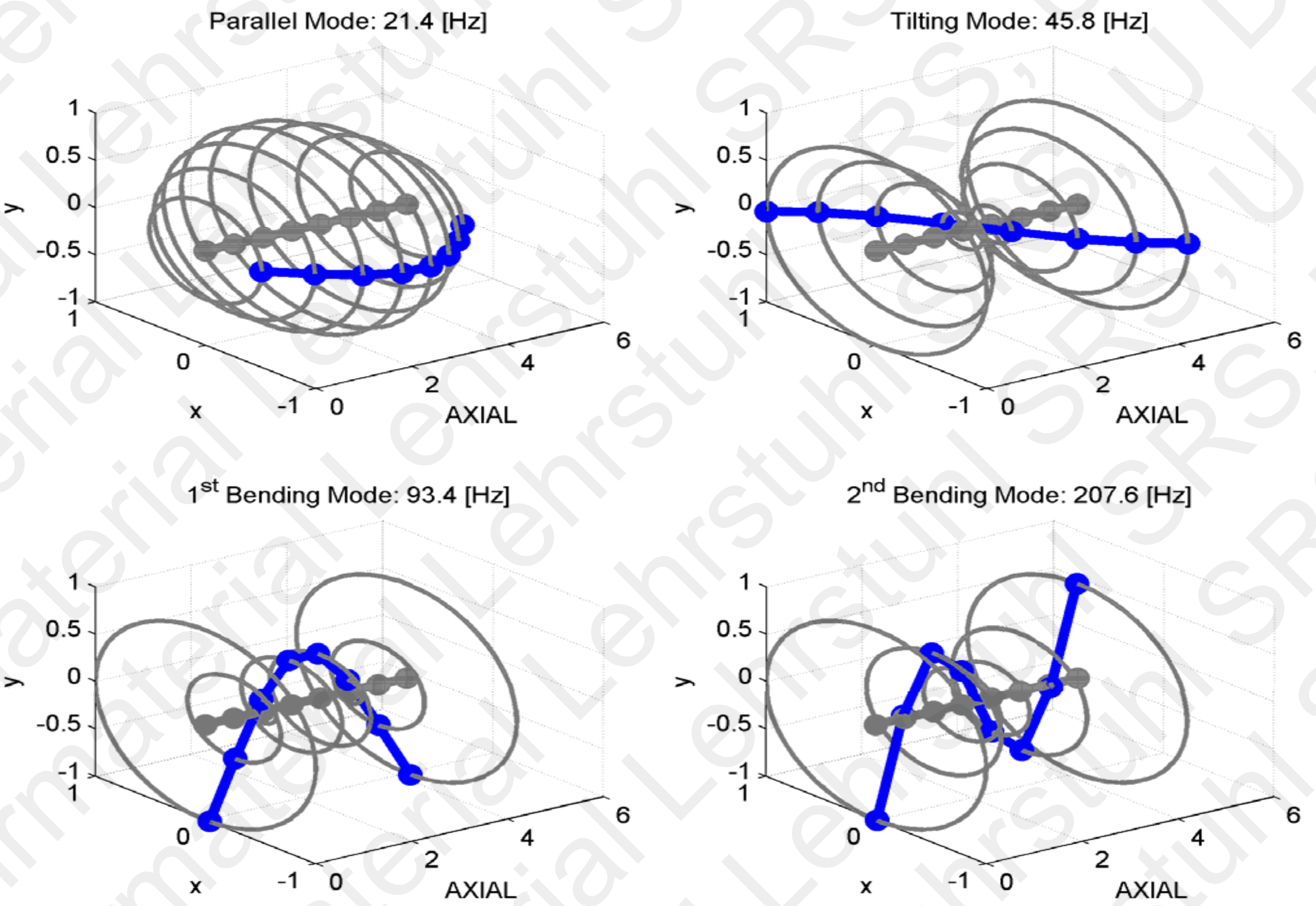

➔ The first four (forward) bending modes are illustated. (Ass.: Rotation speed: 9000 rpm)

I Modeling of the considered fault: crack modeling

Crack model (Gasch, 1976)

$$\begin{bmatrix}\xi\\ \eta\end{bmatrix} = \begin{bmatrix} h+h_\mathrm{a} & 0\\ 0 & h\end{bmatrix}\begin{bmatrix}F_\xi\\ F_\eta\end{bmatrix}$$

$$h_\mathrm{r} = \frac{h_\mathrm{a}}{h}$$

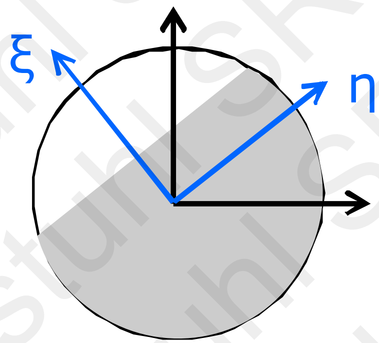

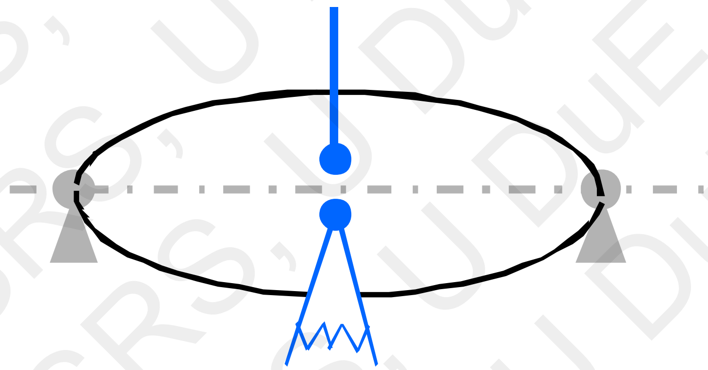

ξ : Deflection in crack direction
F_ξ : Force in crack direction
h : Compliance
h_a : Addtional compliance
h_r : Relative crack compliance

➔ Open crack leads to an increasing compliance in crack direction.
Result 1: Nonlinear dynamical behavior results even in case of linear base systems
Result 2: Linear reference models may not be suitable

Complex behavior of the considered rotor system

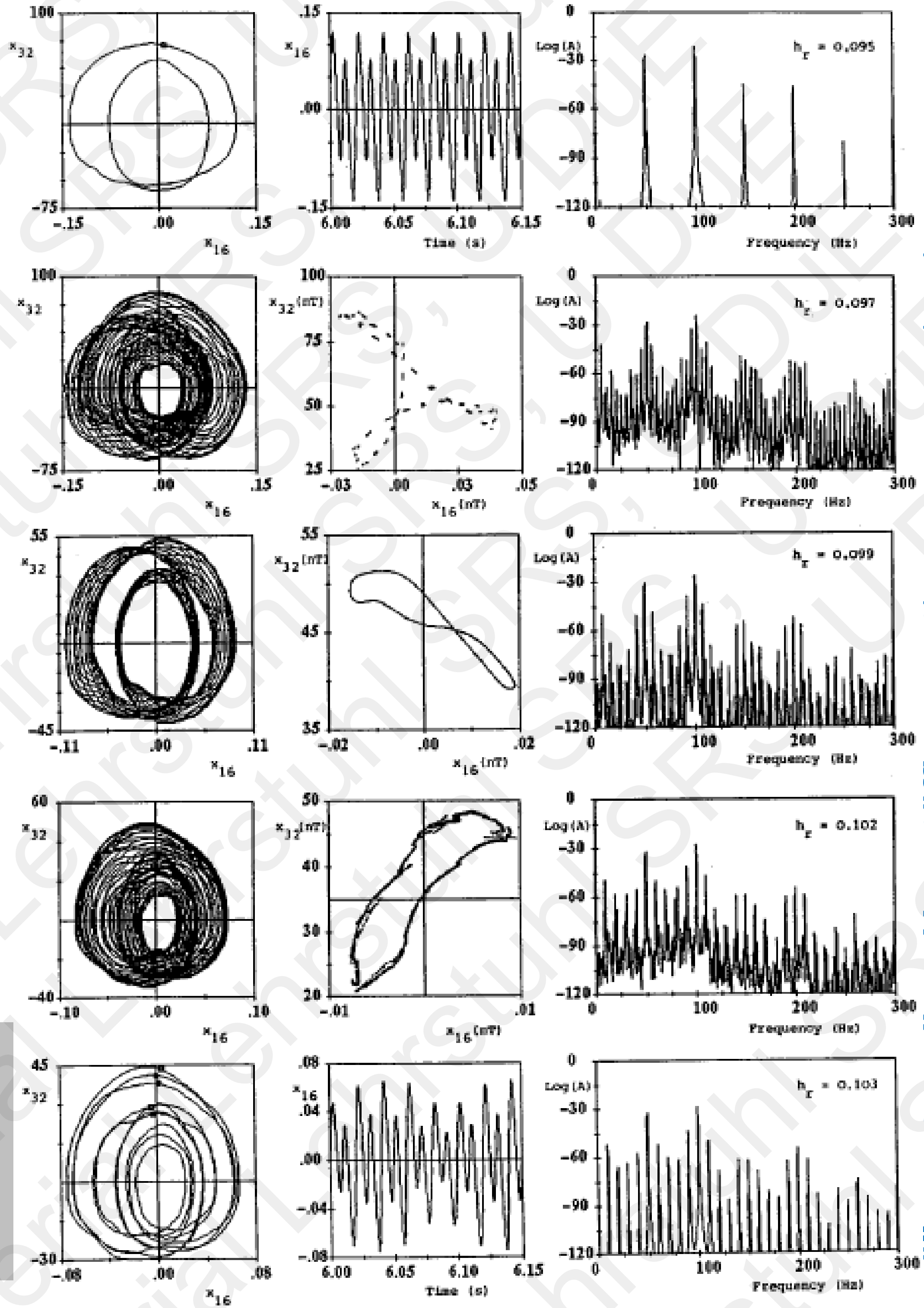

➔ Crack may also lead to complex vibrational behavior depending on crack depth and damping

➔ Difficulties to distinguish and to allocate effects

Müller, P.C.; Bajkowski, J.; Söffker, D.: *Chaotic Motions and Fault Detection in a Cracked Rotor*. Nonlinear Dynamics, Vol. 5, Issue 2, 1994, pp. 233-254.

I Model-based method: PI-Observer*

$$\mathrm{n} \approx \mathrm{Hv}$$
$$\dot{\mathrm{v}} = \mathrm{Fv} + \mathrm{Gu}$$
$$\mathrm{G} = 0, \qquad \mathrm{F} = \begin{bmatrix} 0 & 0 & 1 & 0 \\ 0 & 0 & 0 & 1 \\ -\omega^2 & 0 & 0 & 0 \\ 0 & -\omega^2 & 0 & 0 \end{bmatrix}$$

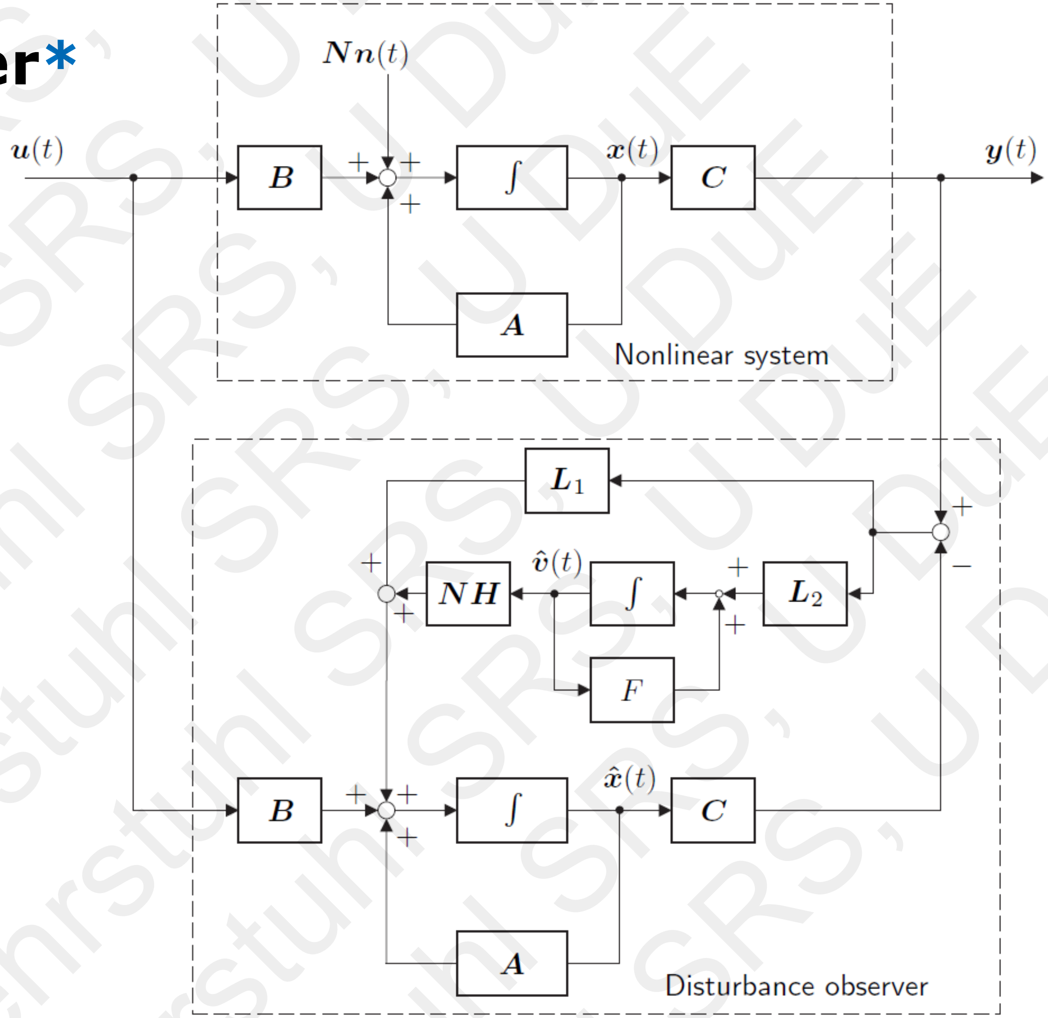

Modeling rotor system with crack

$$\begin{bmatrix} \dot{\mathrm{x}} \\ \dot{\mathrm{v}} \end{bmatrix} = \begin{bmatrix} \mathrm{A} & \mathrm{NH} \\ 0 & \mathrm{F} \end{bmatrix} \begin{bmatrix} \mathrm{x} \\ \mathrm{v} \end{bmatrix} + \begin{bmatrix} \mathrm{B} \\ 0 \end{bmatrix} \mathrm{u}$$
$$\mathrm{y} = \begin{bmatrix} \mathrm{C} & 0 \end{bmatrix} \begin{bmatrix} \mathrm{x} \\ \mathrm{v} \end{bmatrix}$$

Observer

$$\begin{bmatrix} \dot{\hat{\mathrm{x}}} \\ \dot{\hat{\mathrm{v}}} \end{bmatrix} = \begin{bmatrix} \mathrm{A} - \mathrm{L}_1\mathrm{C} & \mathrm{NH} \\ -\mathrm{L}_2\mathrm{C} & \mathrm{F} \end{bmatrix} \begin{bmatrix} \hat{\mathrm{x}} \\ \hat{\mathrm{v}} \end{bmatrix} + \begin{bmatrix} \mathrm{B} \\ 0 \end{bmatrix} \mathrm{u} + \begin{bmatrix} \mathrm{L}_1 \\ \mathrm{L}_2 \end{bmatrix} \mathrm{y}$$

* Söffker, D; Yu, Tie-Jun; Müller, P.C.: *State Estimation of Dynamical Systems with Nonlinearities by using Proportional-Integral Observer.* International Journal of System Science, Vol. 26 (1995), No. 9, pp. 1

➔ Result: the model-based approach allows to estimate the dynamical behavior of crack-equivalent forces and unmeasurable displacements.

Classification system based on two main modules

- Feature extraction module:
  Extraction of reliable features using DWT/RMS
- Classification module:
  Classification of the extracted features using SVM

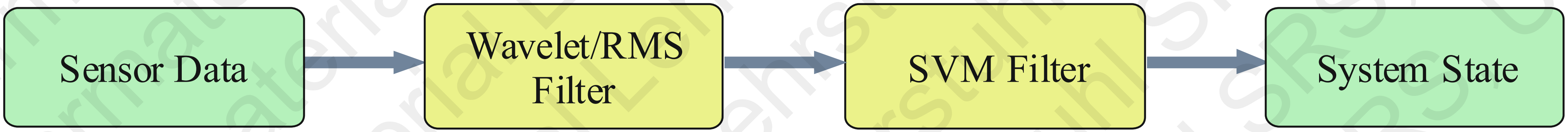

Discrete Wavelet Transform (DWT)

- Comparison of the signals with scaled and shifted mother wavelets
- Use of two complementary wavelet filters to decompose the signal into A. and D. components
- Multiple successive level decomposition is applied to realize a wavelet decomposition tree
- Denoising is realized by selective consideration of components

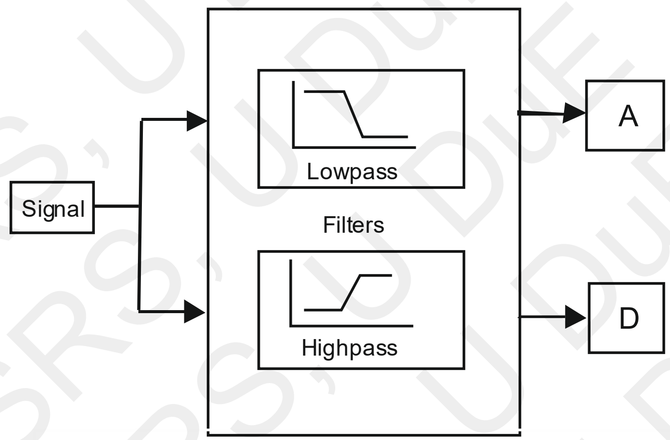

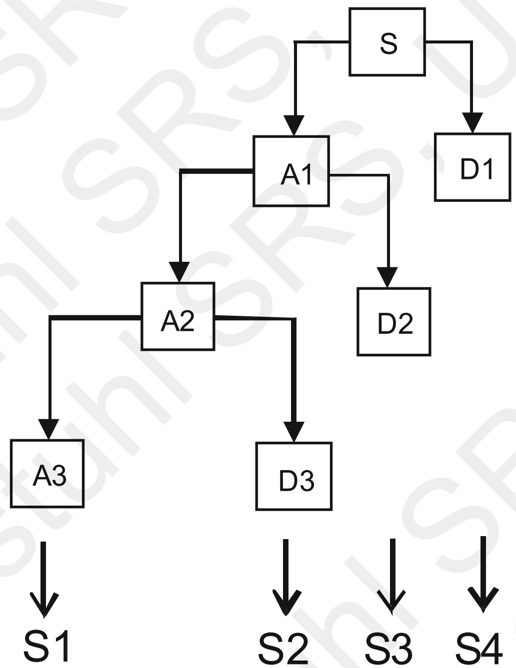

I Learning and classification using Support Vector Machine (SVM)

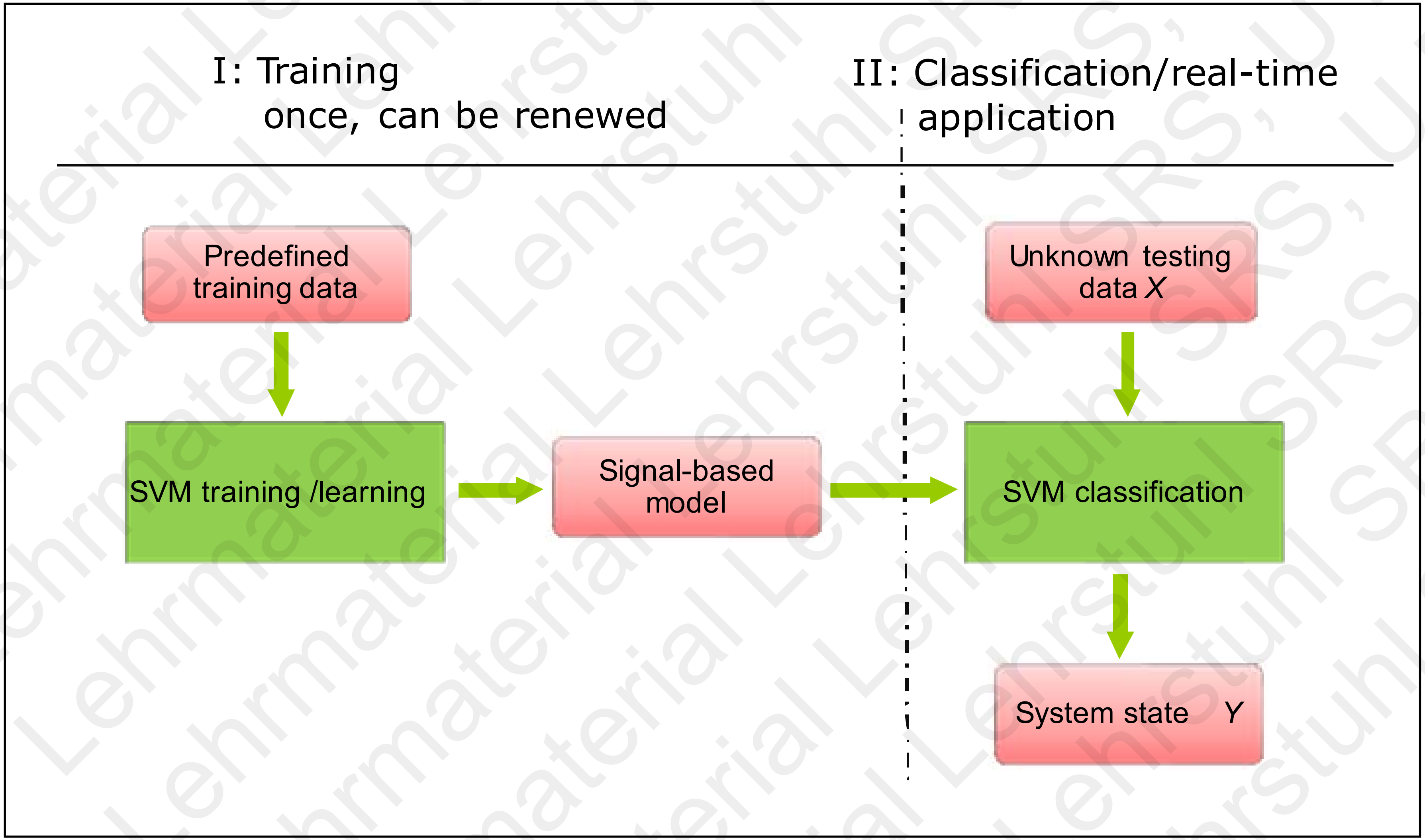

I Results*: model-based approach I

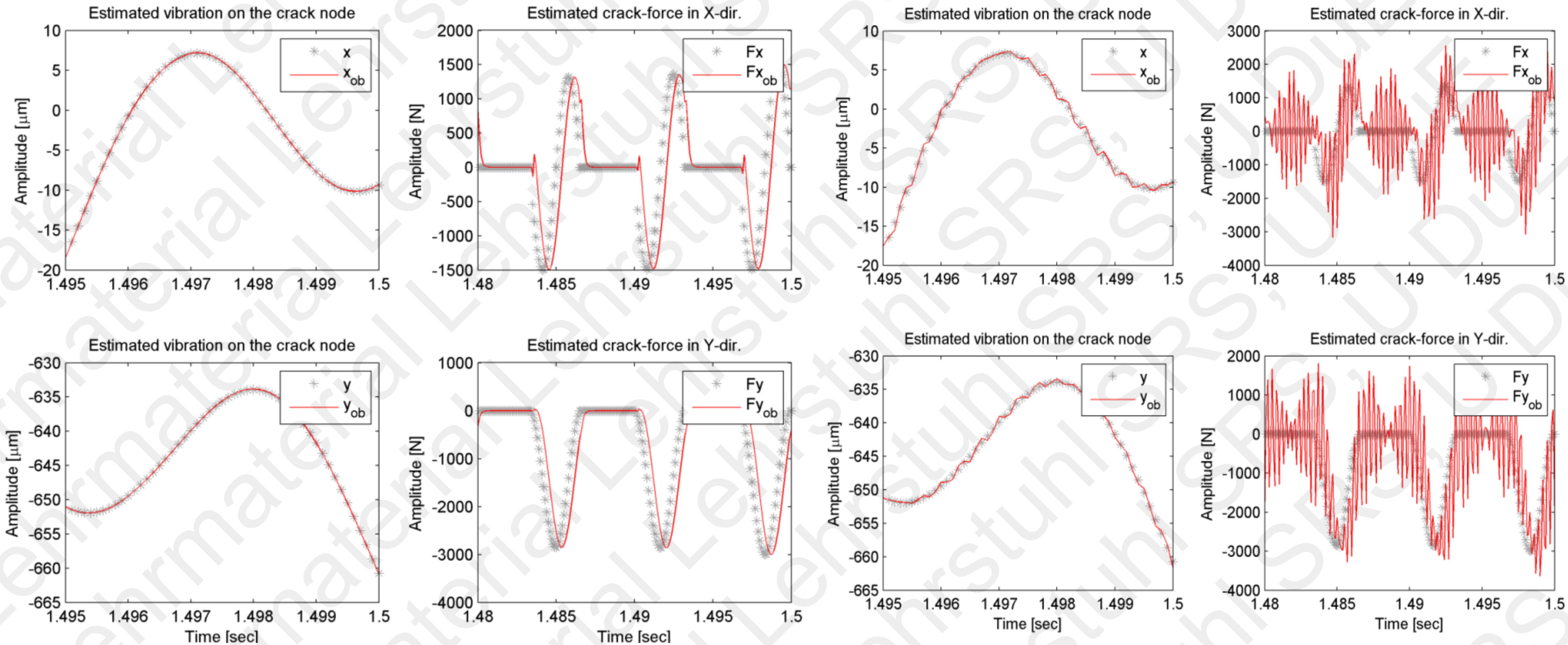

* Söffker, D.; Wei, C.; Wolff, S., Saadawia, M.S.: *Detection of Rotor Cracks: Comparison of an old Model- with a new Signal-based approach*. Nonlinear Dynamics, Vol. 83, 2016, pp. 1153-1170.

➔ Displacement and crack force estimations are perfect in noise-free cases.

➔ The quality of the result depends on the signal (and the model).

I Results*: model-based approach II

Variation of damping

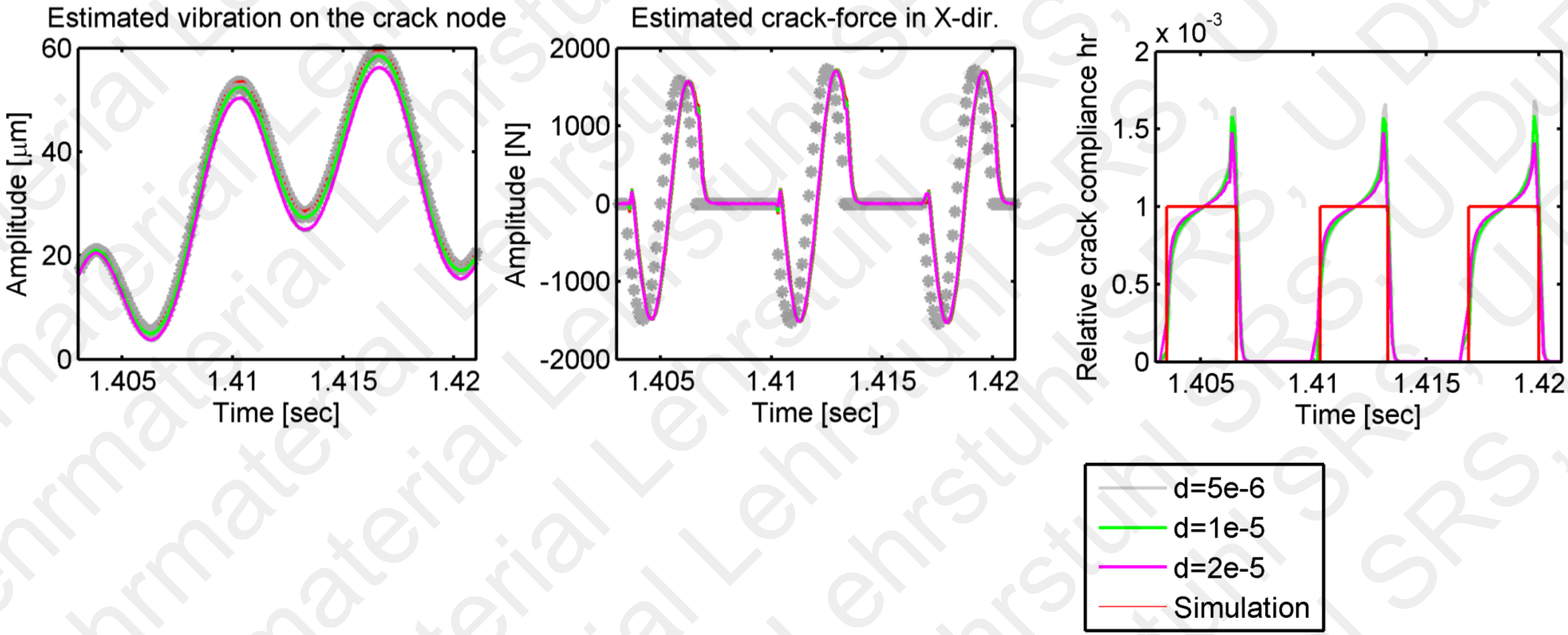

* Söffker, D.; Wei, C.; Wolff, S., Saadawia, M.S.: *Detection of Rotor Cracks: Comparison of an old Model- with a new Signal-based approach*. Nonlinear Dynamics, Vol. 83, 2016, pp. 1153-1170.

➔ No noticeable influence on the estimated displacements and crack force

➔ Detectable effect on the reconstructed compliance hr

I Results*: feature-based approach

Binary SVM classification

- Binary training data
- Position and distance from the separating hyperplane can be used
- Easy to use for prediction of remaining life time

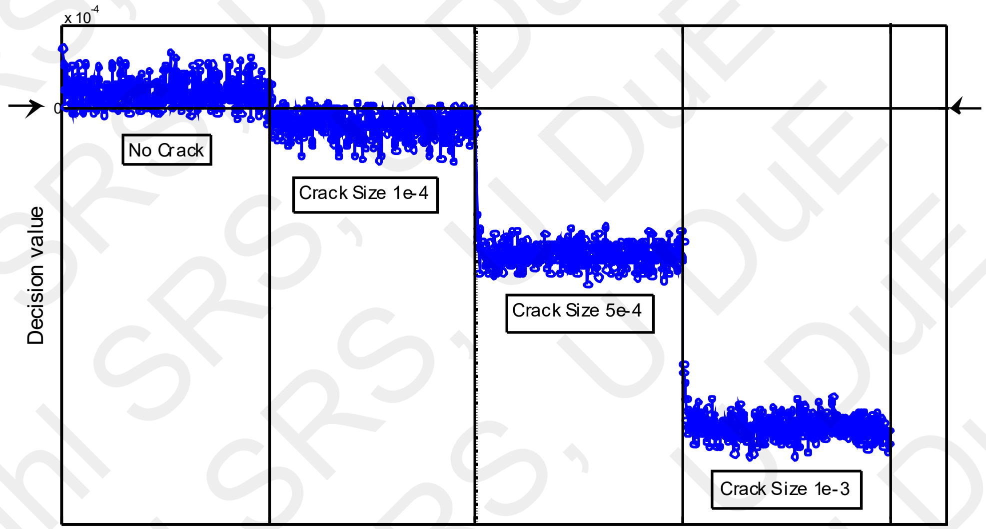

Multiclass SVM classification

- Grouped training data
- Flexible scaling of cracks possible
- Larger implementation effort

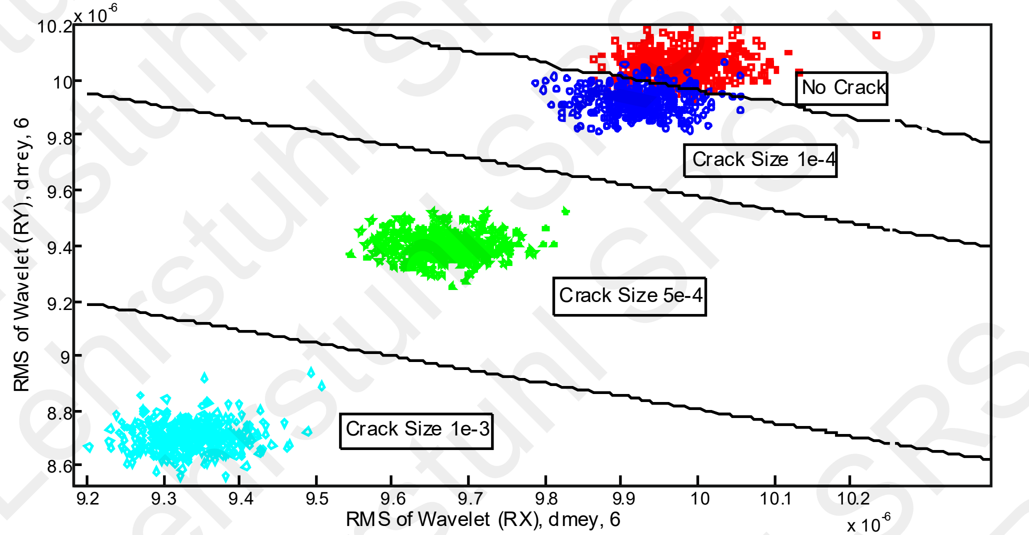

* Söffker, D.; Wei, C.; Wolff, S., Saadawia, M.S.: *Detection of Rotor Cracks: Comparison of an old Model- with a new Signal-based approach*. Nonlinear Dynamics, Vol. 83, 2016, pp. 1153-1170.

II Complex analysis: wear analysis and evolution I

Research goals
- Signal-based classification of wear states
- Signal-based/data-driven lifetime estimation
- How to find suitable features?

- Advantages: - Ability to use systems/components up to the end of lifetime
  - Advanced production reliability due to known remaining lifetime
  - Equipment/spare parts management in context Industry 4.0

- Main wear effects induced by insufficient lubrication
  - Metal-on-metal contact
  - Welding
  - Cracks close to surface
  - Particles
  - Surface fatigue

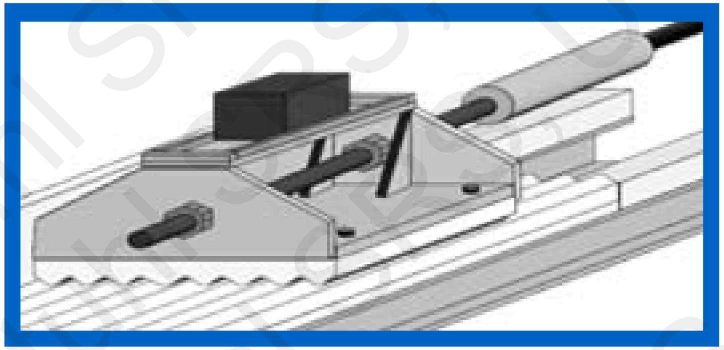

Tribological system

→ Material removal causes Acoustic Emission (AE) and additional friction.
→ Idea I: Acoustic emision can be used as wear indicator.
→ Idea II: Changing frictional behavior used as wear indicator.

Test rig

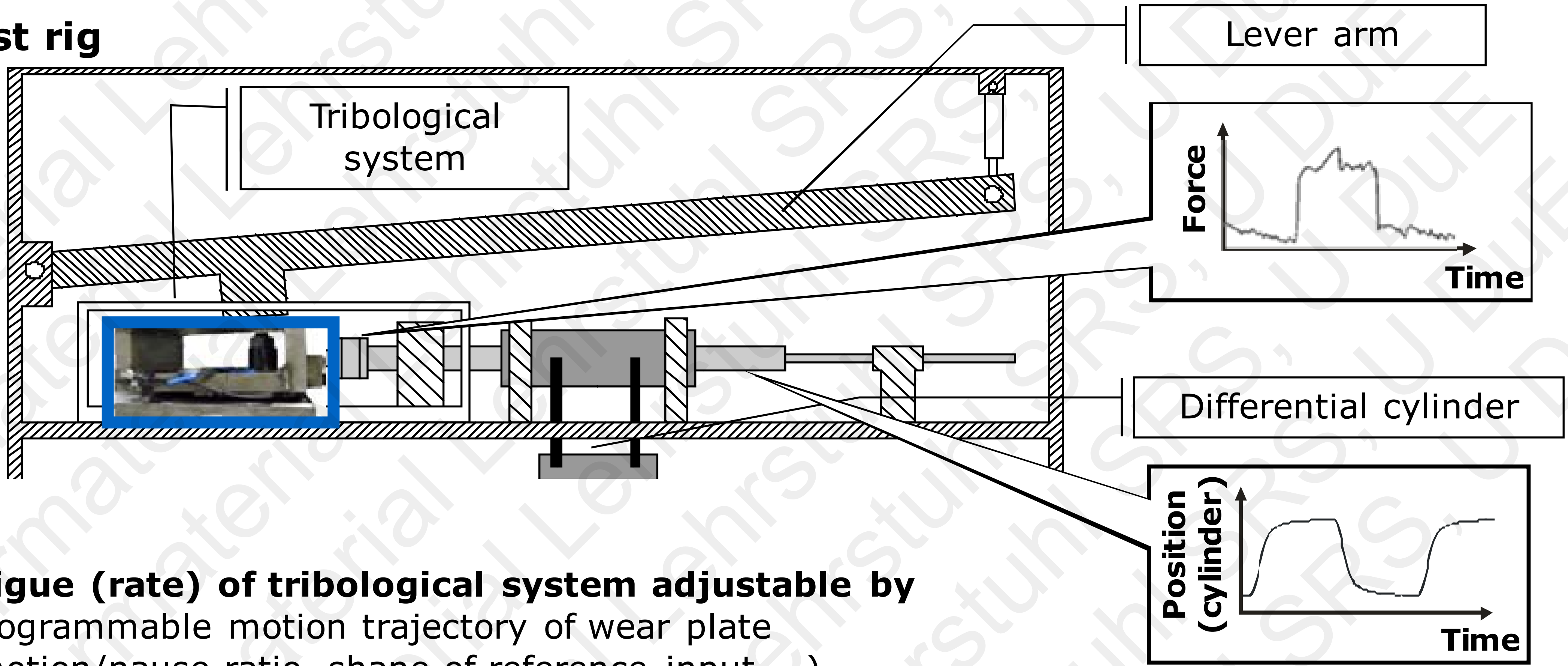

Fatigue (rate) of tribological system adjustable by

- Programmable motion trajectory of wear plate (motion/pause ratio, shape of reference input, …)
- Variable normal force (by lever arm)
- Variable lubrication (not depicted)

II Complex analysis: wear analysis and evolution III

Wear plates after a 20-days endurance test

Surface destruction

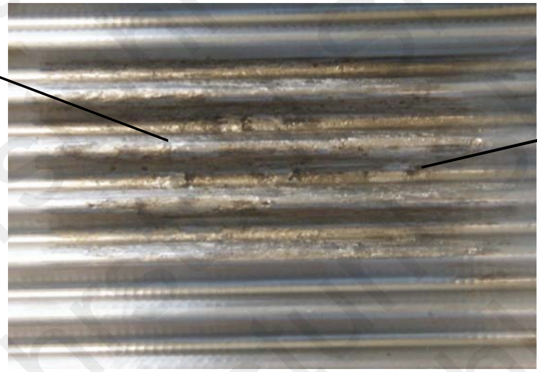

Pittings

Abrasion scratches

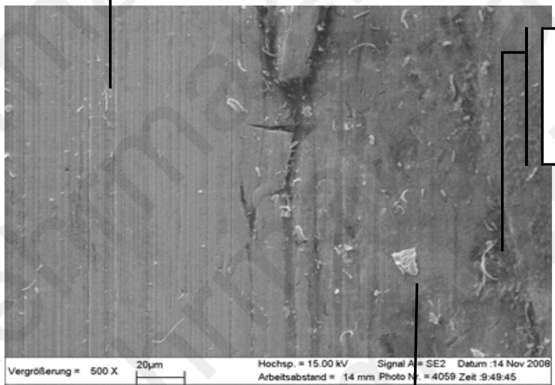

Surface fatigue

Wear debris

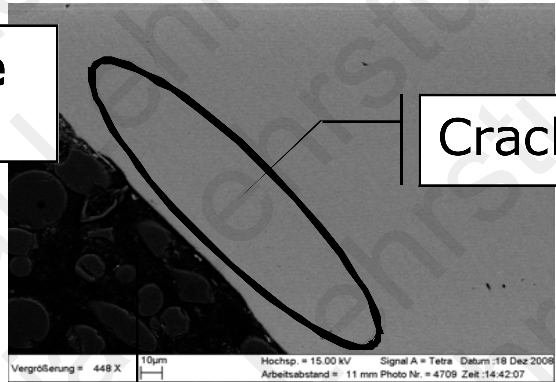

Cracks

Steel pittings

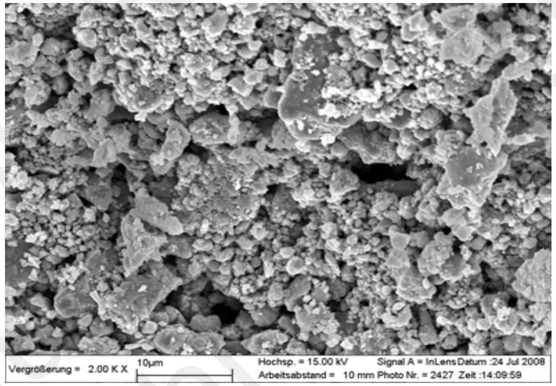

Particles (SEM)

→ Surface fatigue is the main wear mechanism. Additionally abrasion is detected.

Signal processing chain

FPGA-based filtering and analyzing of AE signals

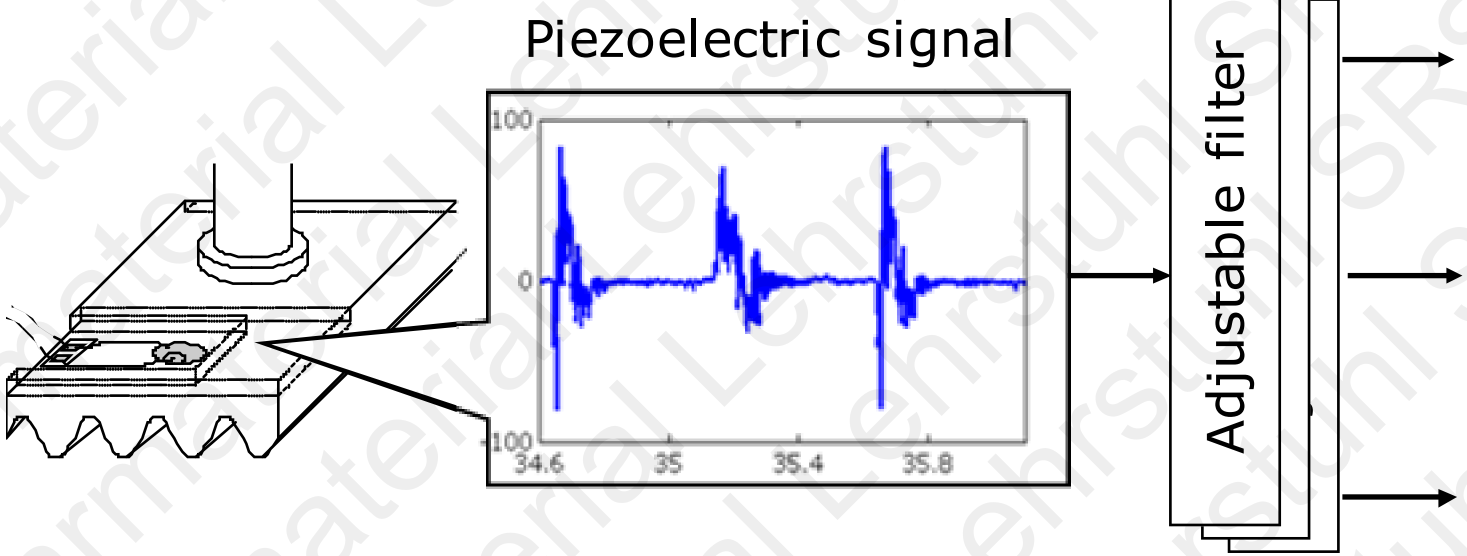

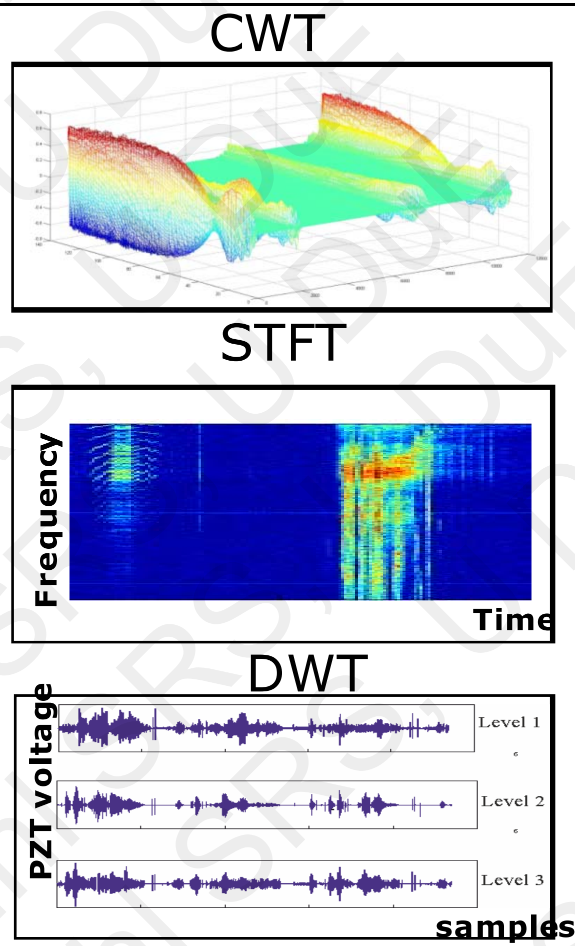

STFT, DWT, and CWT are realized to extract relevant features related to damage.

➔ Strong correlation with typical, time-dependent process information (position, velocity, etc.)
➔ Revealing a connection between material changes (e. g. crack growth) and system damage (probability of failure)

II Experimental results I

AE energy distribution and derived AE accumulation over system usage

- Summation of deterioration-equivalent AE energy: damage accumulation hypothesis to obtain the deterioration-proportional information
- Progression of deterioration-proportional information (accumulated AE energy): indicator of deterioration level

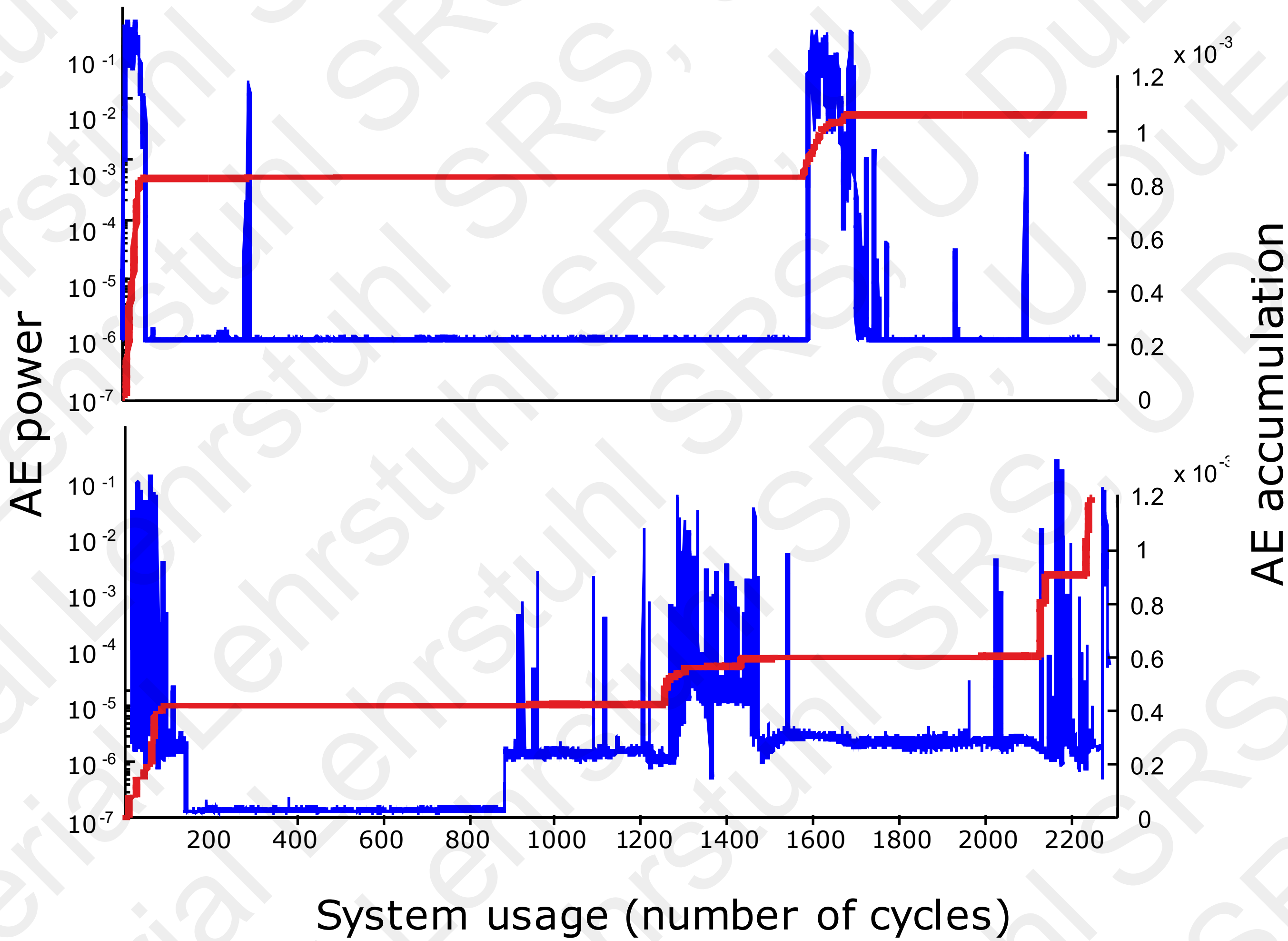

II Experimental results II

Frequency examinations of AE signal

- Distinction between the three major phases of system failure
- Identification of
  - typical patterns
  - transient wear events
  - wear inherent frequencies
- Conclusion from recorded AE signal to state-of-wear

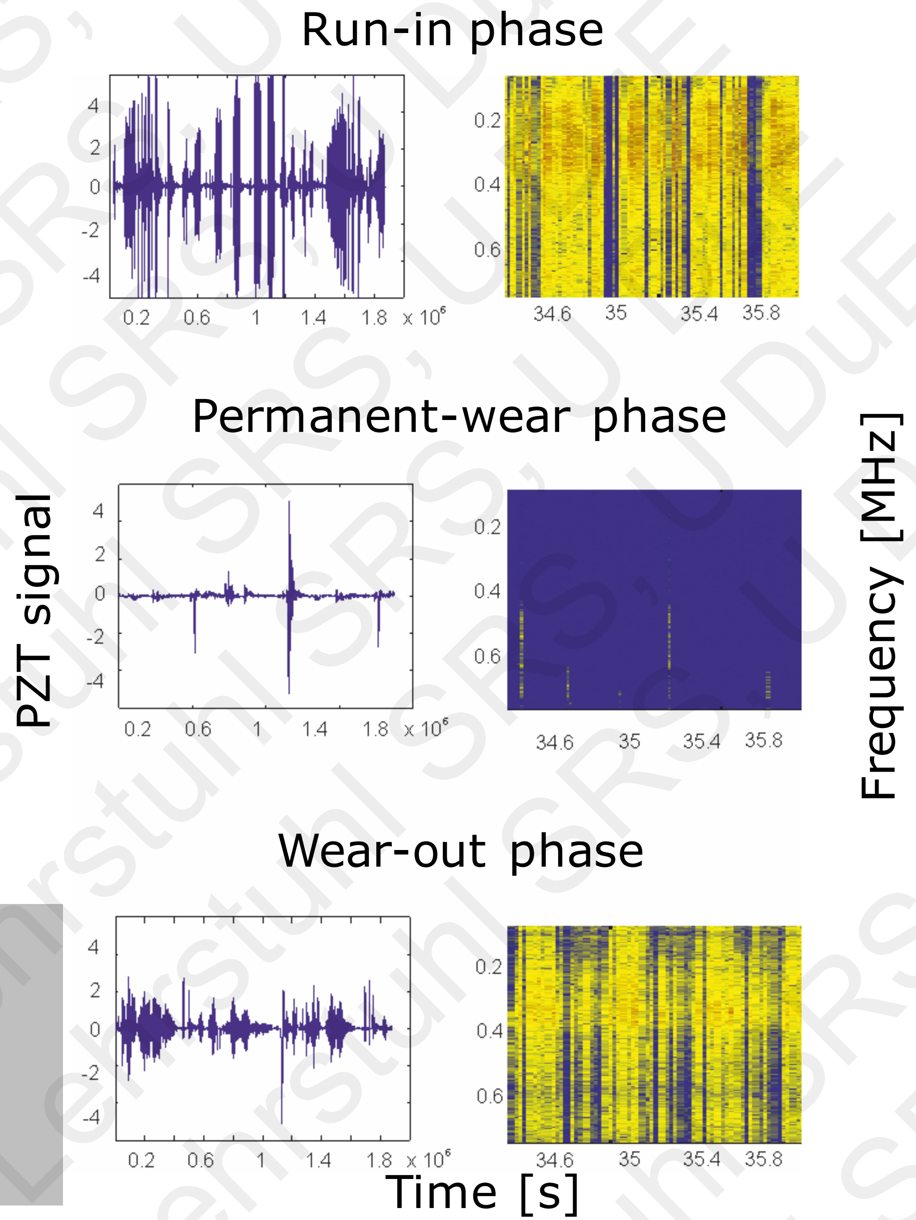

→ The STFT-transformed AE signals during run-in and wear-out phase look similiar.

→ The STFT is not efficient to establish differences between the states. Alternative choice: CWT/DWT

II Experimental results* III

Generation of unique features:
Frequency examinations of AE signal

- Distinction between the three major phases of system operation
- Identification of
  - transient wear events
  - typical patterns

CWT of AE signal

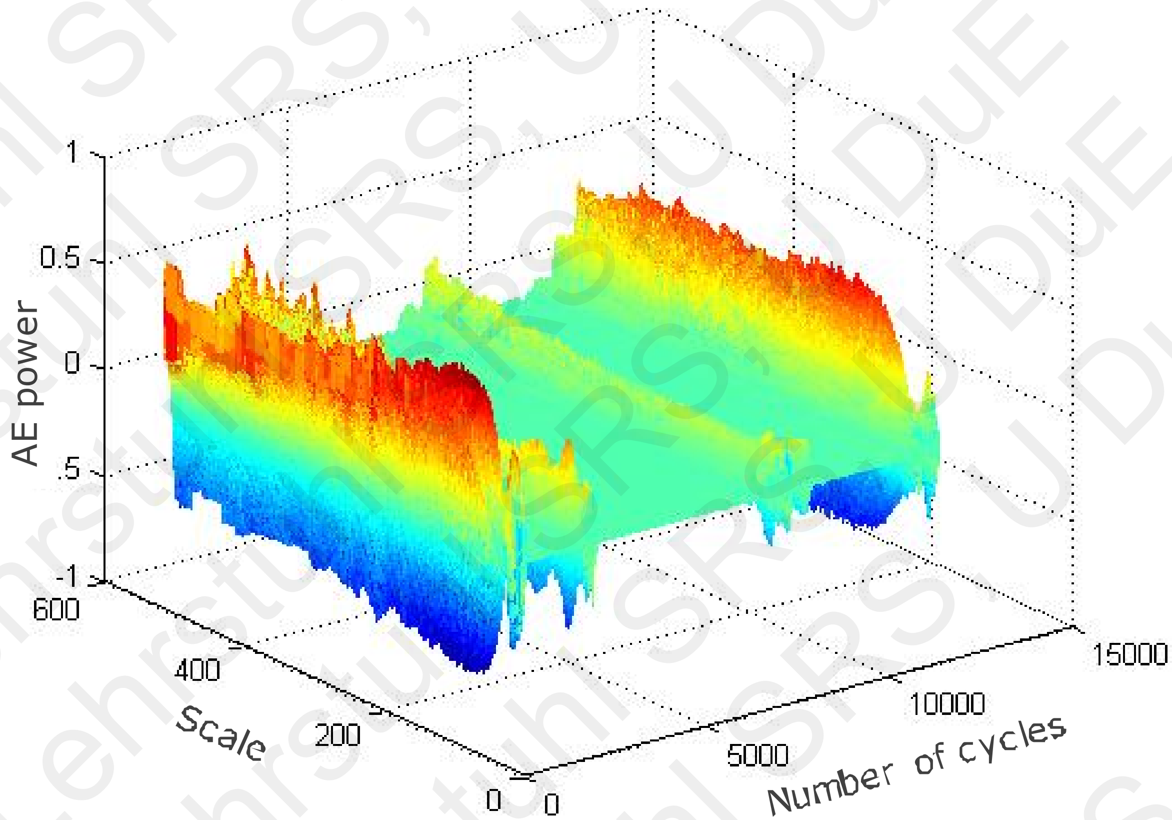

* Baccar, D.; Söffker, D.: *Wear Detection by Means of Wavelet-based Acoustic Emission Analysis*. Mechanical Systems and Signal Processing, Vol. 60-61, August, 2015, pp. 198-207.

➔ Main goal: define unique features connecting recorded AE signals to state-of-wear

II Experimental results IV

CWT coefficients corresponding to frequency range [100kHz , 200kHz]

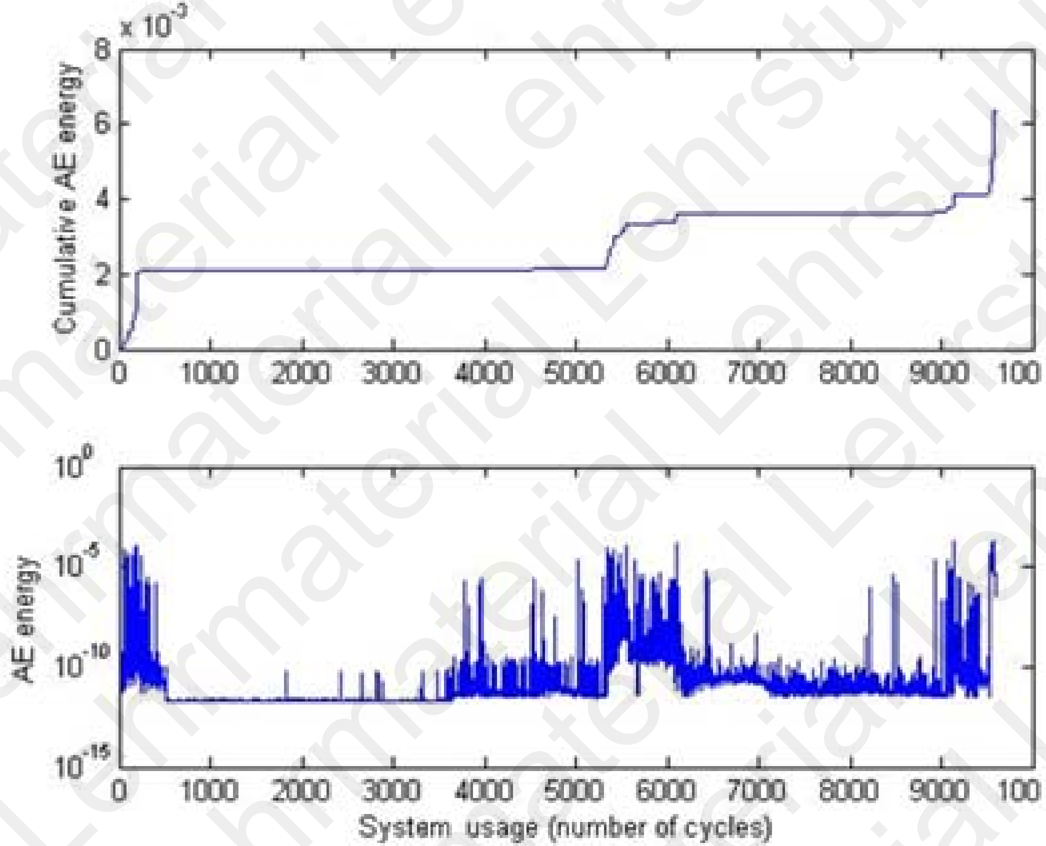

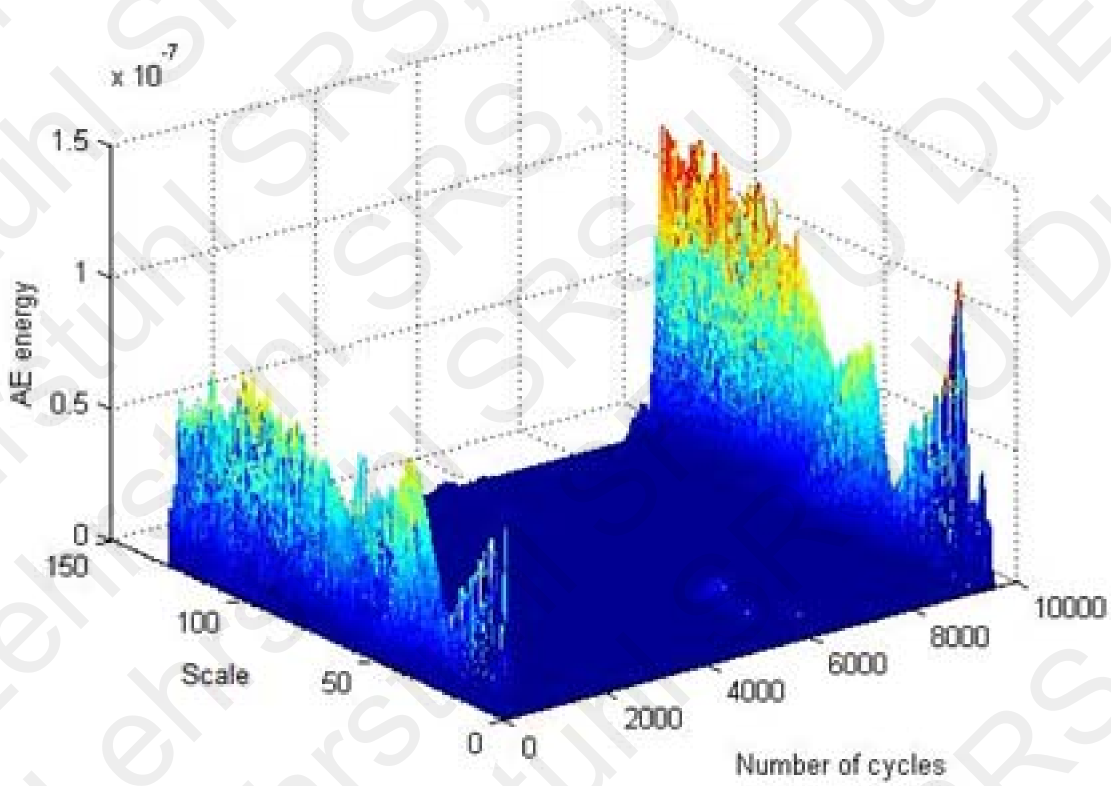

→ Frequency components appear in run-in and wear-out phases.
→ Higher energy content in wear-out phase

II Experimental results V

CWT coefficients corresponding to frequency range [200kHz , 300kHz]

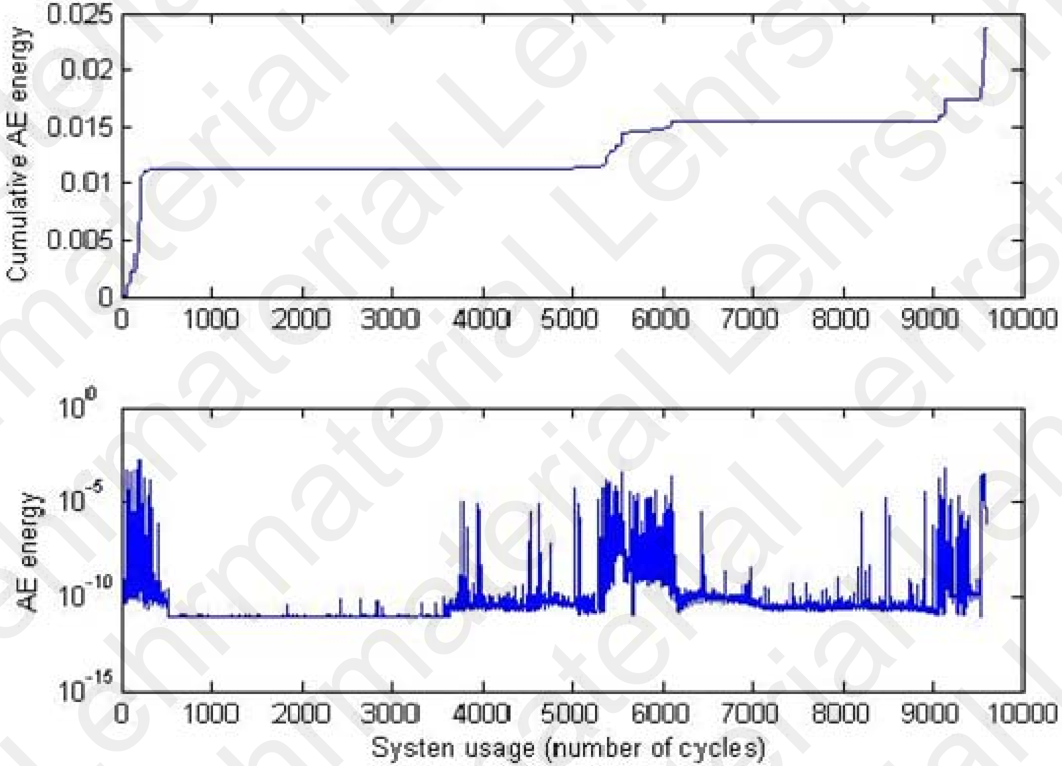

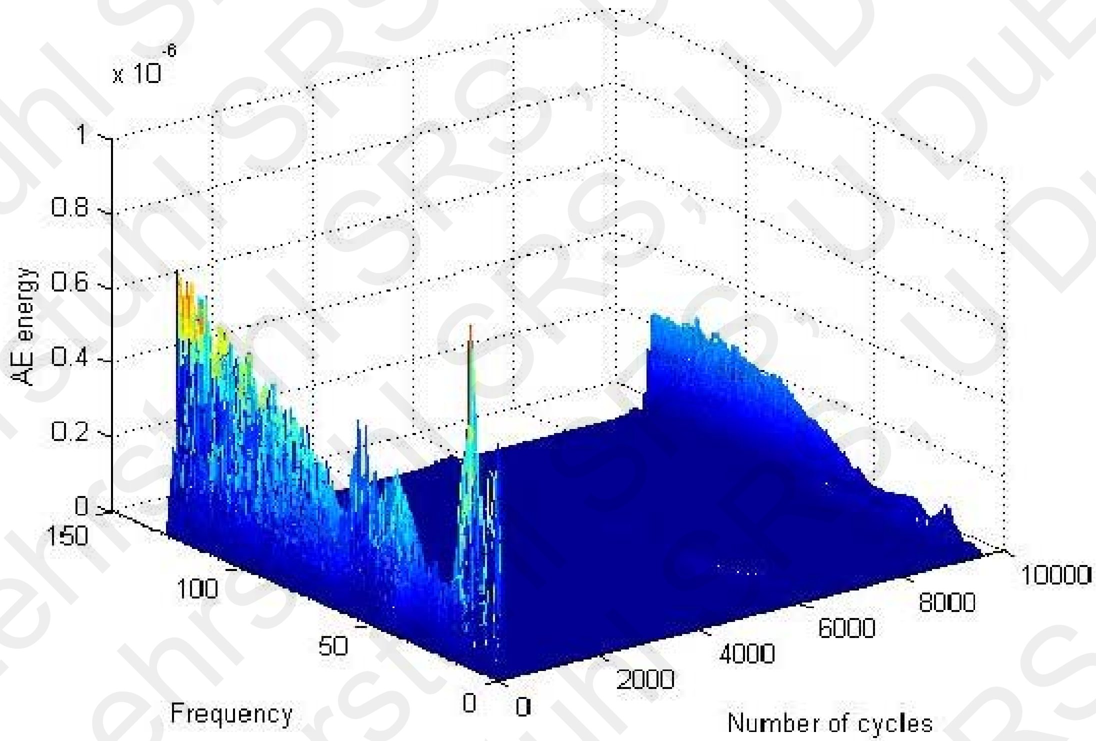

→ Frequency components appear in run-in and wear-out phases.
→ Higher energy content in run-in phase

II Experimental results VI

CWT coefficients corresponding to frequency range [800kHz , 900kHz]

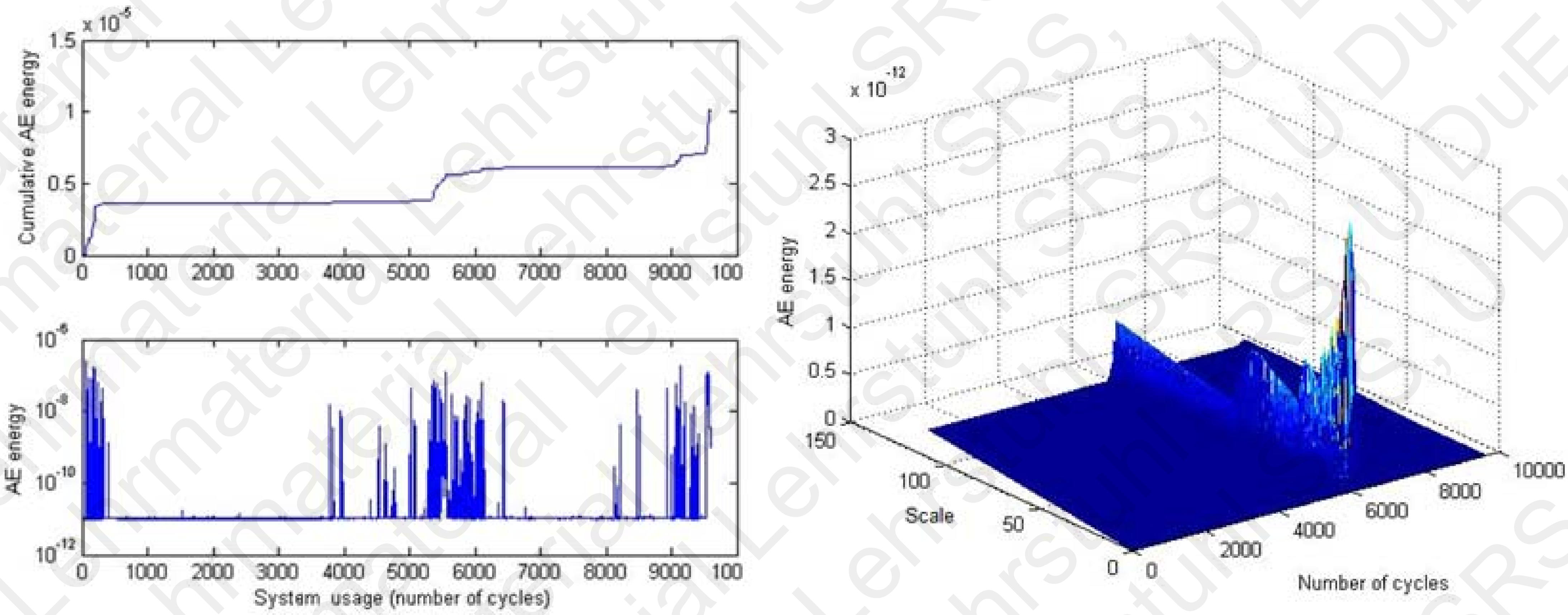

→ Frequency components appear only at the end of permanent phase.
→ Very low energy content

II Experimental results* VII

Differences between maximum amplitude and minimum amplitude of the frequency components in the different process phases

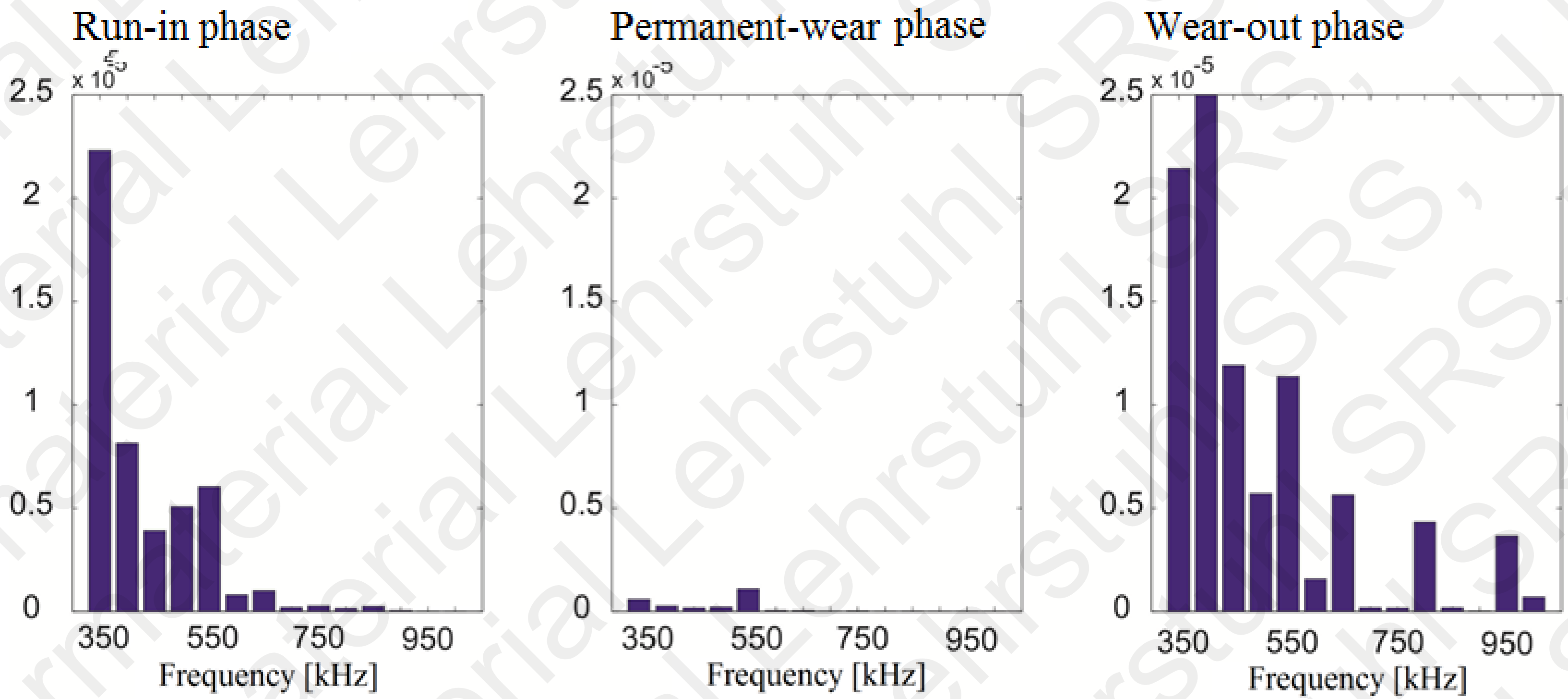

* Baccar, D.; Söffker, D.: *Wear Detection by Means of Wavelet-based Acoustic Emission Analysis.* Mechanical Systems and Signal Processing, Vol. 60-61, August, 2015, pp. 198-207.

➔ Run-in phase: Frequencies from 300 kHz up to 600/700 kHz
➔ Permanent-wear phase: Components about 550 kHz dominate
➔ Wear-out phase: Frequencies close to 1 MHz are observed.

II Diagnosis-oriented filtering using other data*

Use of hydraulic pressure signals effected by friction change

Hydraulic pressure

Generation of characteristic value

Accumulated damage increments (AS)

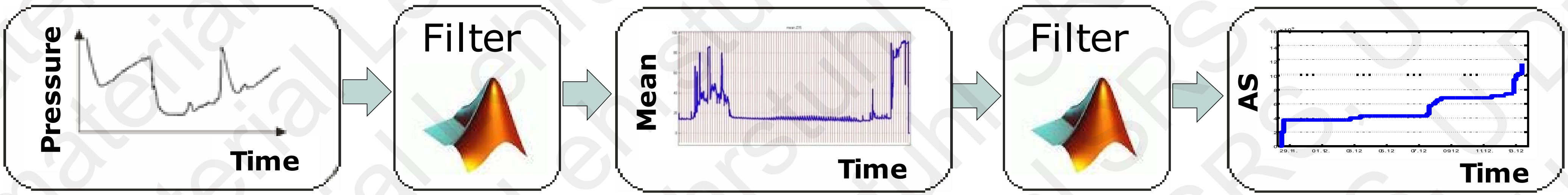

Generation of suitable characteristic value/feature

- Consideration of friction proportional pressure behavior
- Using of sliding window technique
- Sliding window-based calculation of characteristics
- Use of arithmetic mean

* Söffker, D.; Rothe, S.: *New Approaches for Supervision of Systems with Sliding Wear: Fundamental Problems and Experimental Results Using Different Approaches*. Applied Sciences, Vol. 7, 2017, pp. 843.

➔ Generation of characteristics are used for wear state evaluation.

Comparison of the three methods using identical test data

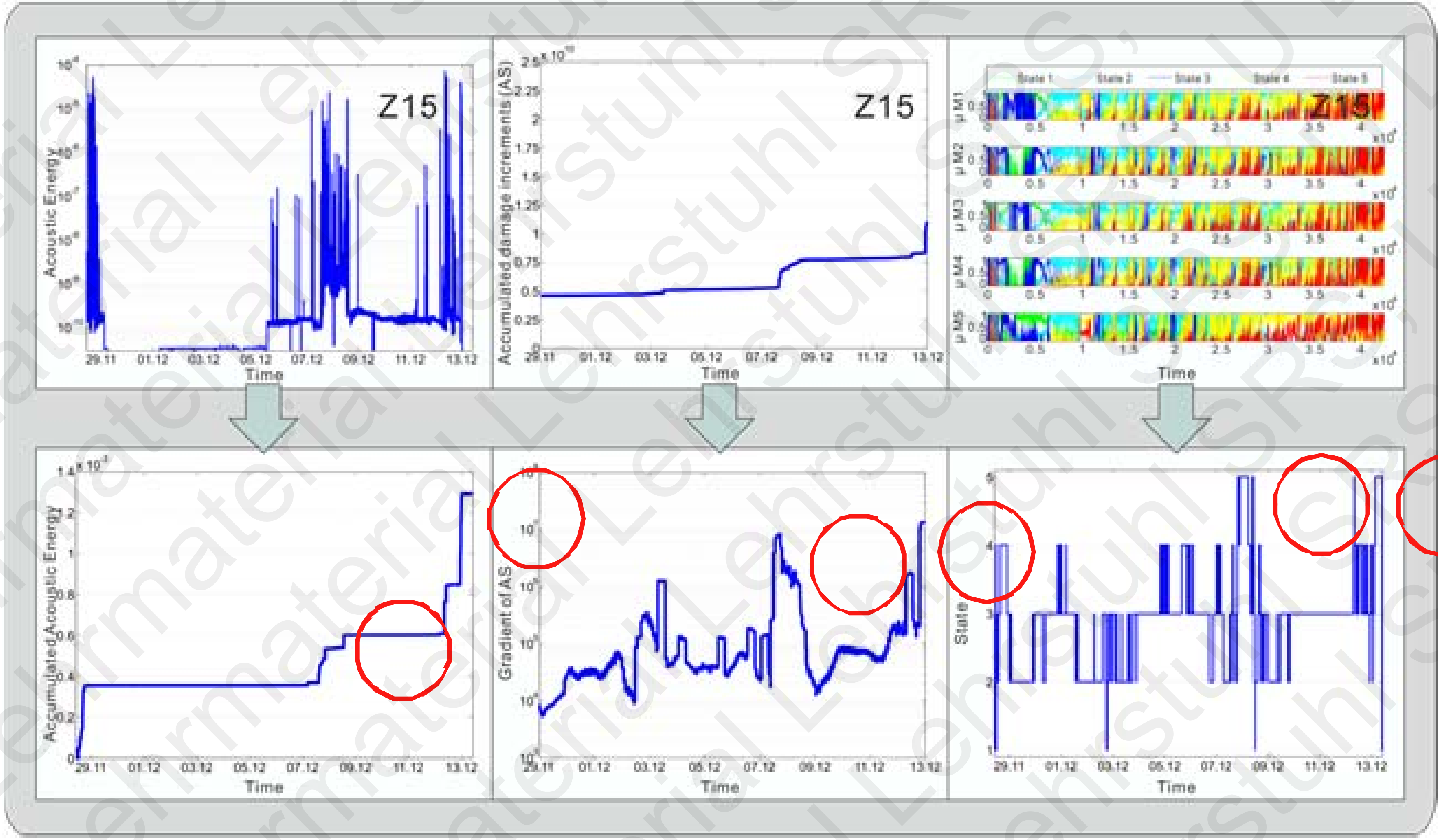

➔ The three different methods show same results. Which one is true? Is there truth behind?

* Söffker, D.; Rothe, S.: *New Approaches for Supervision of Systems with Sliding Wear: Fundamental Problems and Experimental Results Using Different Approaches.* Applied Sciences, Vol. 7, 2017, pp. 843.

Loading of meshing gears

- Cyclic loading
- Combined rolling and sliding
- Different damage modes
  - Micro-pitting (1)
  - Pitting (2)
  - Tooth-root crack (3)

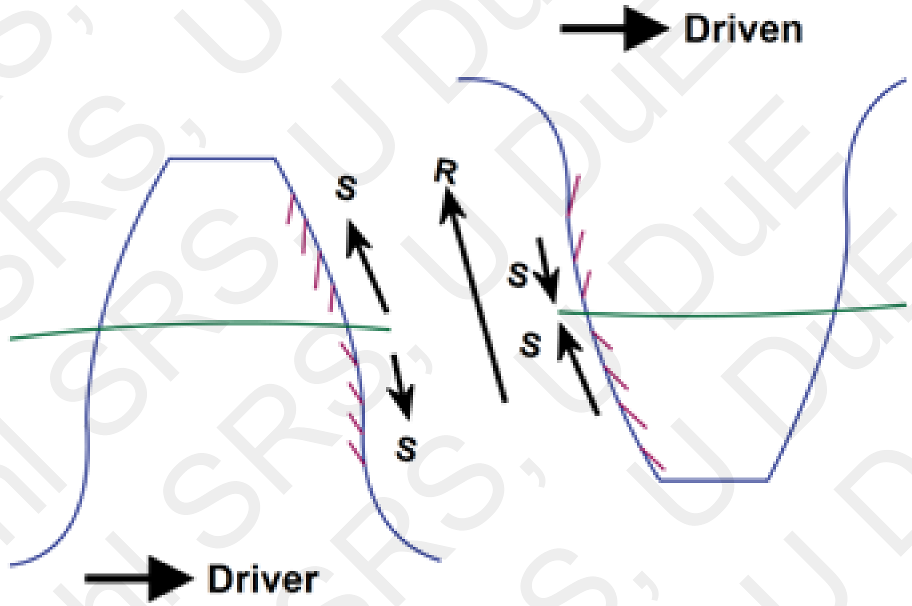

Illustration of gear mesh [Errichello, 2011]

(1)

(2)

(3)


Different damage modes of spur gears

II Experimental setup I

Standard test rig (FZG[1])

- Standardized for wear-testing of lubricated spur gears
- Two cylindrical gear stages (slave and testing gears)
- Static torque loading using calibrated weights
- Different loads indicated by Load Stages (LS)
- Principle of circulating power

	# of teeth	rpm
Wheel	24	1450
Pinion	16	2175

Specification of tested gears

FZG standard test rig

[1] Forschungsstelle für Zahnräder und Getriebebau (FZG)

II Experimental setup II

Measurement equipment

- Custom AE measurement system
- Sensors mounted outside the housing above the pinion of the test gears
- FPGA-based data acquisition

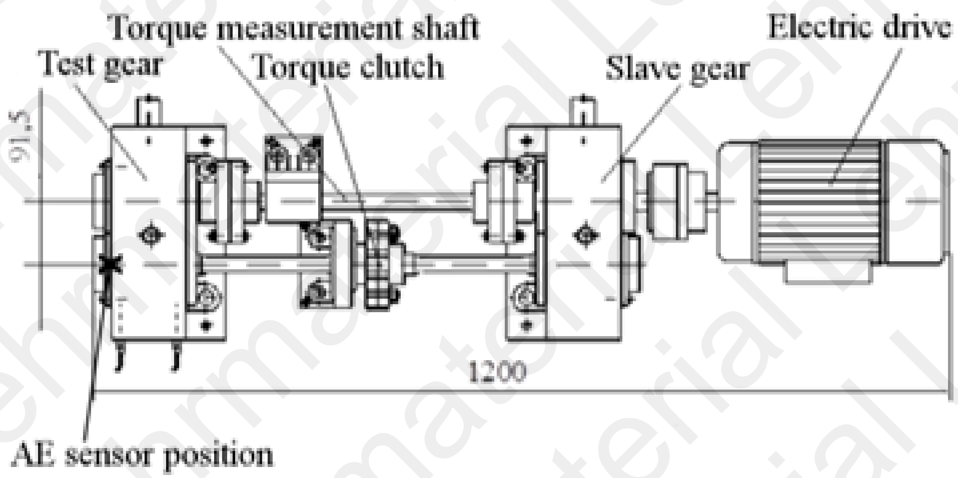

Top view of FZG test rig
showing AE sensor location

© Chair of Industrial and Automotive Drivetrains, Ruhr-Universität Bochum

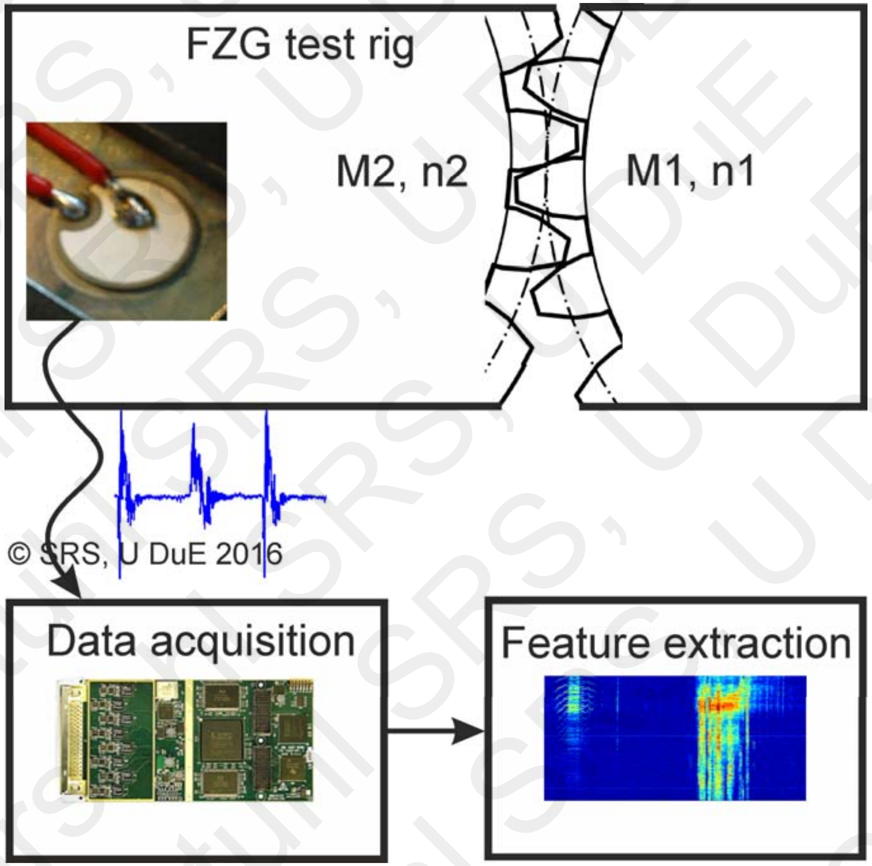

Illustration of
AE measurement system

Time domain signal: Normal operation

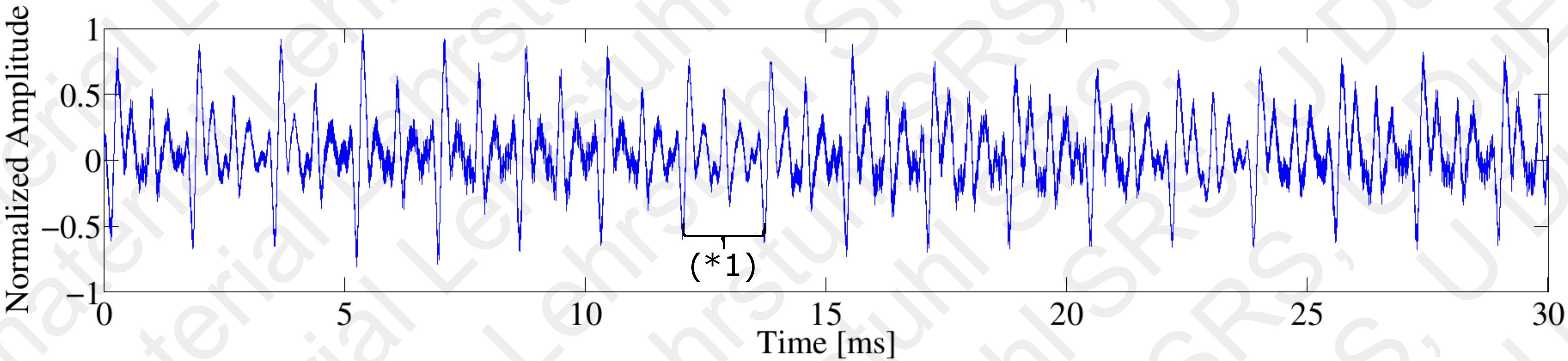

Time domain representation of measurement signal

- Fault-free gears
- Transient, continuous-type waveforms
- Distinct periodic pattern (*1), duration: ~1.7 ms
- Correspondence with meshing frequency: 580 Hz

II Experimental results II

Time domain signal: Pitting fault

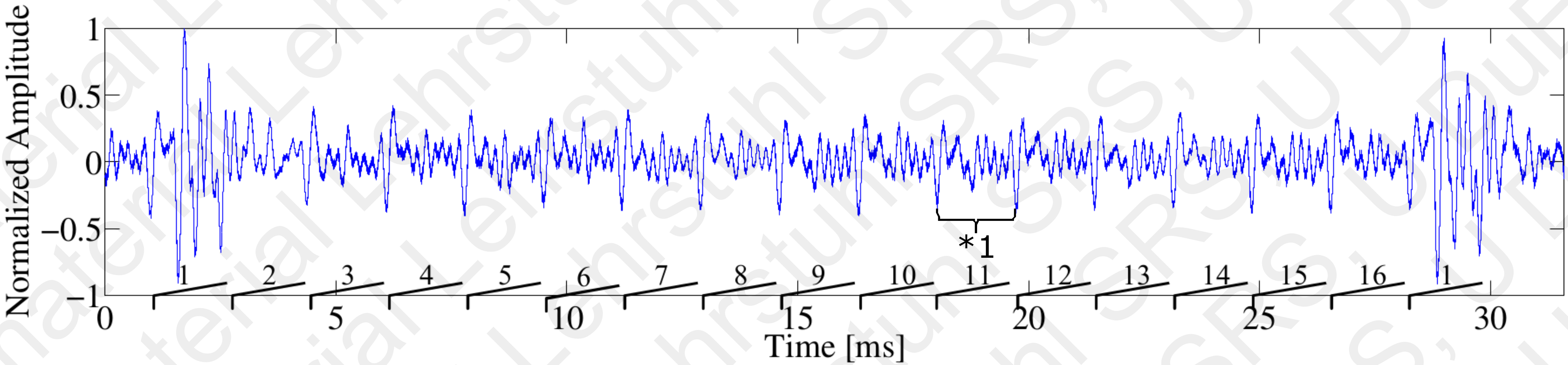

Time domain representation of measurement signal

- Pitting fault at single pinion tooth
- Transient, continuous-type waveforms
- Additional superimposed bursts every 16th period
- Correspondence of periodicity and the number of pinion teeth

➔ Measurement signal: dominated by meshing of the gears

II Experimental results* III

Wavelet analysis: Normal operation

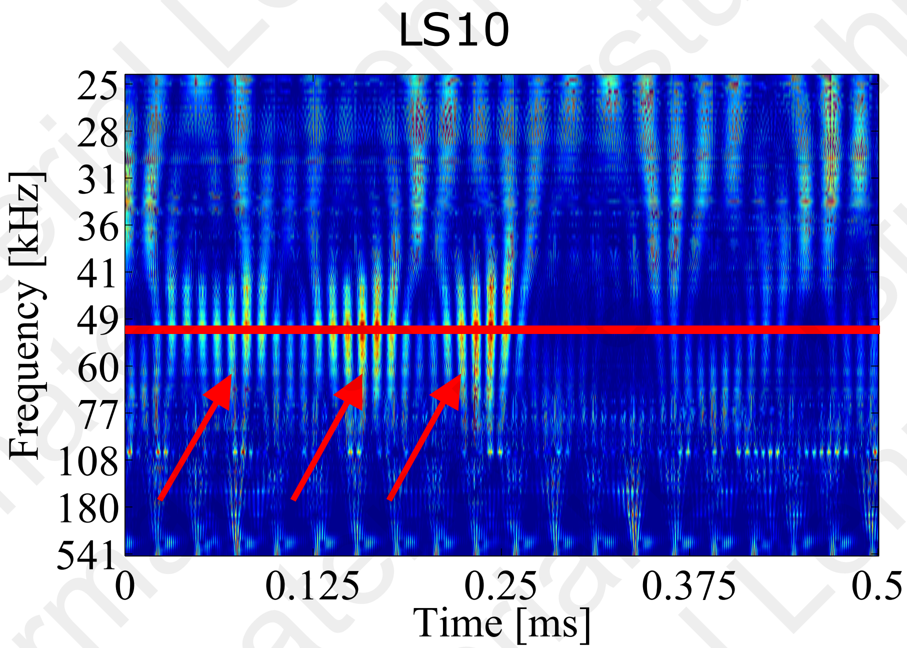

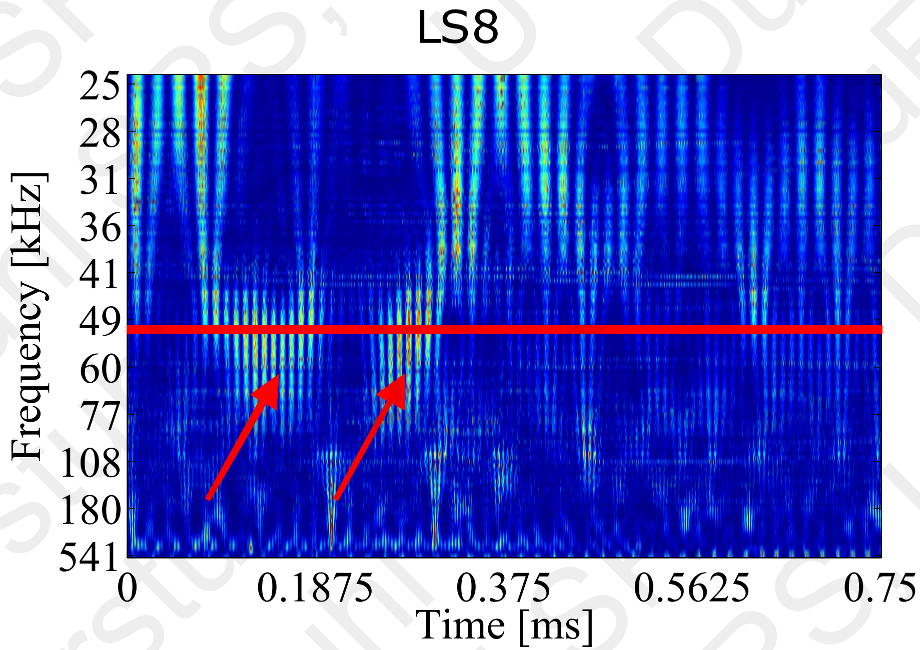

Time-frequency domain representation of measurement signal

- Fault-free gears
- Baseline pattern at frequencies of [40 kHz - 60 kHz], localized in time
- Similar patterns at different loads

* Wirtz, S.F.; Beganovic, N.; Tenberge, T.; Söffker, D.: *Frequency-based damage detection of spur gear using wavelet analysis*. European Workshop on Structural Health Monitoring, Bilbao, Spain, July 5-8, 2016.

II Experimental results* IV

Wavelet analysis: Micro-pitting

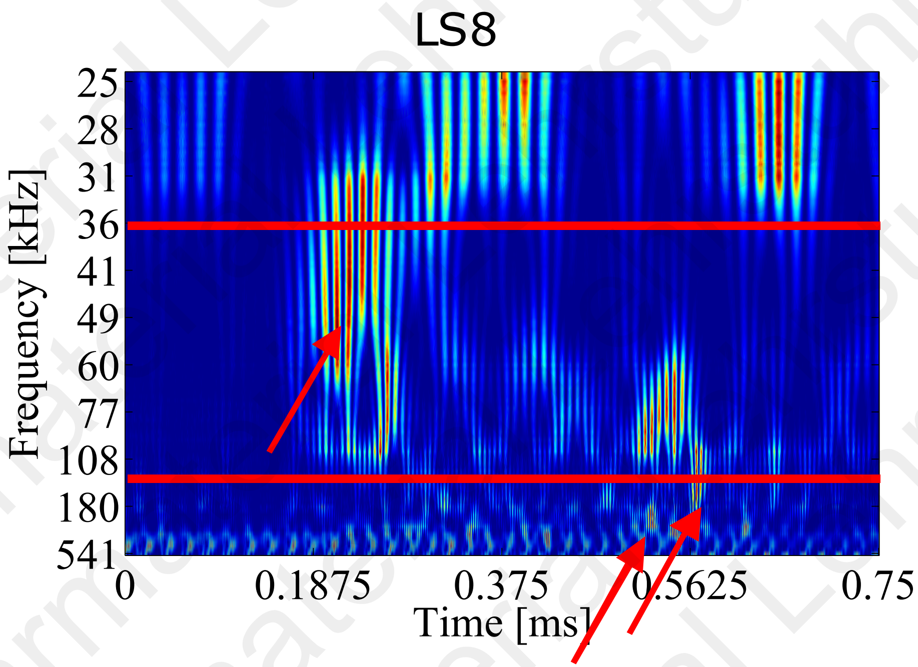

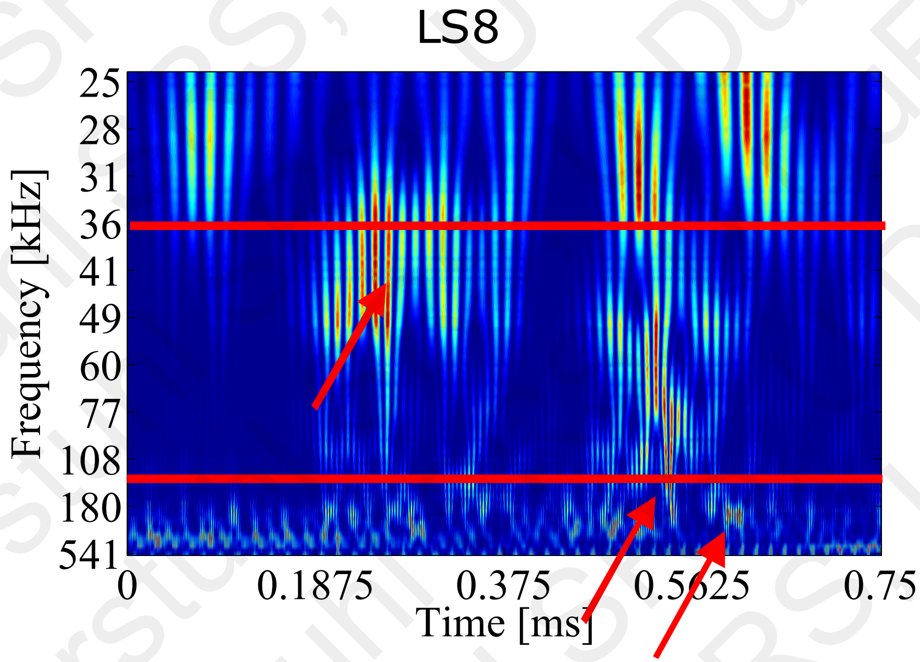

Time-frequency domain representation of measurement signal

- Deteriorated flank surfaces, matte gray appearance indicating micro-pitting
- Shift of baseline pattern down to [30 kHz – 40 kHz]
- Additional peak frequencies above 100 kHz

* Wirtz, S.F.; Beganovic, N.; Tenberge, T.; Söffker, D.: *Frequency-based damage detection of spur gear using wavelet analysis*. European Workshop on Structural Health Monitoring, Bilbao, Spain, July 5-8, 2016.

II Experimental results* V

Wavelet analysis: Pitting

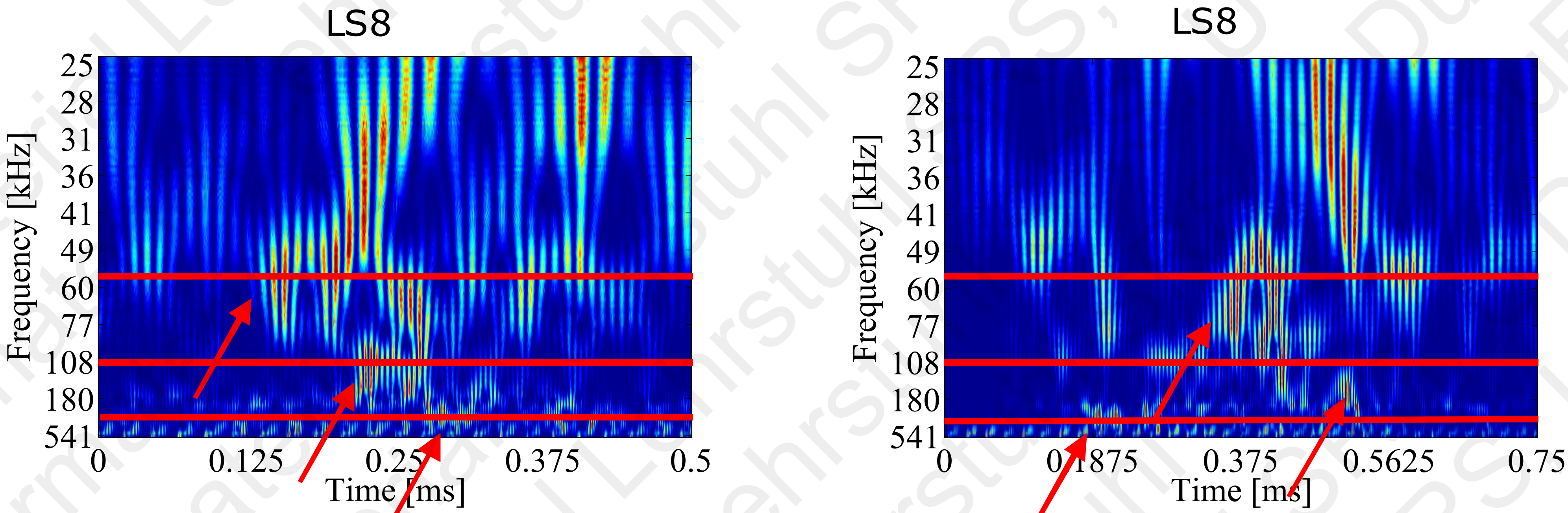

Time-frequency domain representation of measurement signal

- Pitting fault at single pinion tooth, no further surface deterioration
- Peak frequencies similar to baseline pattern at [40 kHz - 60 kHz]
- Additional high-frequency patterns at [100 kHz - 400 kHz]

* Wirtz, S.F.; Beganovic, N.; Tenberge, T.; Söffker, D.: *Frequency-based damage detection of spur gear using wavelet analysis*. European Workshop on Structural Health Monitoring, Bilbao, Spain, July 5-8, 2016.

From sensors to decisions to decision fusion

- Individual feature extraction and classification of sensor signals
- Fusion using reliability of classification results

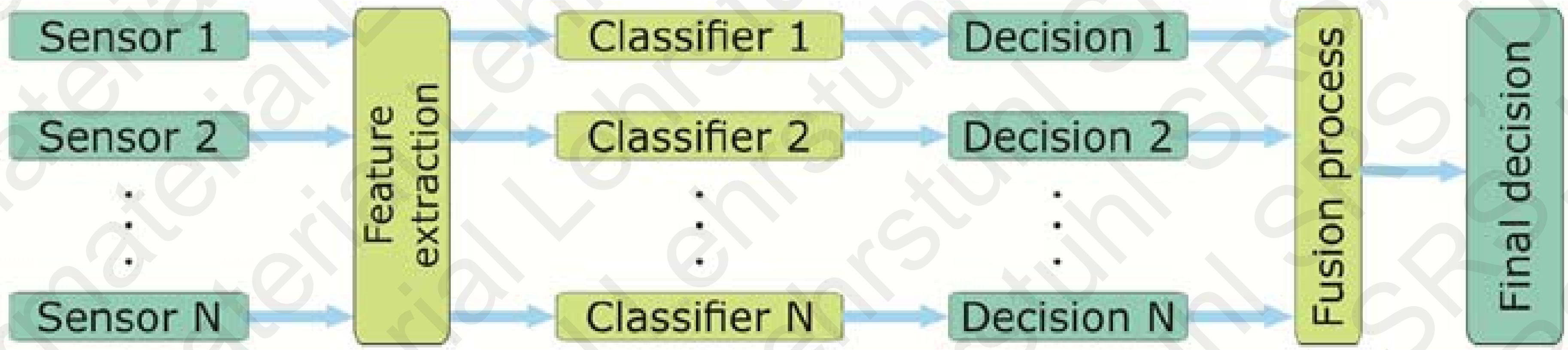

[Al-Shrouf, 2013]

→ Decisions show a certain reliability (correct, wrong)
→ Decisions can be fused with other decisions > decision fusion

II Experimental results of damage detection in composites I

Experimental setup I

- Bending test rig
  - Specimens of composite material
  - Cyclic bending load with different amplitudes and frequencies
- Acoustic Emission (AE): Elastic waves emerging within structures on damage initiation or propagation
- Composite materials: Frequency content of AE waveforms as reliable descriptor of underlying source mechanisms

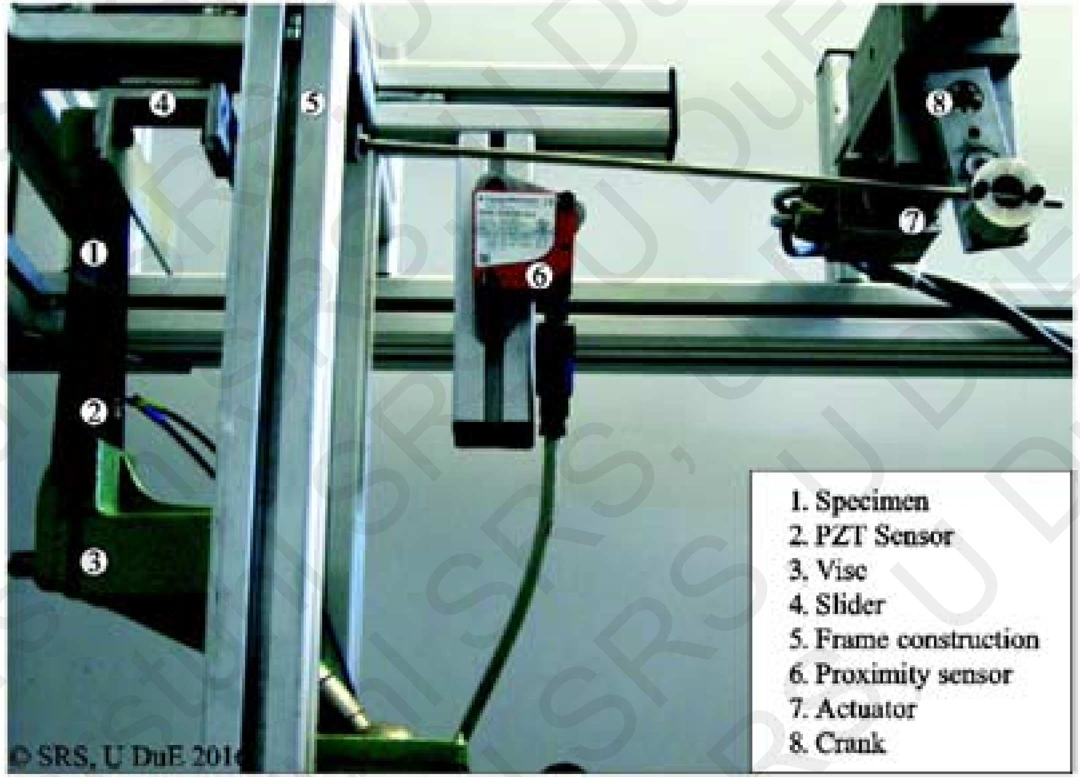

➔ Detection and distinction of damages within the material using frequency-domain features

Experimental setup*

- Specimen dimensions:
  425 x 425 x 1.8 mm^3
- Mounting specimens
  using clamping system
- Quasi-static load applied manually in
  transverse direction
- Sharp cone-shaped tool

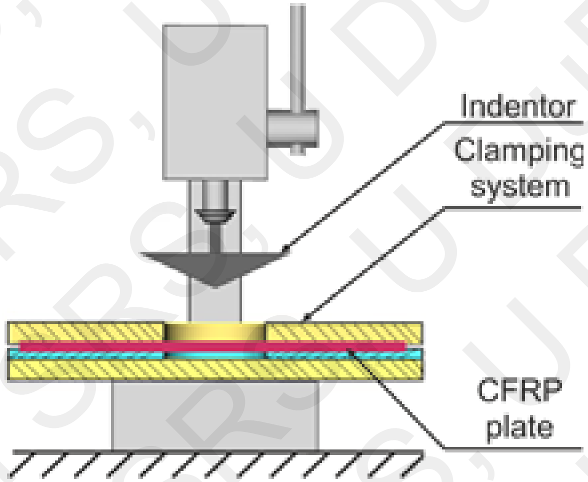

[Baccar, 2017]

Damage pattern

- Top side: indentation marks
- Bottom side: extensive damage
  - Delamination
  - Broken fibers
  - Crack

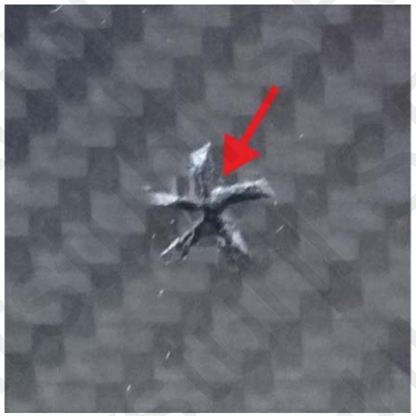

Top

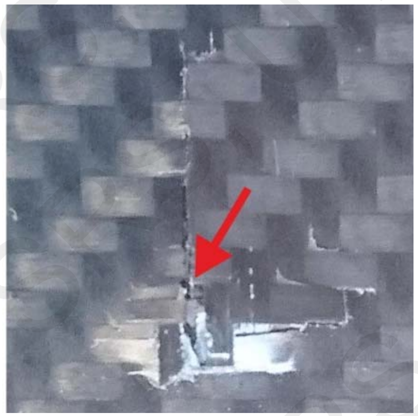

Bottom

* Baccar, D.; Söffker, D.: Identification and Classification of Failure Modes in Laminated Composites by using a Multivariate Statistical Analysis of Wavelet Coefficients. Mechanical System and Signal Processing, Vol. 96, 2017, pp. 77-87.

→ Generation of data samples according to specific damages

II Experimental results* of damage detection in composites III

Data samples with unknown labels

- Two independent specimens subjected to identical testing procedure
- Measurement series of each specimen containing a total of 25(*) to 120 (**) datasets
- Five different excitation frequencies [2 Hz - 6 Hz]
- Five different amplitudes [6 mm - 18 mm]
- Four considered damages
  - Class 1: Delamination
  - Class 2: Matrix crack
  - Class 3: Debonding
  - Class 4: Fiber breakage
- Three classification algorithms
  - Support Vector Machine (SVM)
  - K-Nearest Neighbor (KNN)
  - Artificial Neural Network (ANN)

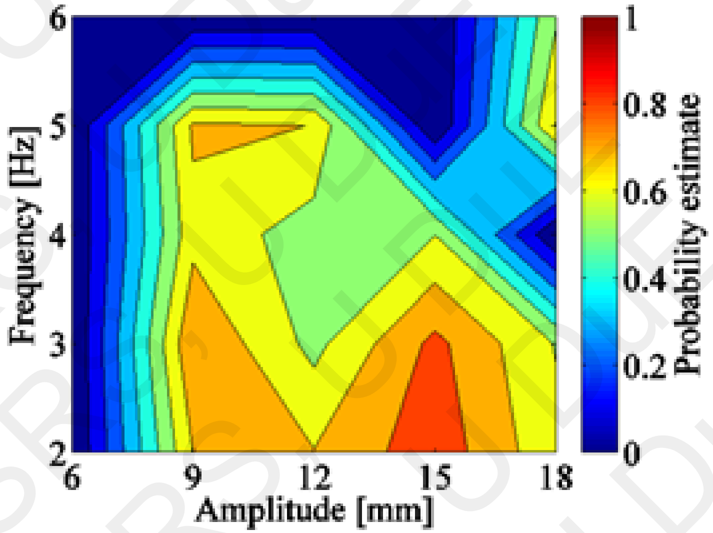

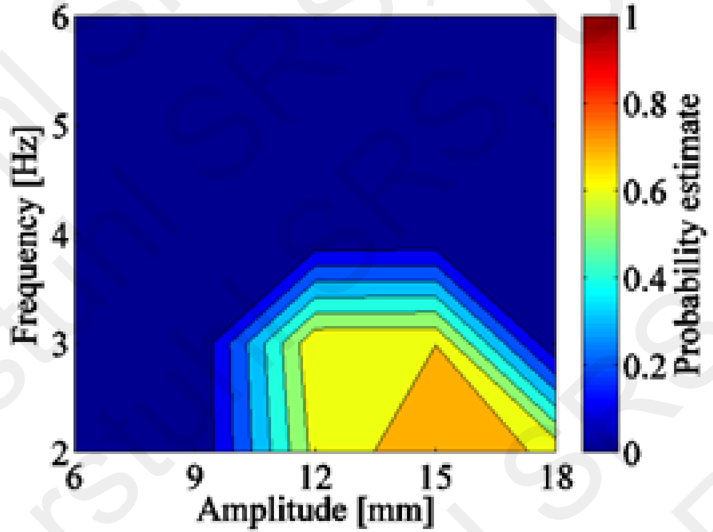

* Wirtz, S.F.; Beganovic, N.; Söffker, D.: *Investigation of damage detectability in composites using frequency-based classification of Acoustic Emission measurements*. Structural Health Monitoring, 2018, pp. 1-12.

II Experimental results*,** of damage detection in composites IV

Results of classification and fusion of data samples with unknown labels I

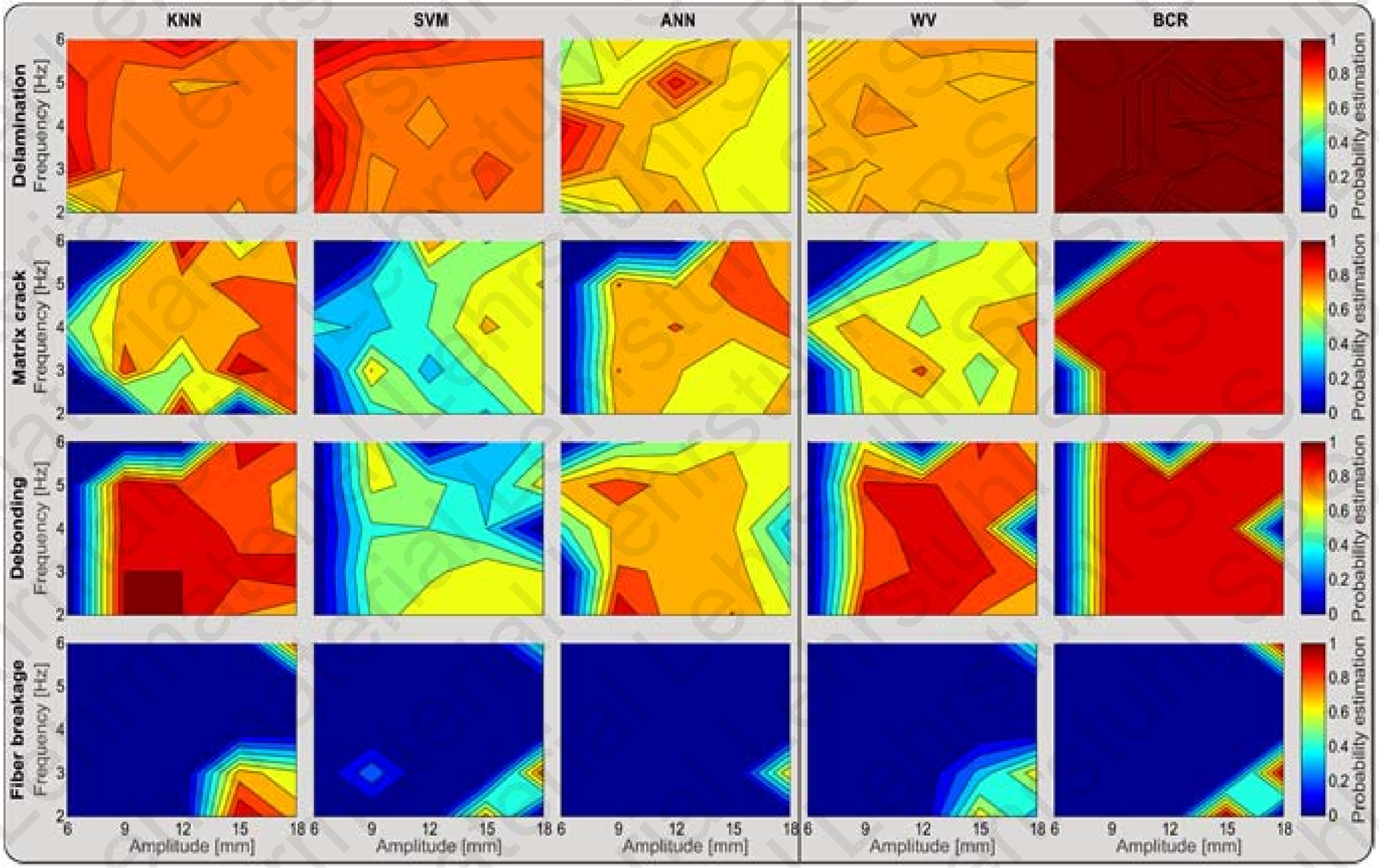

II Experimental results*,** of damage detection in composites V

Results of classification and fusion of data samples with unknown labels II

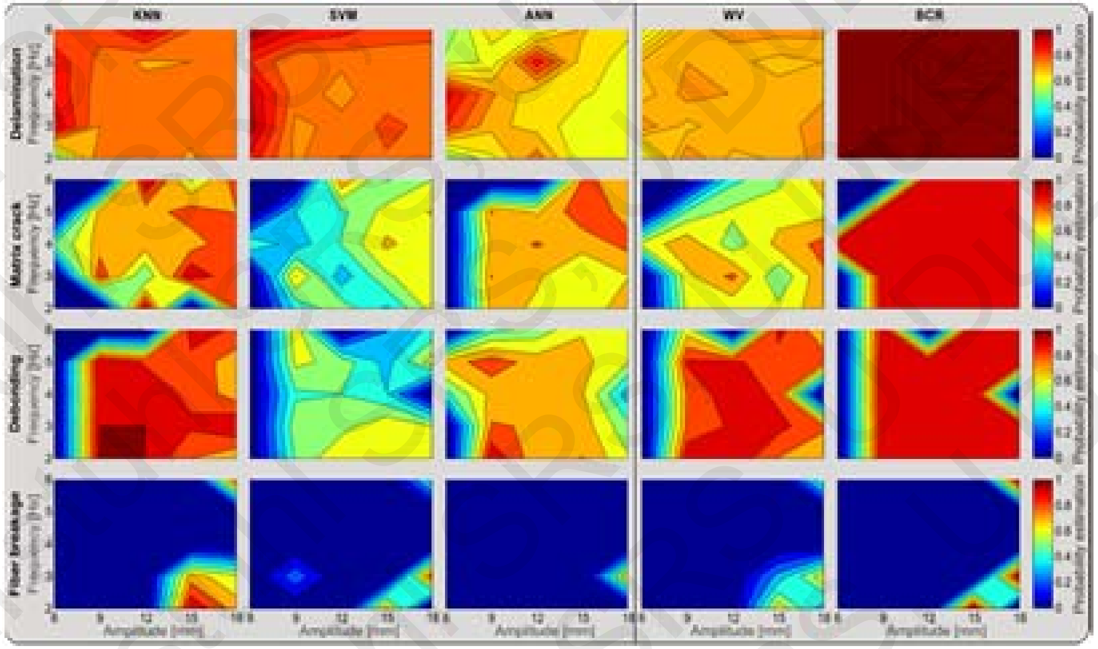

* Wirtz, S.F.; Beganovic, N.; Söffker, D.: *Investigation of damage detectability in composites using frequency-based classification of Acoustic Emission measurements*. Structural Health Monitoring, 2018, pp. 1-12.

** Rothe, S.; Wirtz, S.F.; Kampmann, G.;Nelles, O.; Söffker, D.: *Ensure the reliability of damage detection in composites by fusion of differently classified Acoustic Emission measurements*. In: Chang, F.K.; Kopsaftopoulos (Ed.): Structural Health Monitoring 2017, Stanford, USA, September 12-14, 2017, pp. 1380-1387.

➔ Structure of fused results show similarities to all individual results
➔ BCR: Crisper decision for one class (0 % or over 80 % probability estimation)
➔ A new problem occurs: **Is the automatic generated statement correct?**

Classification results and fusion
Complete datasets
as validation and test

- ➔ RKHS and SVM show the best individual results regarding the accuracy, the average recall, and the average FAR.
- ➔ Using WV the performance cannot be improved.
- ➔ BCR shows higher performance measure values for all average measures.
- ➔ Precision, recall, and FAR of class one is best using only SVM.

		ANN	KNN	RKHS	SVM	WV	BCR
Accuracy		92.50	95.00	96.67	96.67	95.83	97.50
Precision	Class 1	83.33	91.67	91.67	95.65	91.67	92.00
	Class 2	91.30	91.67	95.65	92.00	91.67	100.00
	Class 3	95.65	100.00	100.00	100.00	100.00	100.00
	Class 4	100.00	100.00	100.00	100.00	100.00	100.00
	Class 5	92.31	92.31	96.00	96.00	96.00	96.00
	Ø	92.52	95.13	96.66	96.73	95.87	97.60
Recall	Class 1	83.33	91.67	91.67	91.67	91.67	95.83
	Class 2	87.50	91.67	91.67	95.83	91.67	91.67
	Class 3	91.67	91.67	100.00	95.83	95.83	100.00
	Class 4	100.00	100.00	100.00	100.00	100.00	100.00
	Class 5	100.00	100.00	100.00	100.00	100.00	100.00
	Ø	92.50	95.00	96.67	96.67	95.83	97.50
FAR	Class 1	4.17	2.08	2.08	1.04	2.08	2.08
	Class 2	2.08	2.08	1.04	2.08	2.08	0.00
	Class 3	1.04	0.00	0.00	0.00	0.00	0.00
	Class 4	0.00	0.00	0.00	0.00	0.00	0.00
	Class 5	2.08	2.08	1.04	1.04	1.04	1.04
	Ø	1.87	1.25	0.83	0.83	1.04	0.62

* Rothe, S. et al.: *Ensure the reliability of damage detection in composites by fusion of differently classified Acoustic Emission measurements*. In: Chang, F.K.; Kopsaftopoulos (Ed.): Structural Health Monitoring 2017, Stanford, USA, September 12-14, 2017, pp. 1380-1387.

Classification results and fusion

Complete datasets as validation and test

- ➔ WV and BCR show **worse** performance than the individual classifiers RKHS and SVM.
- ➔ Static Ensemble Selection shows best fusion results for fusion of ANN and SVM although ANN has worst individual results.
- ➔ **Improvement of results compared to individual results not possible**

		ANN	KNN	RKHS	SVM	WV	BCR	BCR 1+4
Accuracy		92.50	95.00	96.67	96.67	95.83	95.83	96.67
Precision	Class 1	83.18	91.86	91.63	95.46	91.63	91.63	95.46
	Class 2	91.88	92.10	95.71	92.31	92.10	92.10	92.31
	Class 3	95.46	100.00	100.00	100.00	100.00	100.00	100.00
	Class 4	100.00	100.00	100.00	100.00	100.00	100.00	100.00
	Class 5	92.49	92.49	96.16	96.16	96.16	96.16	96.16
	Ø	92.60	95.29	96.70	96.78	95.98	95.98	96.78
Recall	Class 1	83.34	91.67	91.67	91.67	91.67	91.67	91.67
	Class 2	87.50	91.67	91.67	95.84	91.67	91.67	95.84
	Class 3	91.67	91.67	100.00	95.84	95.84	95.84	95.84
	Class 4	100.00	100.00	100.00	100.00	100.00	100.00	100.00
	Class 5	100.00	100.00	100.00	100.00	100.00	100.00	100.00
	Ø	92.50	95.00	96.67	96.67	95.83	95.83	96.67
FAR	Class 1	4.17	2.08	2.08	1.04	2.08	2.08	1.04
	Class 2	2.09	2.09	1.04	2.09	2.09	2.09	2.09
	Class 3	1.04	0.00	0.00	0.00	0.00	0.00	0.00
	Class 4	0.00	0.00	0.00	0.00	0.00	0.00	0.00
	Class 5	2.08	2.08	1.04	1.04	1.04	1.04	1.04
	Ø	1.87	1.25	0.83	0.83	1.04	1.04	0.83

* Rothe, S. et al.: *Ensure the reliability of damage detection in composites by fusion of differently classified Acoustic Emission measurements*. In: Chang, F.K.; Kopsaftopoulos (Ed.): Structural Health Monitoring 2017, Stanford, USA, September 12-14, 2017, pp. 1380-1387.

How Data-driven approaches works?

- Supervised data-driven approaches (SVM, KNN, ANN, RT, HMM, Regression-based …, ….) are using data (input, output, both) and given classifying knowledge
- Non-supervised approaches (K-means, ANN, GM, HMM, …) are using data (input, output, both) and internally generate internal relations > IF data-sets are extreme large > BIG-DATA (using other analytical tools)
- Feeding the approaches with data and knowledge leads to so-called data-driven models > trained **data-driven I/O-models** establishing relations between I/O
  > feed the algorithms with data => train the model (Training)
  > use the trained model with unknown data => test/apply the model (Test)
- Training is denoted as learning > **Machine learning** denotes automated modeling
- Several approaches compete for 'free lunch'.
- In case of classification: detection rate, false alarm rate etc. (ROC) are used for evaluation.

➔ Data-driven/Machine Learning/Training: similar terms for generating data-based models
➔ Established models are not related to first principles.

How Data-driven approaches works?

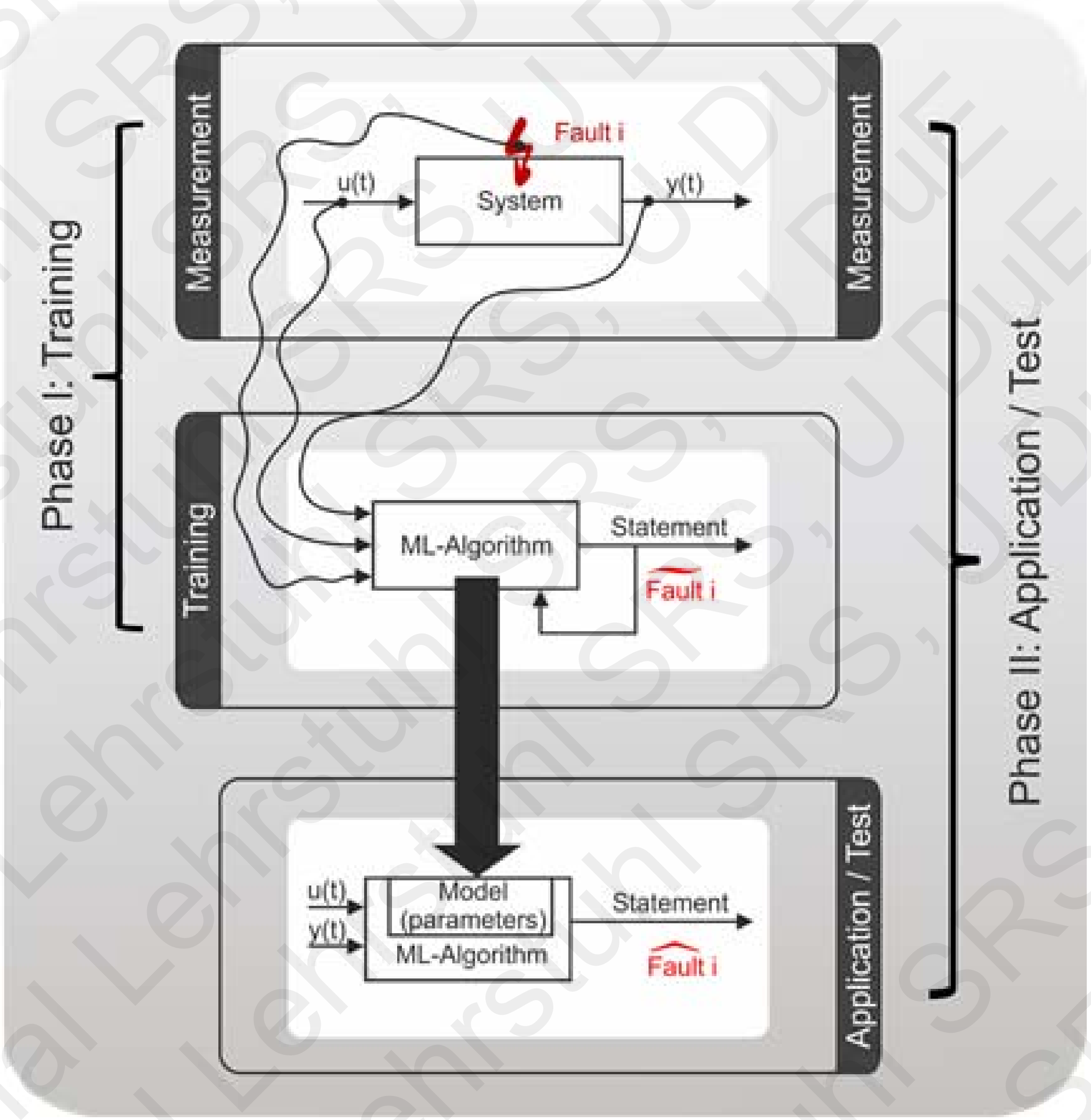

- ➔ Advantages:
  easy to establish.
- ➔ Disadvantages:
  - Difficult to interprete
    (beside the statement itself)
  - Not necessary reliable
  - Wrong generalizability.

III Example: Establishment of a data-driven RUL model I

Remaining useful lifetime as key variable within the Prognostic health management (PHM) view

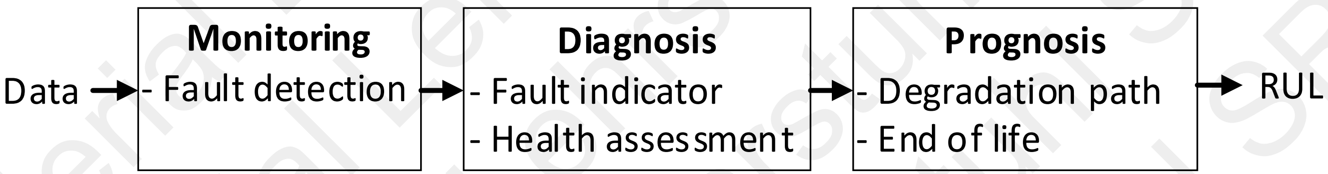

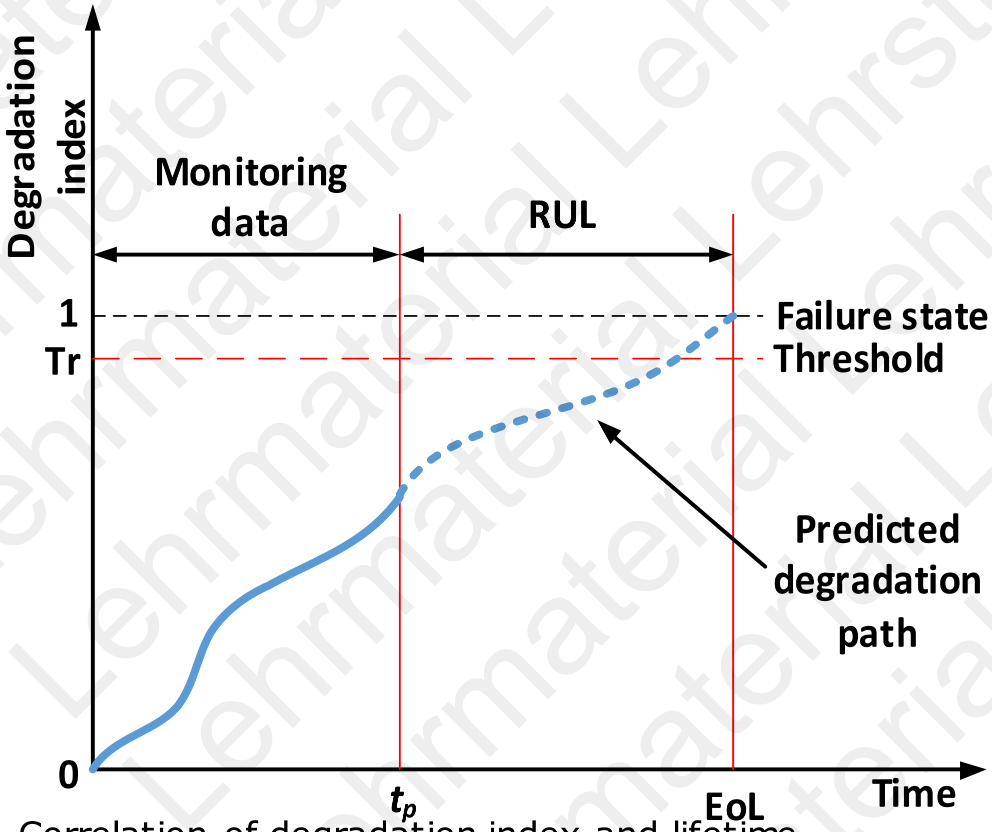

Correlation of degradation index and lifetime

- RUL: distance from prediction time (t_p) to end of life (EoL) time

$$\text{RUL} = \text{EoL} - t_p \; ; \; \text{EoL} > t_p$$

- EoL: based on predicted degradation path exceeding threshold (Tr) and reach failure state

III Example: Establishment of a data-driven RUL model II

Prognostic process based on state machine scheme

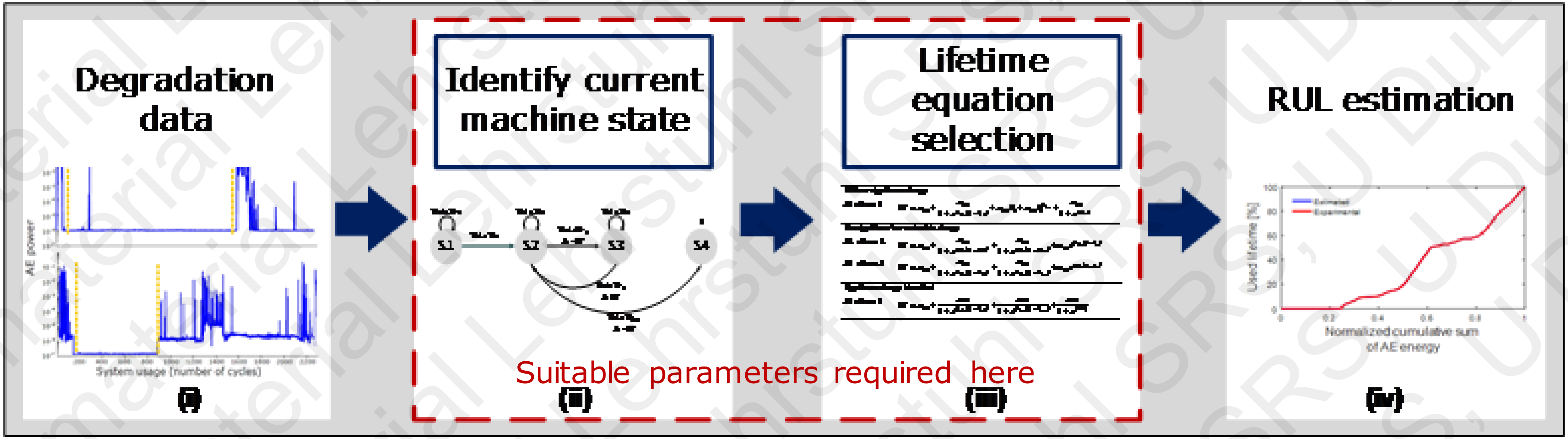

Process flow:

(i) Degradation data as prognostic model input

(ii) Identification of current machine state

(iii)Selection and parameter definition corresponding of state specific lifetime equation

(iv)Estimation of overall RUL based on state-specific lifetime equations contribution

➔ Required suitable parameters (thresholds and design variables) has to be defined.

III Example: Establishment of a data-driven RUL model III

State machine model: illustrative example (concept)

- All states correspond to **three degradation phases**
- State selection according to **threshold (Tr)** and input **decreasing/increasing trend (DT/~DT)**
- Possible state **transition paths**:
  i- From S1 (initial state) to S2 if Tr_1 exceeded
  ii- From S2 to S3 if Tr_2 exceeded and input increase (~DT)
  iii- From S3 to S2 if Tr_2 exceeded and input decrease (DT)
  iv- From S2 to S4 if Tr_{diff} exceeded and input increase (~DT)

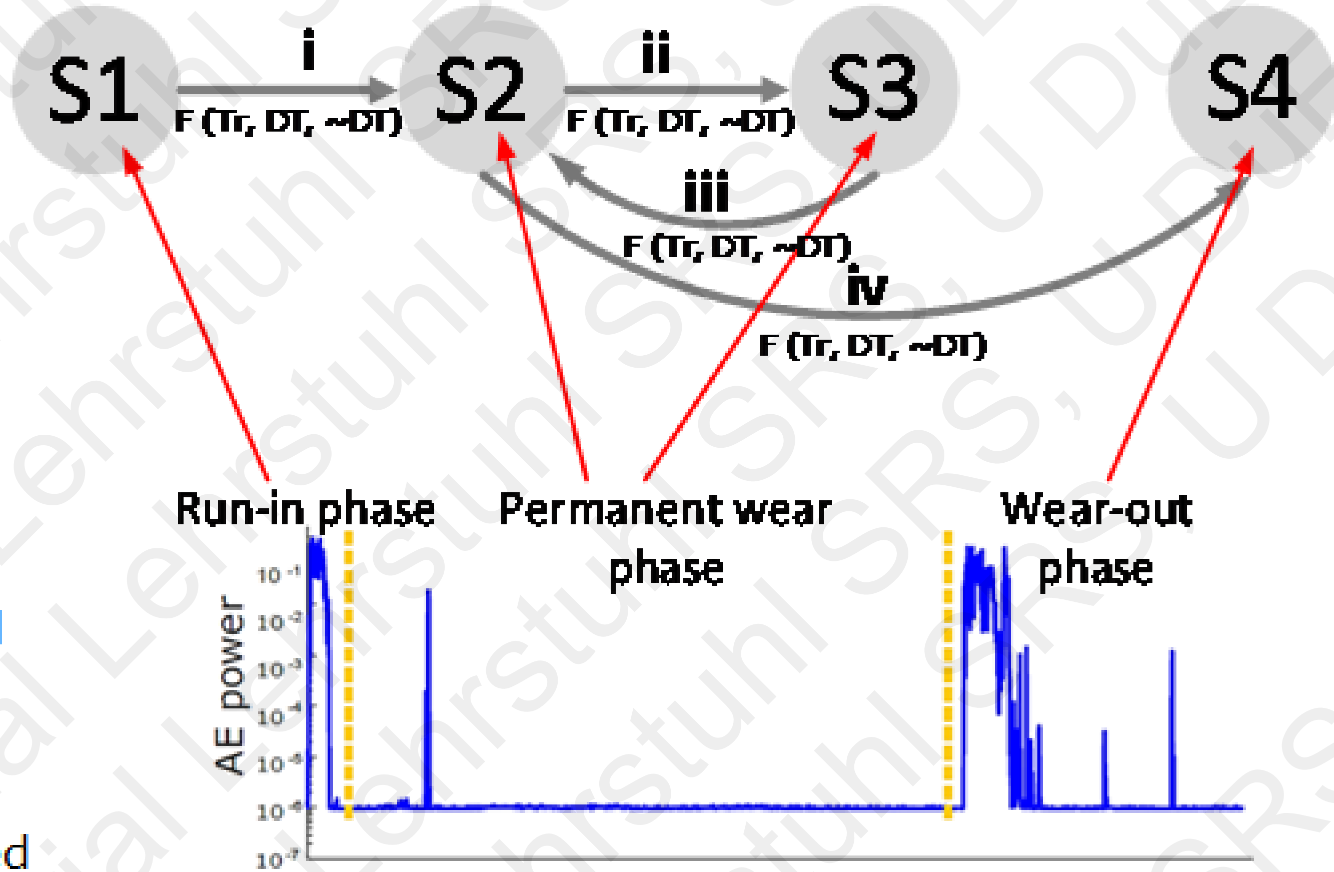

III Example: Establishment of a data-driven RUL model IV

A simple model: Type I*

- Feature values of AE data directly used as input to prognostic model
- Thresholds are **subject of optimization**
- Threshold 1 (Tr_1) **excluded** from sorting procedure of NSGA-II

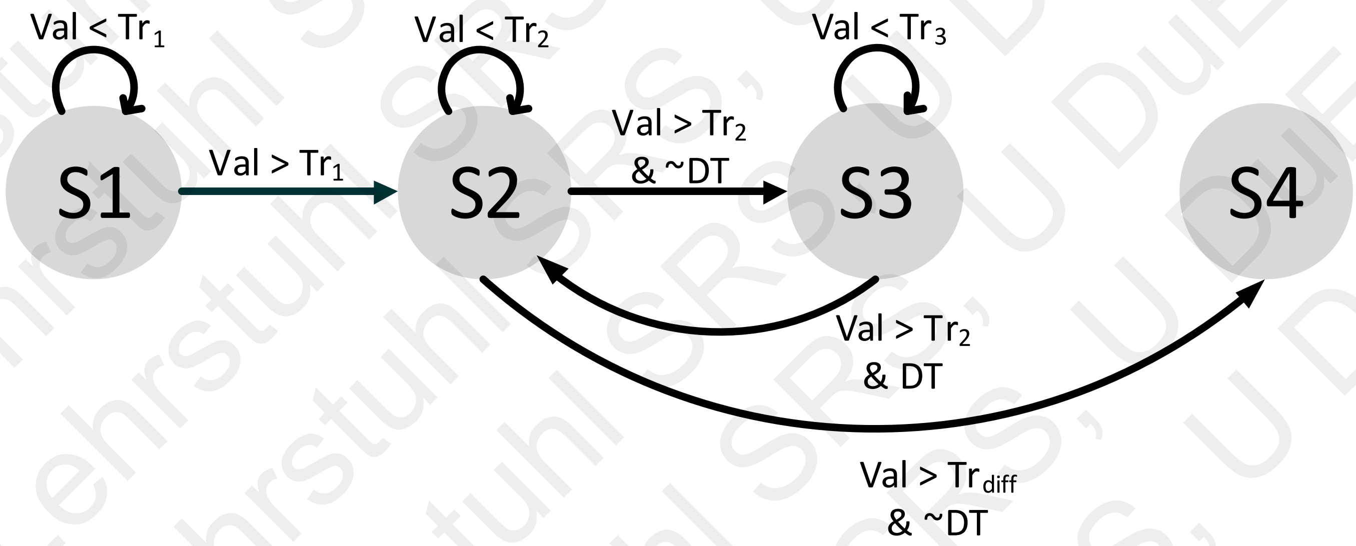

State-machine topology

Val	Feature value
Tr	Threshold
S	State-machine
DT	Decreasing trend
~DT	Increasing trend

* Beganovic, N.; Söffker, D.: *Remaining lifetime modeling using State-of-Health estimation*. Mechanical Systems and Signal Processing, Vol. 92, 2017, pp. 107-123.

Lifetime equation for model type I*

- Each state leads to identical lifetime equations [Weng, 2013]
- 36 design parameters identified by optimization

S1: $$LT = a_{10} + \frac{a_{11}}{1 + e^{a_{12}(F_1 - a_{13})}} + \frac{a_{14}}{1 + e^{a_{15}(F_1 - a_{16})}} + \frac{a_{17}}{1 + e^{a_{18}F_1}}$$

S2: $$LT = a_{20} + \frac{a_{21}}{1 + e^{a_{22}(F_1 - a_{23})}} + \frac{a_{24}}{1 + e^{a_{25}(F_1 - a_{26})}} + \frac{a_{27}}{1 + e^{a_{28}F_1}}$$

S3: $$LT = a_{30} + \frac{a_{31}}{1 + e^{a_{32}(F_1 - a_{33})}} + \frac{a_{34}}{1 + e^{a_{35}(F_1 - a_{36})}} + \frac{a_{37}}{1 + e^{a_{38}F_1}}$$

S4: $$LT = a_{40} + \frac{a_{41}}{1 + e^{a_{42}(F_1 - a_{43})}} + \frac{a_{44}}{1 + e^{a_{54}(F_1 - a_{46})}} + \frac{a_{47}}{1 + e^{48F_1}}$$

LT	Consumed lifetime (%)
a_{xy}	Design variable
F_1	Feature value

* Beganovic, N.; Söffker, D.: *Remaining lifetime modeling using State-of-Health estimation*. Mechanical Systems and Signal Processing, Vol. 92, 2017, pp. 107-123.

Model type II*

- Accumulated AE data used as input to prognostic model
- Thresholds are **subject of optimization**
- State 3 is **divided** into state 3a and state 3b for more flexibility

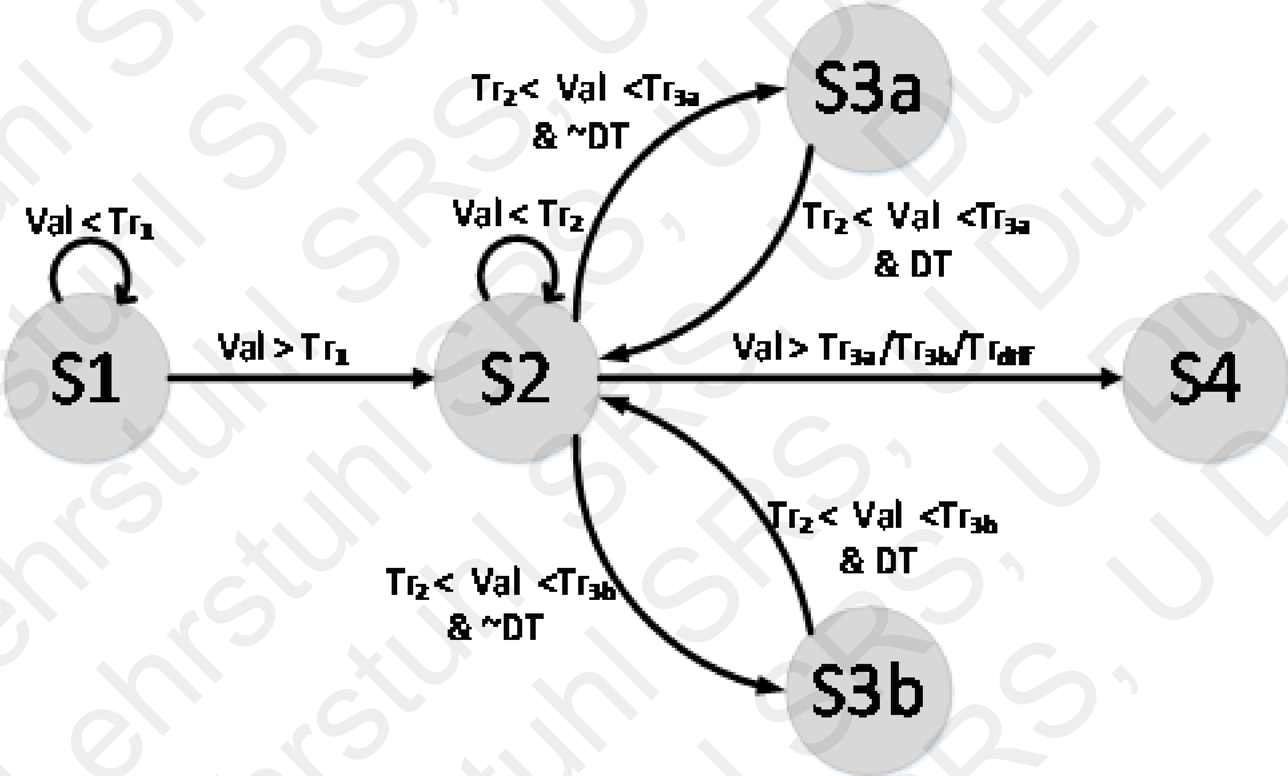

State-machine topology

Val	Feature value
Tr	Threshold
S	State-machine
DT	Decreasing trend
~DT	Increasing trend

* Jihin, R.; Söffker, D.; Beganovic, N.: *Integrated Prognostic Model For RUL Estimation Using Threshold Optimization*. In: Chang, F.K.; Kopsaftopoulos (Ed.): Structural Health Monitoring 2017, Stanford, USA, September 12-14, 2017, pp. 640-647.

Lifetime equation for model type II*

- Each state leads to different lifetime equations
- 45 design parameters identified by optimization

Without significant change

S1: $$LT = a_{10} + \frac{a_{11}}{1 + e^{a_{12}(F_2 - a_{13})}} + a_{14}F_2 + a_{15}F_2^{a_{16}} + \frac{a_{17}}{1 + e^{a_{18}F_2}}$$

Not significant but noticeable change

S2: $$LT = a_{20} + \frac{a_{21}}{1 + e^{a_{22}(F_2 - a_{23})}} + \frac{a_{24}}{1 + e^{a_{25}(F_2 - a_{26})}} + a_{27}e^{a_{28}(1 - F_2)}$$

S3a: $$LT = a_{30} + \frac{a_{31}}{1 + e^{a_{32}(F_2 - a_{33})}} + \frac{a_{34}}{1 + e^{a_{35}(F_2 - a_{36})}} + a_{37}e^{a_{38}(1 - F_2)}$$

S3b: $$LT = a_{40} + \frac{a_{41}}{1 + e^{a_{42}(F_2 - a_{43})}} + \frac{a_{44}}{1 + e^{a_{45}(F_2 - a_{46})}} + a_{47}e^{a_{48}(1 - F_2)}$$

Significant change identified

S4: $$LT = a_{50} + \frac{a_{51}}{1 + e^{a_{52}(F_2 - a_{53})}} + \frac{a_{54}}{1 + e^{a_{55}(F_2 - a_{56})}} + \frac{a_{57}}{1 + e^{a_{58}F_2}}$$

LT	Consumed lifetime (%)
a_{xy}	Design variable
F_2	Feature value

III Example: Establishment of a data-driven RUL model VIII

Optimization of the prognostic model using NSGA-II

- Parameters optimization using NSGA-II
- Fixed thresholds prone to error when not set to optimal variables [Bai, 2016]
- Objective functions: minimize discrepancies between observed (measured) and predicted (based on the model) lifetime

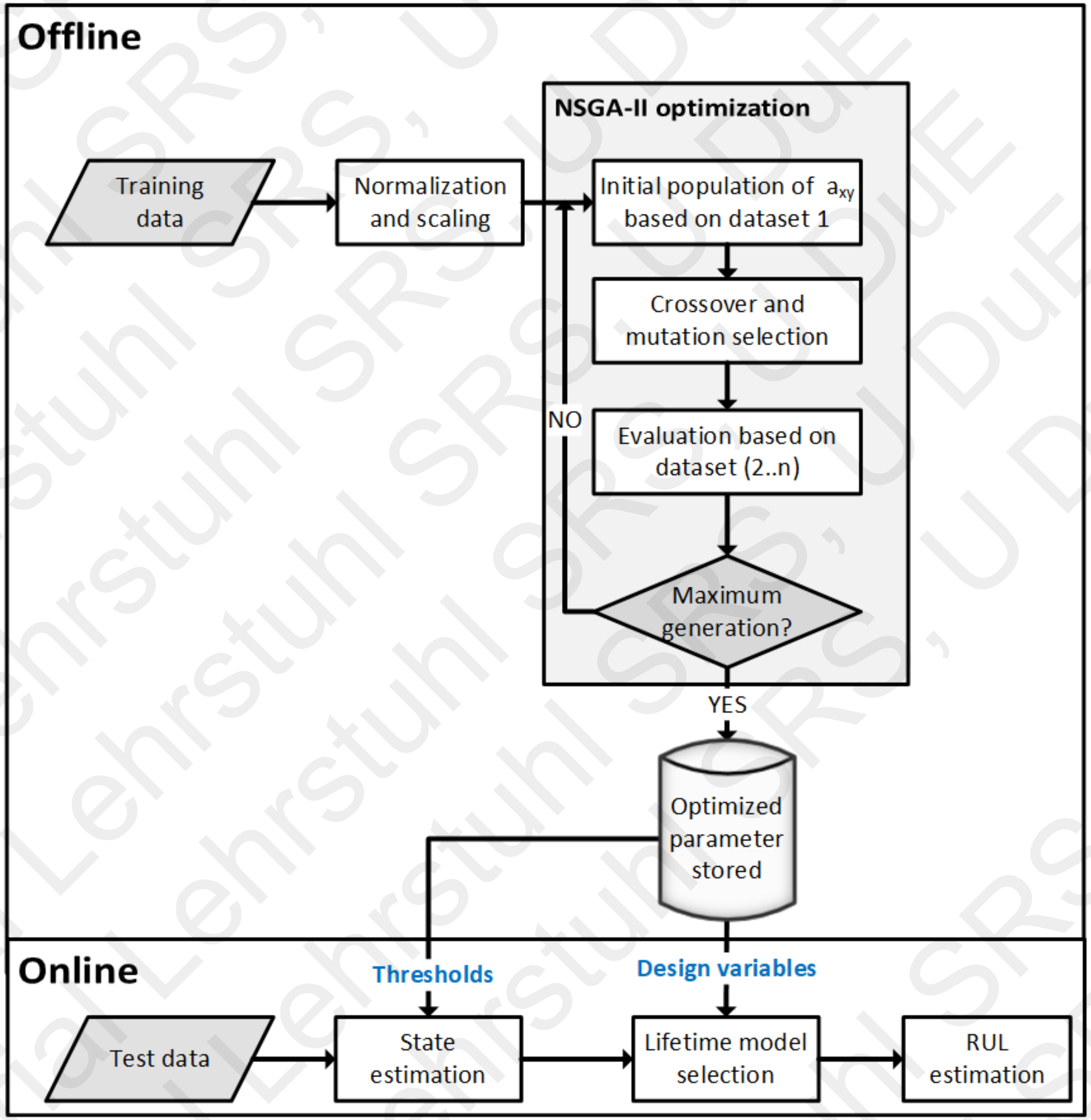

Application of experimental data

- Prognostic models deployed using experimental data from tribology test at Chair SRS, U DuE
- Consist of two metal plates sliding on each other (in exact operating conditions)
- Wear progress due to tribological effect
- Generate AE energy until life ended (run-to-failure data)
- Dataset used (different test runs)
  - Training: Z15, Z20, Z21, Z22
  - Test: Z16, Z24

Tribology test rig

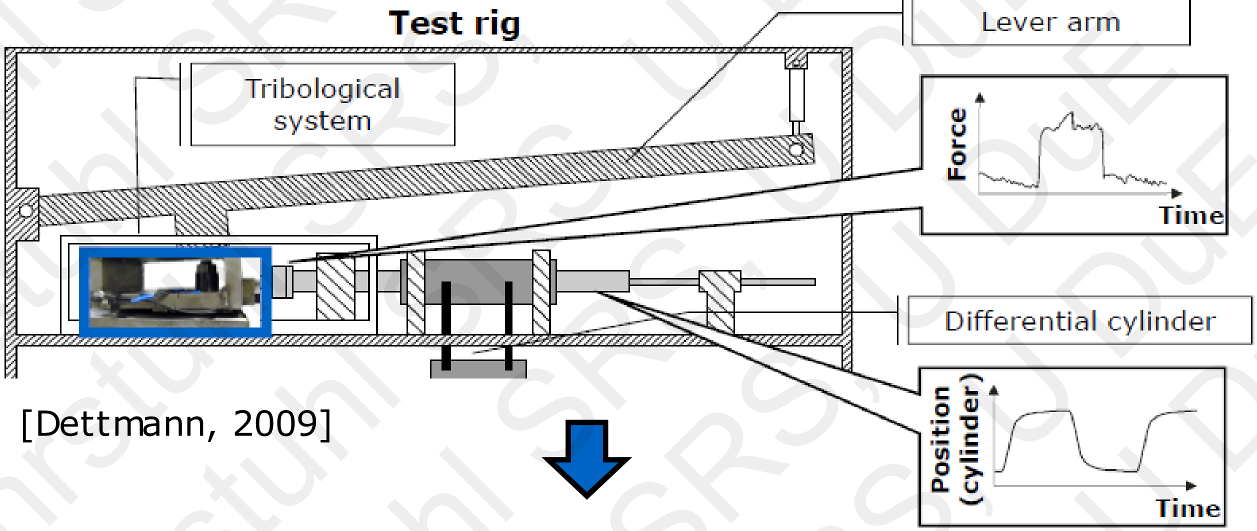

[Dettmann, 2009]

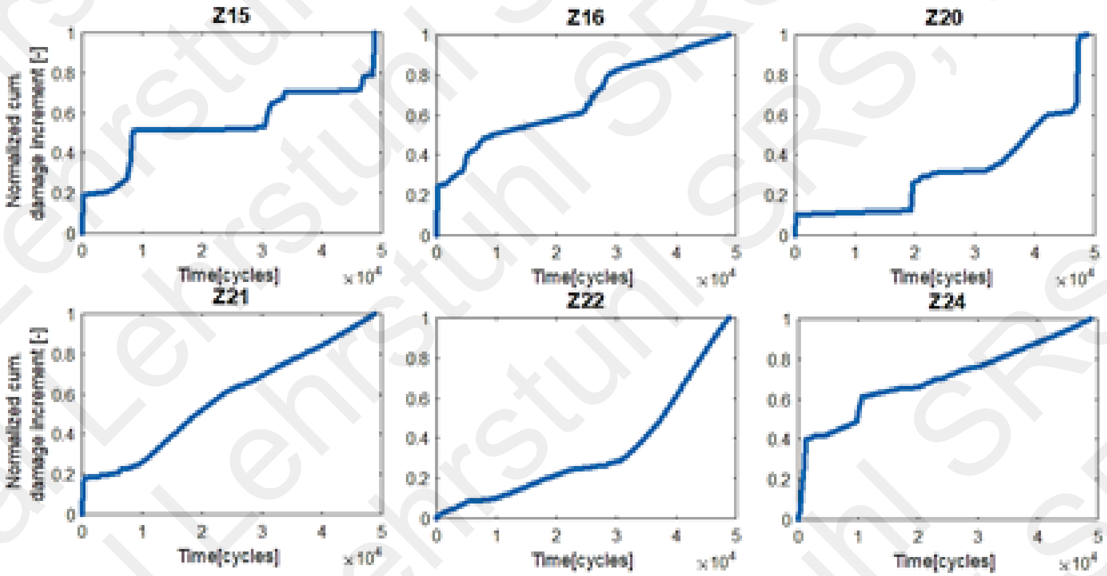

III Example: Establishment of a data-driven RUL model X

Model evaluation: performance criteria

- Efficiency measurement based on overall RUL prediction
- Performance evaluation using Root Squared Error (RSE), Mean Squared Error (MSE) and Absolute Error (ABE)

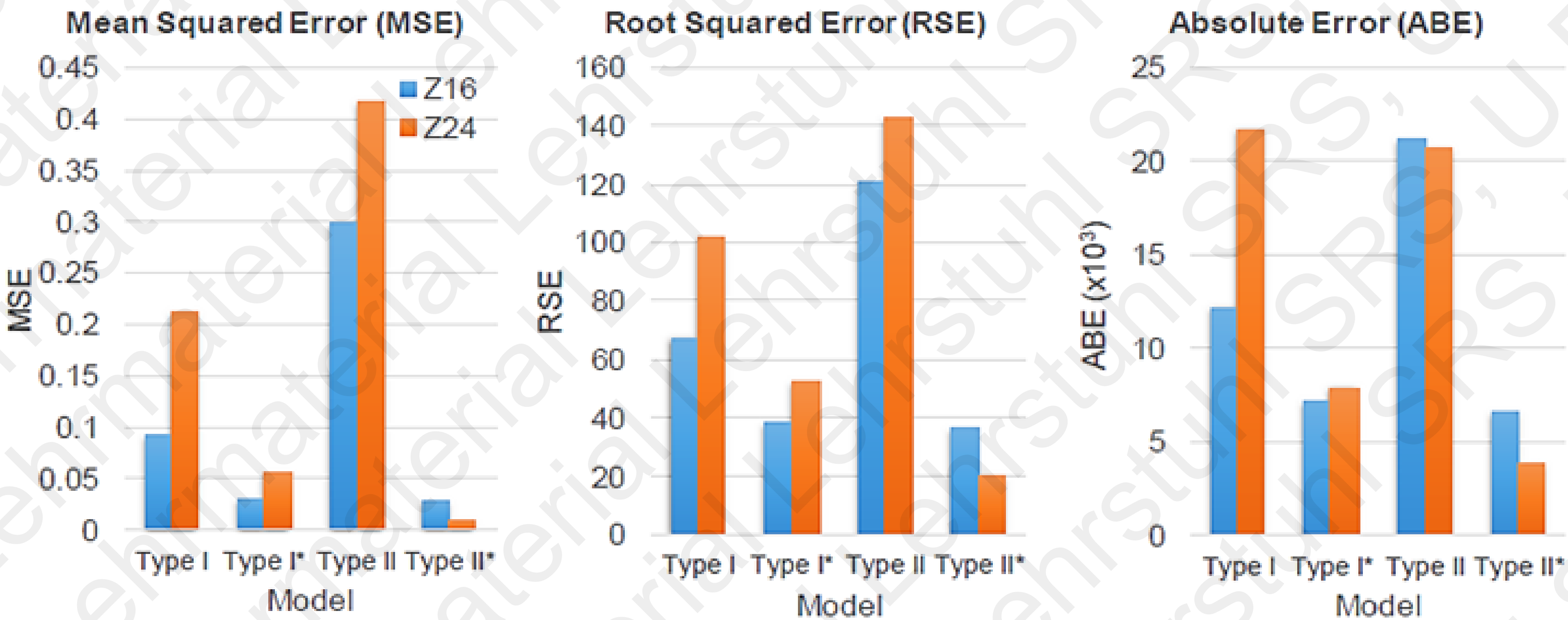

➔ Less errors obtained by model type II* compared to other models

III Example: Establishment of a data-driven RUL model XI

Evaluation: end of life estimation

- Prediction of EoL based on n % available measurement data
- Real EoL considered when system reach 100 % lifetime
- Closer to 100 % better EoL prediction

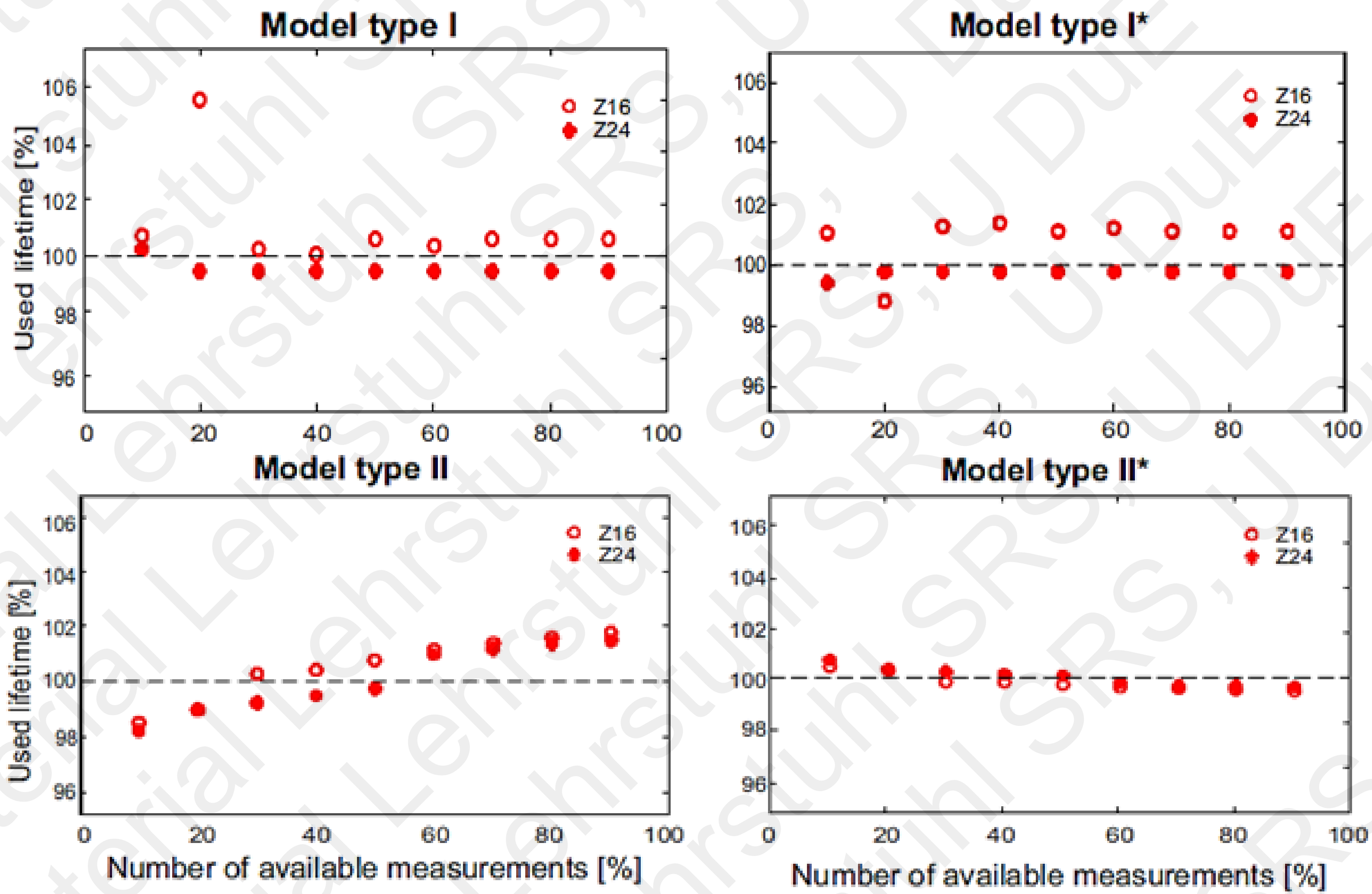

➔ Type I*: Able to estimate lifetime from the beginning (20/25/30%) of system life
➔ Type II*: Perfect estimations (errors ±1%) of EoL at the very beginning of lifetime

III Example: Establishment of a data-driven RUL model XII

Simple fold cross-validation

- EoL estimated using model type II* for six training and test datasets variations
- Observation based on number of available measurement and lifetime prediction

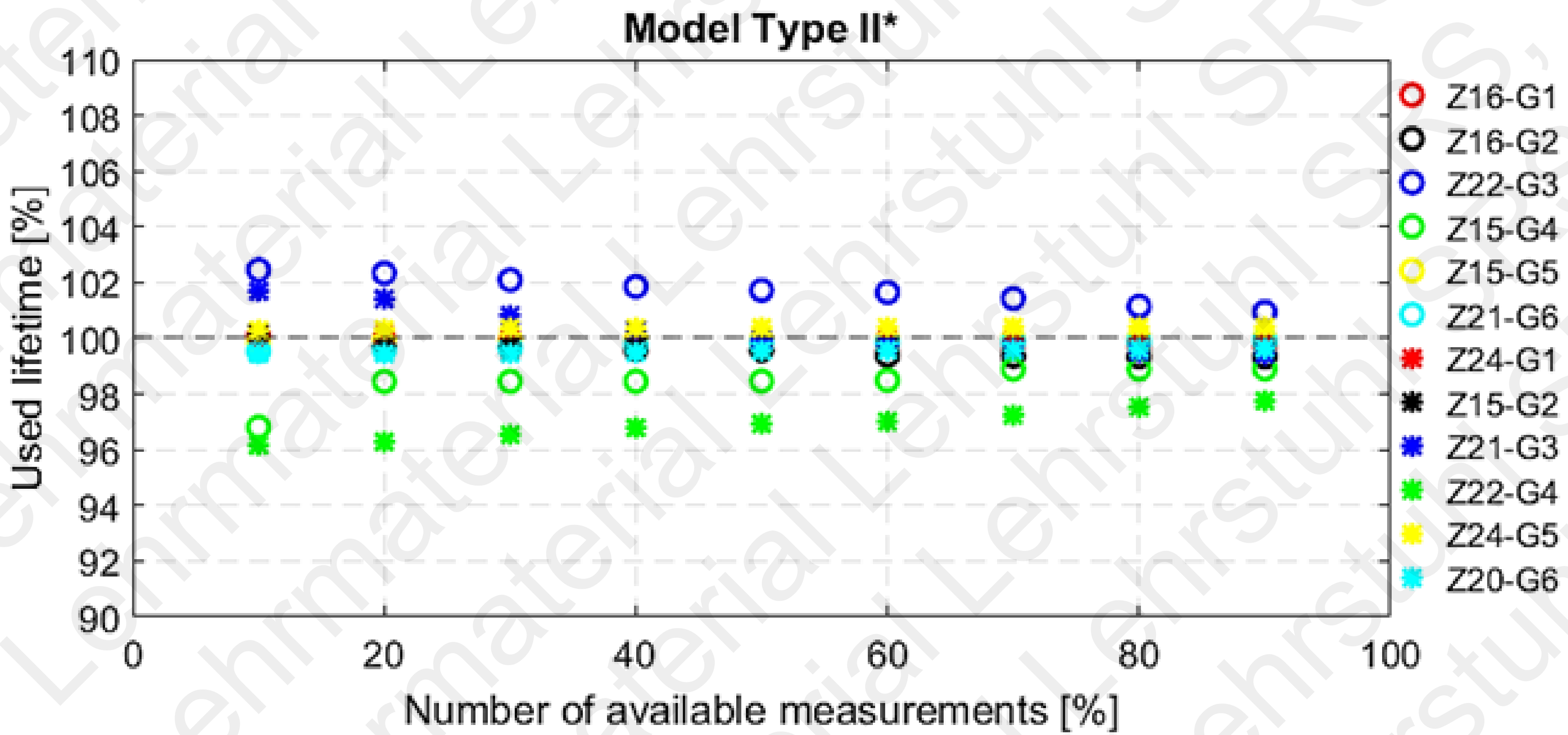

Group	Test dataset
G1	Z16,Z24
G2	Z16,Z15
G3	Z22, Z21
G4	Z15, Z22
G5	Z15, Z24
G6	Z21, Z20

➔ Estimated results independent from training and test datasets variations

IV Next step: BIG DATA-based modeling and analysis I

What are the changes and the key ideas in this ‚new world'?

	Scheme	How ?	For what ?
Signal-based	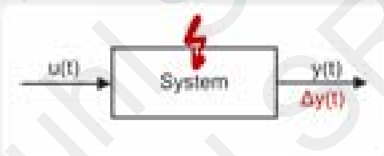	• Use of Δy(t) for FDI	• Interpretation of Δy(t) by expert (human, artificial)
Model-based	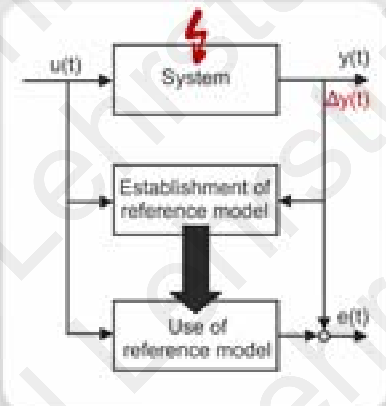	• Use of I/O-relation (u(t), y(t)) for generation of reference model • Use of residuum e(t) for FDI	• Best case: Interpretation not required • Worst case: Residuum allows only fault detection
Data-driven	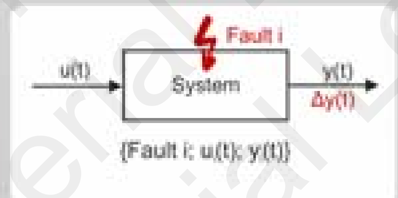	• Use of I/O-relation and label information • ML-Algorithm determines suitable model parameters using training data • Use of model to distinguish between different faults	• Model is not interpretable (Exception: Residuum allows only fault detection) • Model validation is challenging • Reliability depends on operating conditions and the environment

➔ We use (as users):
Suitably choosen Machine-learning approaches

➔ We get:
Automated modeling and decision making

We lose(*):

- Interpretability

- Robustness

IV Next step: BIG DATA-based modeling and analysis II

A new type of modeling:
we have to learn about the options, the risk,
and how to evaluate the results obtained

- Machine learning provides a large variety of new obtions
  - Modeling > instead of 1st principle-based I/O-models
  - Classification > instead of logic or thresholds
  - Numerical results > replacing classical numerical models (experimental modeling)
- Risk:
  Even easy to generate
  data-driven models are even models
- Evaluation
  - becomes part of the election process,
  - is crucial for risk analysis, and
  - ensure robustness by defining bounds.

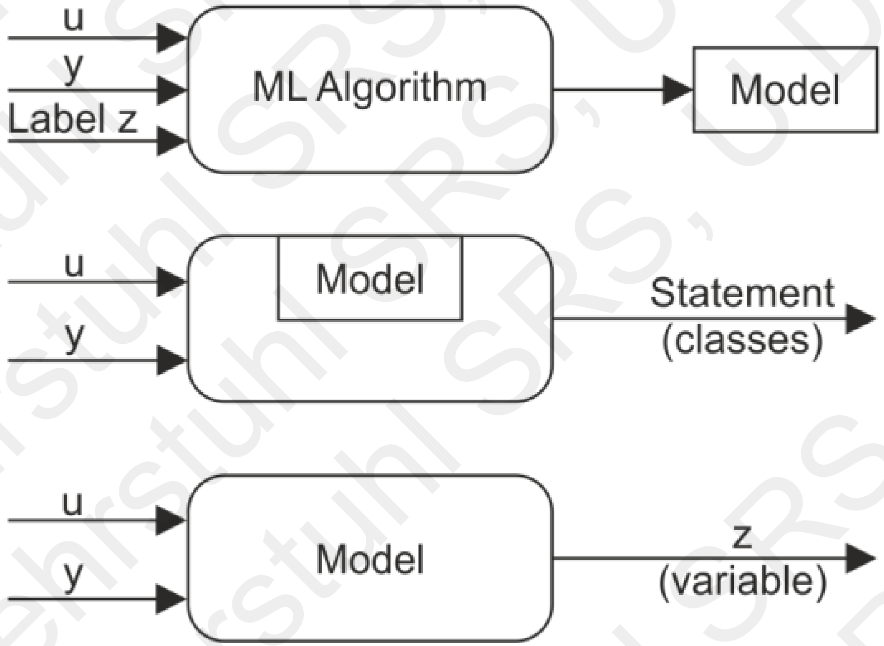

➔ ROC-based evaluation of data-driven approaches becomes crucial.

A new type of modeling: now we have the tool to
- compare apples with pears and
- connect storks and babies

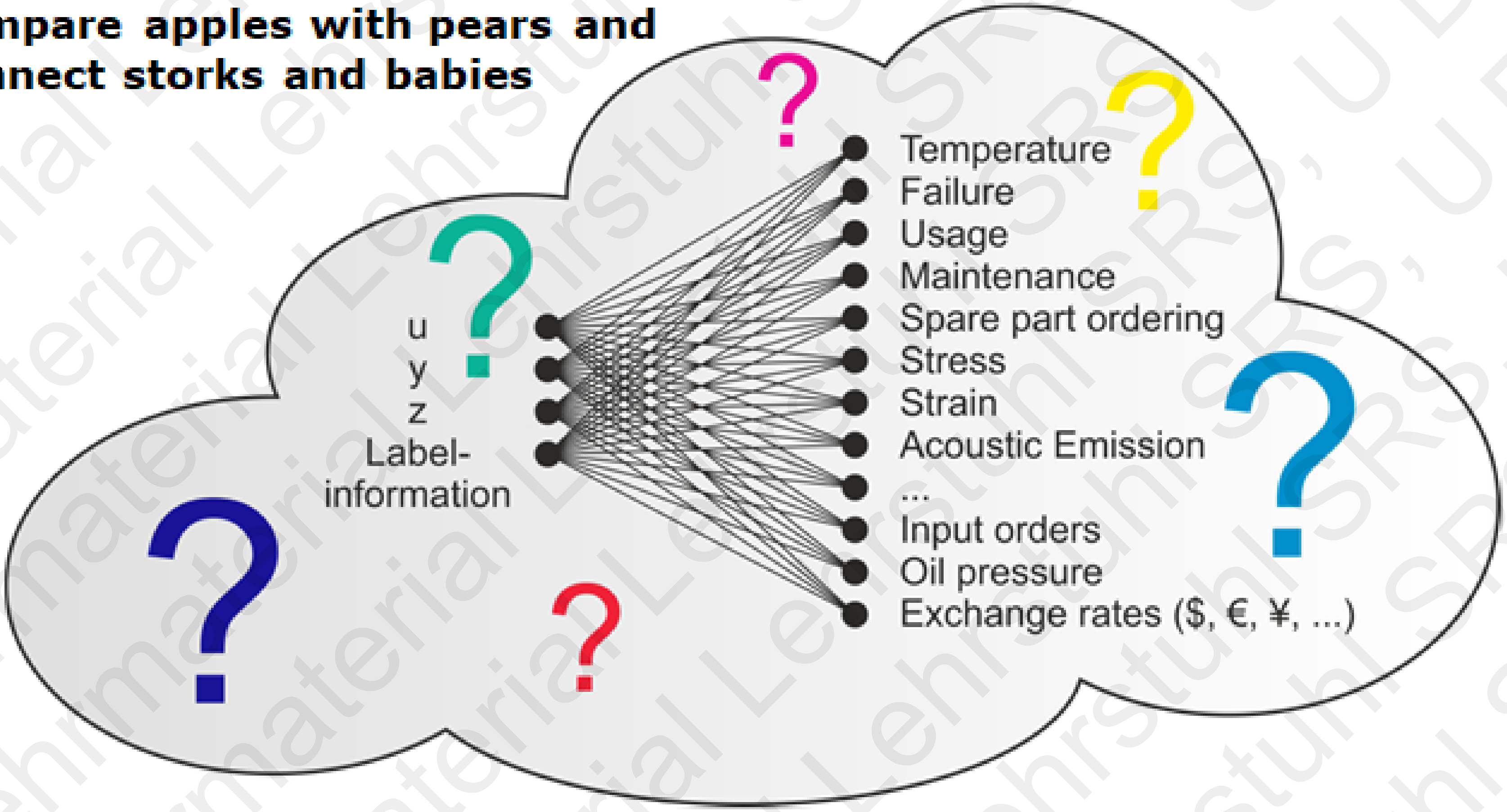

➔ Increasing the horizon with allow to go the next steps
- fault > failure > RUL > maintainance > spare part logistics
➔ Do not forget to check causal mechanisms behind.

Summary, conclusion, and outlook

Summary and conclusion

- Introduction to signal-, model-, data-driven FDI/NDT
  - Examples: crack rotor, sliding surfaces, damaged gears, damaged CFRP plates
  - Lessions learned:
    > More clear fault-related statement (less interpretation required)
    > Easy application of data-driven approaches (ML)
- Data-driven approaches allow complex modeling of complex relation
  - Examples: health status of tribological system, damage distinction of damaged CFRP plates, Remaining Useful Life (RUL)
  - Lessions learned:
    > Modeling is possible even no physical model exists.
    > Detection rate+ has to be considered.
    > BIG-DATA is similar to small data approaches (ML-based, critical aspects)

Outlook

- Big data relations (NDT-maintaince) will be considered in the near future.
- Reliability(*,**) and interpretability has to considered and improved.

* Rothe, S.; Wirtz, S.F.; Kampmann, G.;Nelles, O.; Söffker, D.: *Ensure the reliability of damage detection in composites by fusion of differently classified Acoustic Emission measurements.* In: Chang, F.K.; Kopsaftopoulos (Ed.): Structural Health Monitoring 2017, Stanford, USA, September 12-14, 2017, pp. 1380-1387.

** Wirtz, S.F.; Beganovic, N.; Söffker, D.: *Investigation of damage detectability in composites using frequency-based classification of Acoustic Emission measurements.* Structural Health Monitoring, 2018, pp. 1-12.

From data-driven NDT of systems to BIG DATA-based modeling

Dirk Söffker

Chair of Dynamics and Control (SRS)
University of Duisburg-Essen

soeffker@uni-due.de
www.srs.uni-due.de

Introduction: Performance measures

Individual-based performance measures

- Overall effectiveness of a classifier

$$Accuracy = \frac{TP+TN}{TP+TN+FP+FN}$$

- Classification error

$$Error\ rate = \frac{FP+FN}{TP+TN+FP+FN}$$

- False alarm rate/false positive rate

$$FAR = \frac{FP}{TN+FP}$$

- Reliability of positive classification

$$Precision = \frac{TP}{TP+FP}$$

- Detection rate (DR)/sensitivity/effectiveness to classify positive labels

$$Recall = \frac{TP}{TP+FN}$$

- Effectiveness to classify negative labels

$$Specificity = \frac{TN}{TN+FP}$$

- Weighted harmonic mean of recall and precision

$$F\text{-}score = \frac{(1+\beta^2)Recall \cdot Precision}{\beta \cdot Precision + Recall}$$

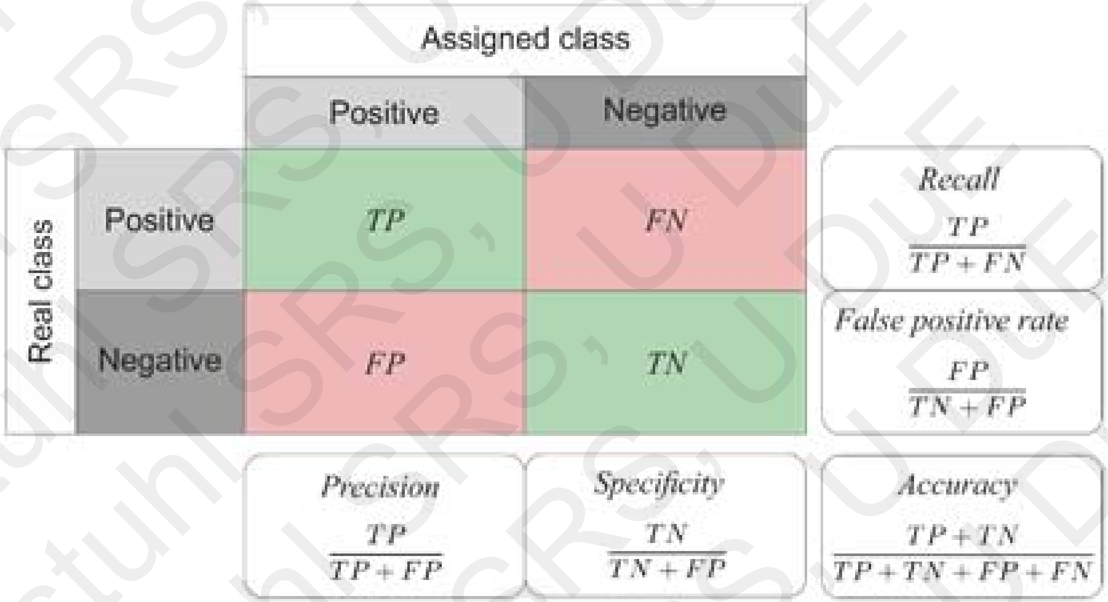

TP	True Positive
TN	True Negative
FP	False Positive
FN	False Negative

Intention and option: modeling and recognition of human driver behavior

Dirk Söffker
www.srs.uni-due.de

(based on common work with
Arezoo Sarkheyli-Hägele, Qi Deng, Olga Muthig, and Jiao Wang)

UNIVERSITÄT DUISBURG ESSEN

Chair of Dynamics and Control (SRS)
University of Duisburg-Essen

Motivation I

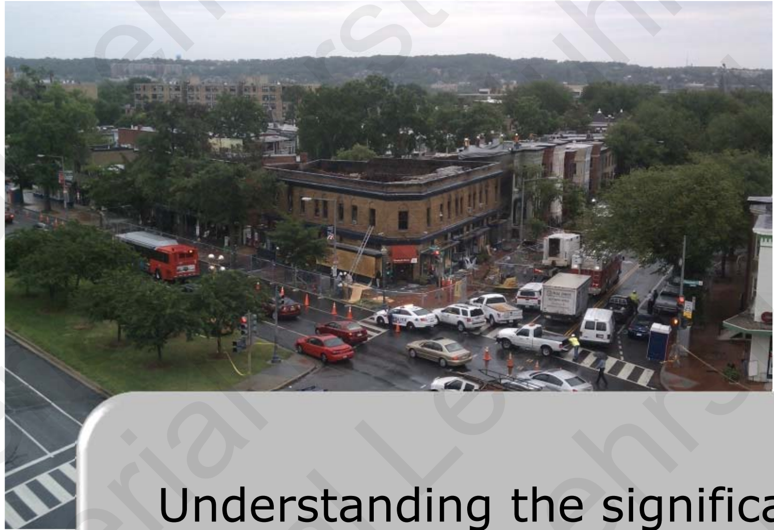

spital]

Understanding the significance of the current situation in light of pertinent operator goals improves situation awareness.

[Endsley, 1995]

[goldcoastbulletin.com.au]

[edtosavetheworld.files.wordpress]

Motivation II

Challenges

- Driver assistance systems and autonomous driving are becoming popular.
- Related approaches are not really reliable.
- Difficulties in modeling real traffic scenarios and human behaviors

[goldcoastbulletin.com.au]

Goals of this presentation

- Modeling individual human behavior with respect to situation recognition and intention prediction
- Maximization of the reliability of related approaches with respect to detection rate (DR) and false alarm rate (FAR)

➔ Here: improvement of real-time situation recognition and intention prediction accuracy

Motivation III

Overall goal:

Development of an individualized situation and intention recognition for different human drivers/operators

Use of driver specific knowledge for supervision and assistance

- Establishing reliable situation and intention recognition
- Close the loop:
  driver/operator <> supervision <> interface/automated system

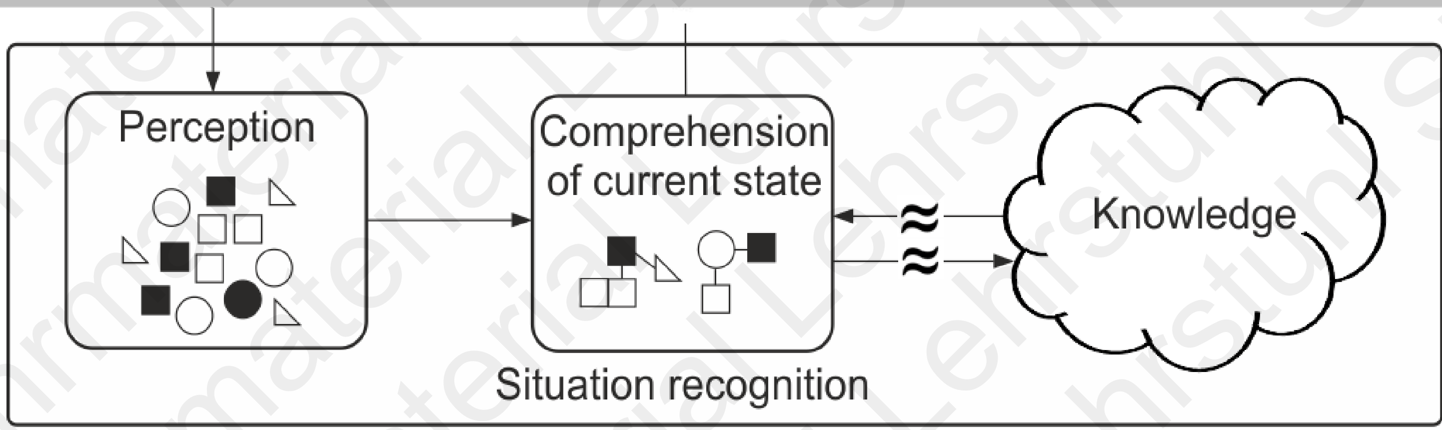

Söffker, D.:
Intention and option: Modeling and recognition of human …

Outline

- Motivation
- Situation-Operator-Modeling (SOM) approach
  - Formalizing interaction
  - Generating the action space
  - Integration within the driver-vehicle loop
- Situation recognition using SOM-based CBR
  - Concept of CBR-based modeling of interaction
  - Generalization and individualization
  - Application and results
- Intention prediction using FL-HMM
  - Concept of FL-HMM for prediction of human behaviors
  - Application and results
- Next step: closing the loop
- Summary and outlook

Situation-Operator-Modeling (SOM) approach I

Approach: Situation-Operator Modeling (SOM)*

- Modeling event-discrete structural variable systems
- Simuliar to ‘state-action’ paradigm but
  - using internal structure for modeling
  - allowing modeling of discrete-event action sequences

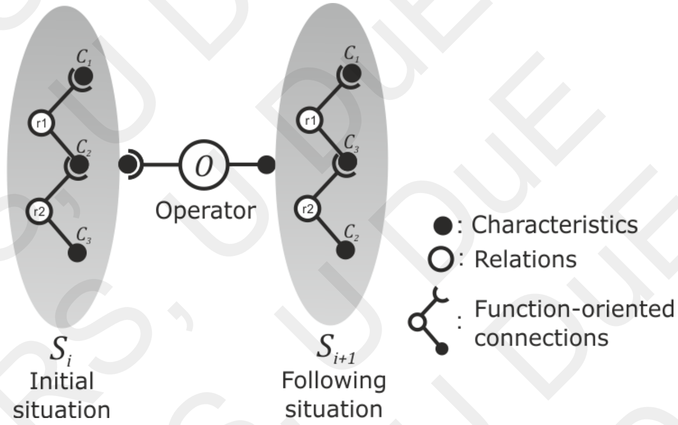

Graphical illustration of situation and operator [Söffker, 2001]

Abilities

- Interpretation of real world events using Situation and Operator by means of
  - Characteristics defining situations and operators
  - Relation between characteristics/features
- Use of a formalizable model for knowledge representation
- Generation of an action space using sequences of situations and operators

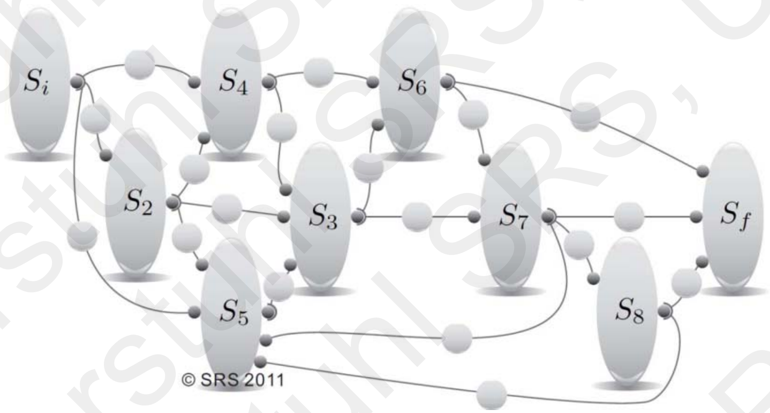

Sample of an action space [Langer and Söffker, 2014]

* Söffker, D.: From human-machine-interaction modeling to new concepts constructing autonomous systems: a phenomenological engineering-oriented approach. Journal of Intelligent and Robotic Systems, Vol. 32, Issue 2, 2001, pp. 191-205

➔ Application of SOM for knowledge modeling

Situation-Operator-Modeling (SOM) approach II

Prefilter: from sensors to situation

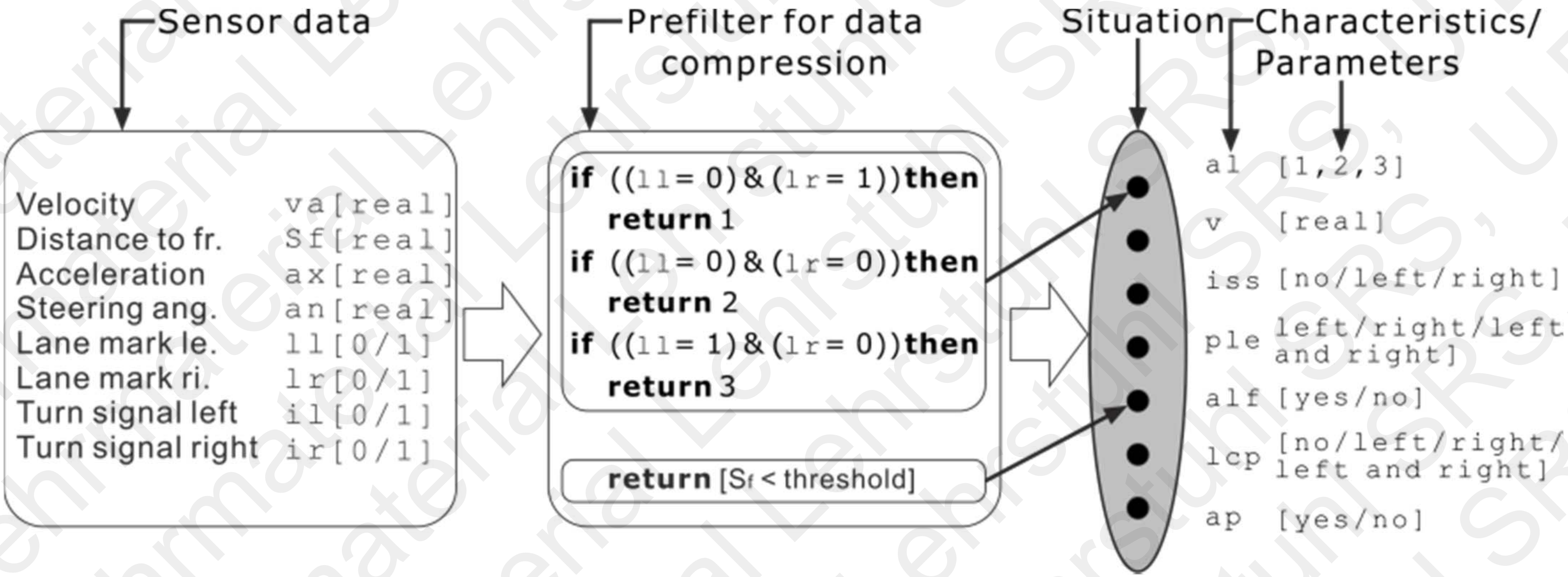

➔ Use of SOM and prefilters connecting measurements and (high-level) SOM-based state

Situation-Operator-Modeling (SOM) approach III

Defining situations and generating action space based on SOM:
Generating the action space

- Automated definition of action space
- Definition of possible actions
- Definition of useful actions
- Evaluation of alternative action options
- Definition of action sequences for given goals

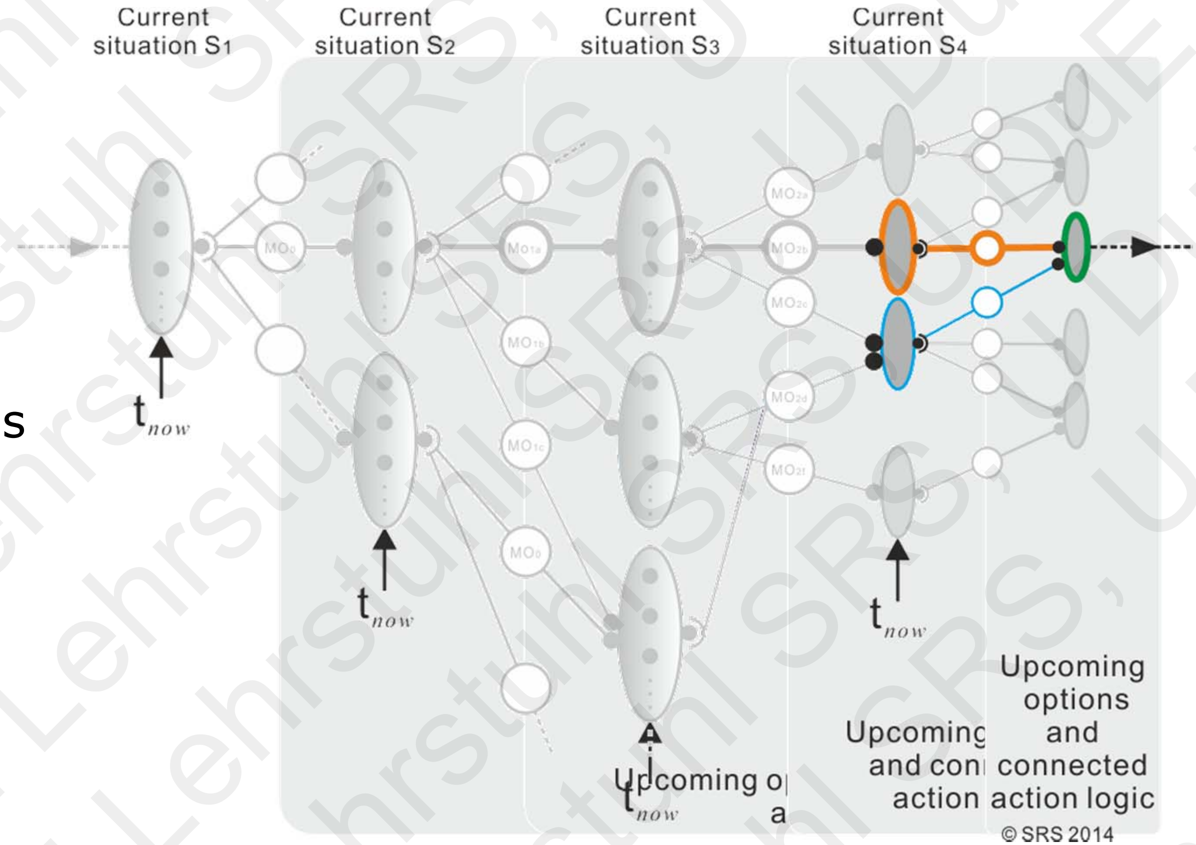

Action options within an action space

➔ Generation of i) all options, ii) best options, and iii) best paths
➔ Detection of critical states and transitions

Situation-Operator-Modeling (SOM) approach III

Integration within the driver vehicle loop

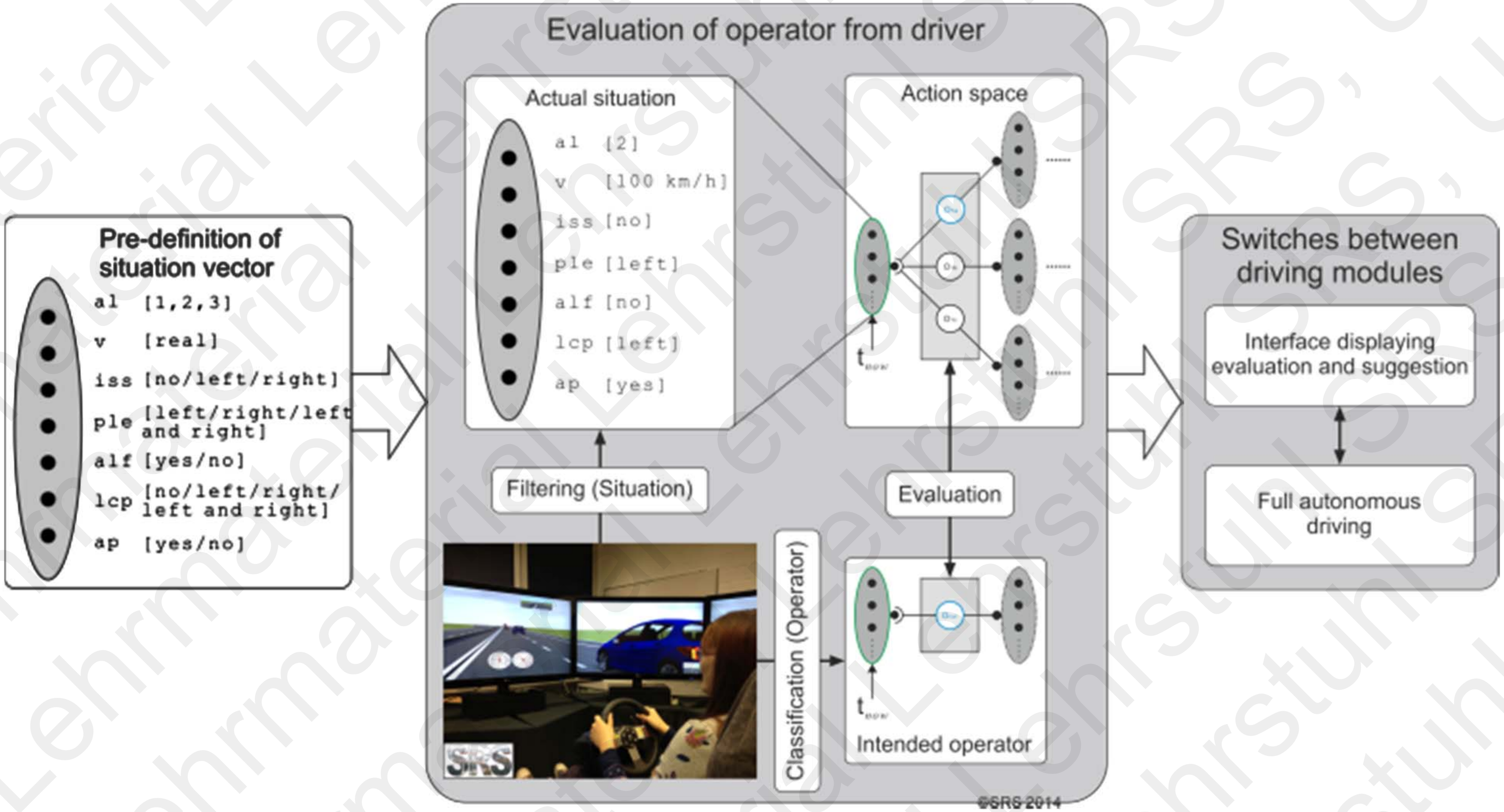

➔ Formalized action sequence modeling within a restricted environment allows assistance

Söffker, D.:
Intention and option: Modeling and recognition of human …

Situation recognition using SOM-based CBR I *

Case base

- Fuzzy object-oriented knowledge base
- Storage of the modeled cases as class objects

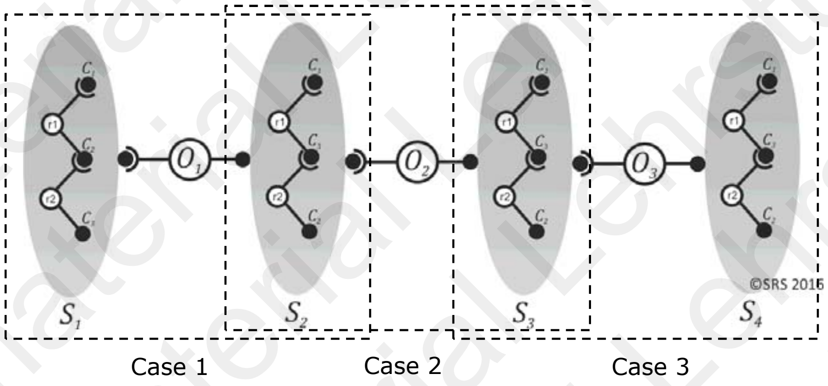

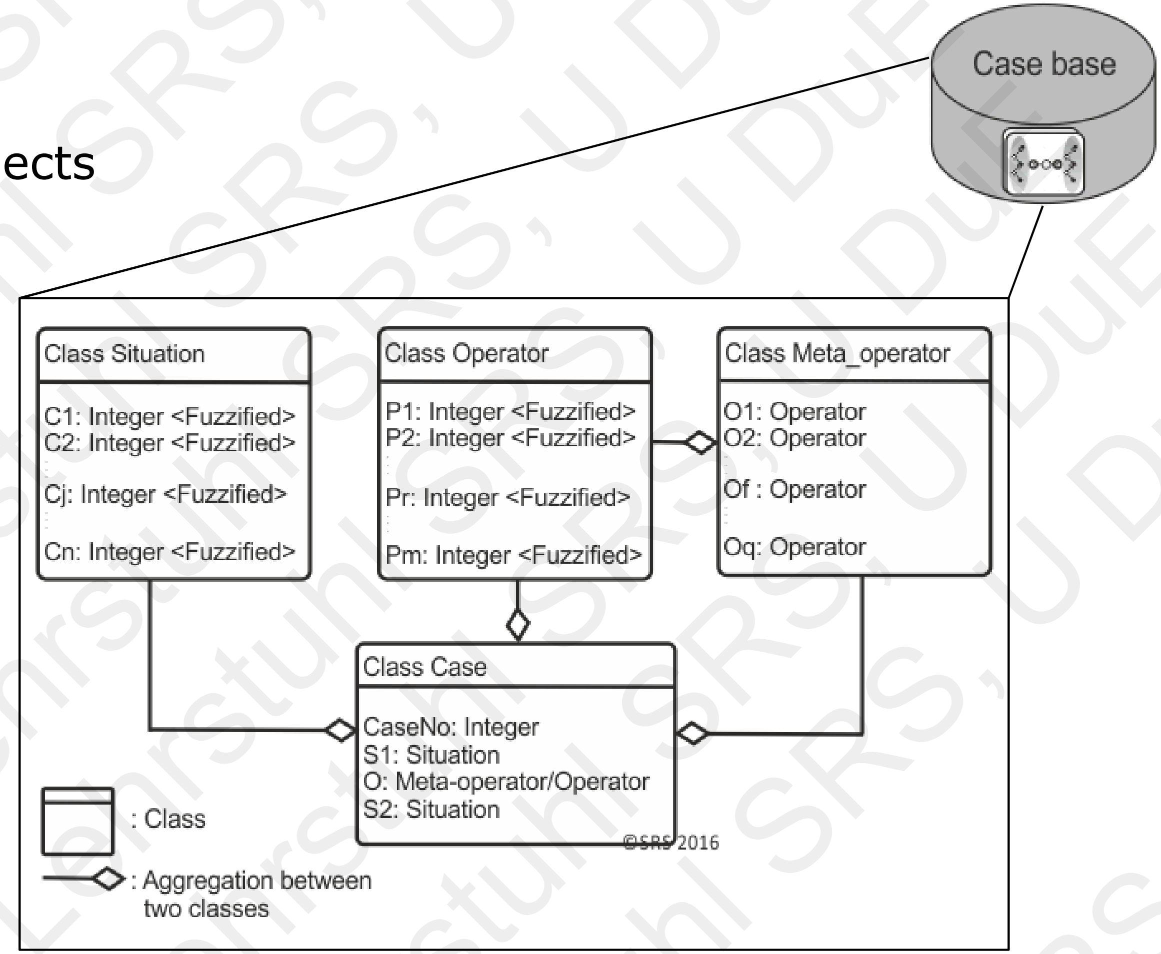

- Retrieving the cases as rules

$$Case_1 : if\ (S_1)\ \&\ (O_1)\ then\ S_2;\ end;$$
$$Case_2 : if\ (S_2)\ \&\ (O_2)\ then\ S_3;\ end;$$
$$Case_3 : if\ (S_3)\ \&\ (O_3)\ then\ S_4;\ end.$$

* Sarkheyli-Hägele, A.; Söffker, D.: Learning and representation of event-discrete situations for individualized situation recognition using fuzzy SOM-based CBR.
Engineering Applications of Artificial Intelligence, 72, 2018, pp. 357-367.

Situation recognition using SOM-based CBR II

Fuzzy SOM-based CBR process

- Fuzzification
- Retrieve (KNN**)
- Reuse (inference) and defuzzification
- Revise
- Reconfiguration of M.F.* and fuzzification
- Retain
- Feature selection (density-based algorithm)
- Case base indexing (KNN**)

Knowledge base

- Case base
- M.F.* design parameters (DB-FDP)
- Relevant features for indexing (DB-IX)
- Indexed case base

*: Membership function
**: K-Nearest Neighbor

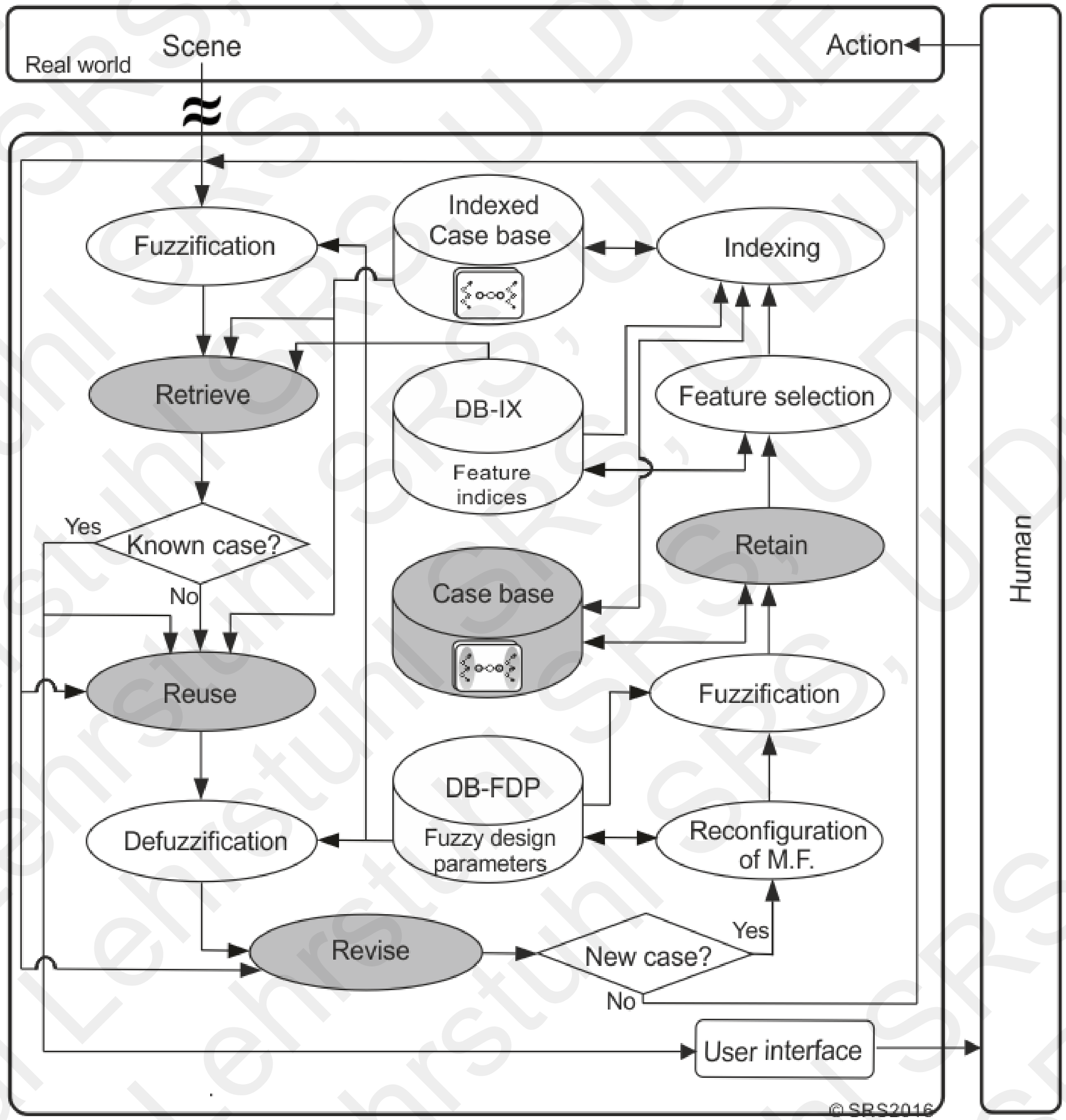

Fuzzy SOM-based CBR cycle

Situation recognition using SOM-based CBR III

Experiment: Lane-change situation recognition

Situation recognition of movements of
ego-vehicle from the current lane to the adjacent lane

Situation patterns

- Lane-keeping (LK)
- Lane-change to left (LCL)
- Lane-change to right (LCR)

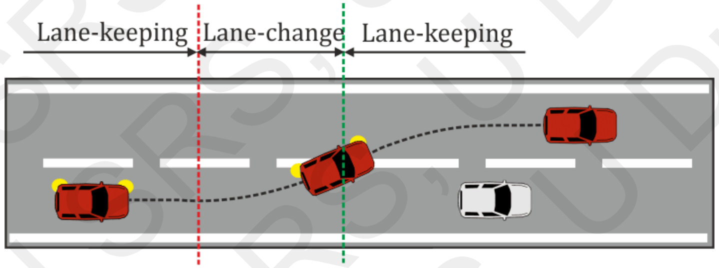

Labeled situation

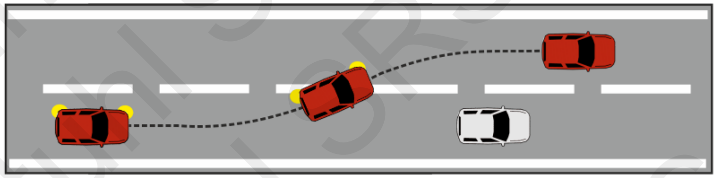

Lane-change to left

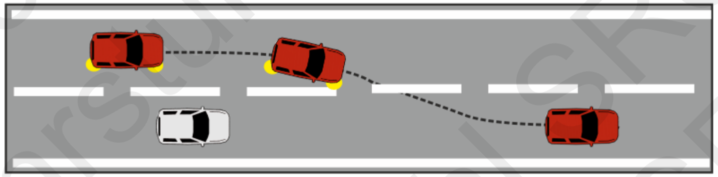

Lane-change to right

Abilities

- Learning different behaviors and
  new experiences of individual drivers
- Evaluating the confidence of actual situations
  to change the lane based on experiences

Goals

- Realization of fuzzy SOM-based CBR approach
- Evaluation of learning for situation recognition
- Evaluation of individualized situation recognition

Söffker, D.:
Intention and option: Modeling and recognition of human …

Situation recognition using SOM-based CBR IV

Experiment: scenario description

- Considering 6 test drivers
- Several driving using simulator
- Driving conditions
  - Simulation of a highway with two driving lanes including winding road
  - Several vehicles in the same driving lane
  - Possibility of two lane-change maneuvers per minute in average

Situation assessment

- Defined using a set of characteristics
- Update every 0.05 s

Operators for lane-change

- Use of steering wheel
- Use of accelerator pedal

Number	Characteristic	Range
1	Velocity of ego-vehicle [km/h]	[0 220]
2	Lane number	{1,...,4}
3	Distance to vehicle in front [m]	[0 250]
4	Distance to vehicle left-front [m]	[0 250]
5	Distance to vehicle right-front [m]	[0 250]
6	Distance to vehicle left-behind [m]	[0 250]
7	Distance to vehicle right-behind [m]	[0 250]
8	Distance to vehicle behind [m]	[0 250]
9	Velocity of vehicle in front [km/h]	[0 220]
10	Velocity of vehicle left-front [km/h]	[0 220]
11	Velocity of vehicle right-front [km/h]	[0 220]
12	Velocity of vehicle left-behind [km/h]	[0 220]
13	Velocity of vehicle right-behind [km/h]	[0 220]
14	Velocity of vehicle behind [km/h]	[0 220]
15	TTC for vehicle in front [s]	[0 12]
16	TTC for vehicle left-front [s]	[0 12]
17	TTC for vehicle right-front [s]	[0 12]
18	TTC for vehicle left-behind [s]	[0 12]
19	TTC for vehicle right-behind [s]	[0 12]
20	TTC for vehicle behind [s]	[0 12]
21	Accelerator pedal	[0 1]
22	Break pedal	{1,...,6}
23	Gearbox	{1,...,4}
24	Indicator	{0,1}
25	Heading angle between ego-vehicle and road	[-3.14 +3.14]
26	Steering wheel angle for ego-vehicle	[-3.14 +3.14]

Set of characteristics

Situation recognition using SOM-based CBR V

Experiment phases

- Offline training: Learning
- Online training: Situation recognition and learning *,**
- Test: Situation recognition

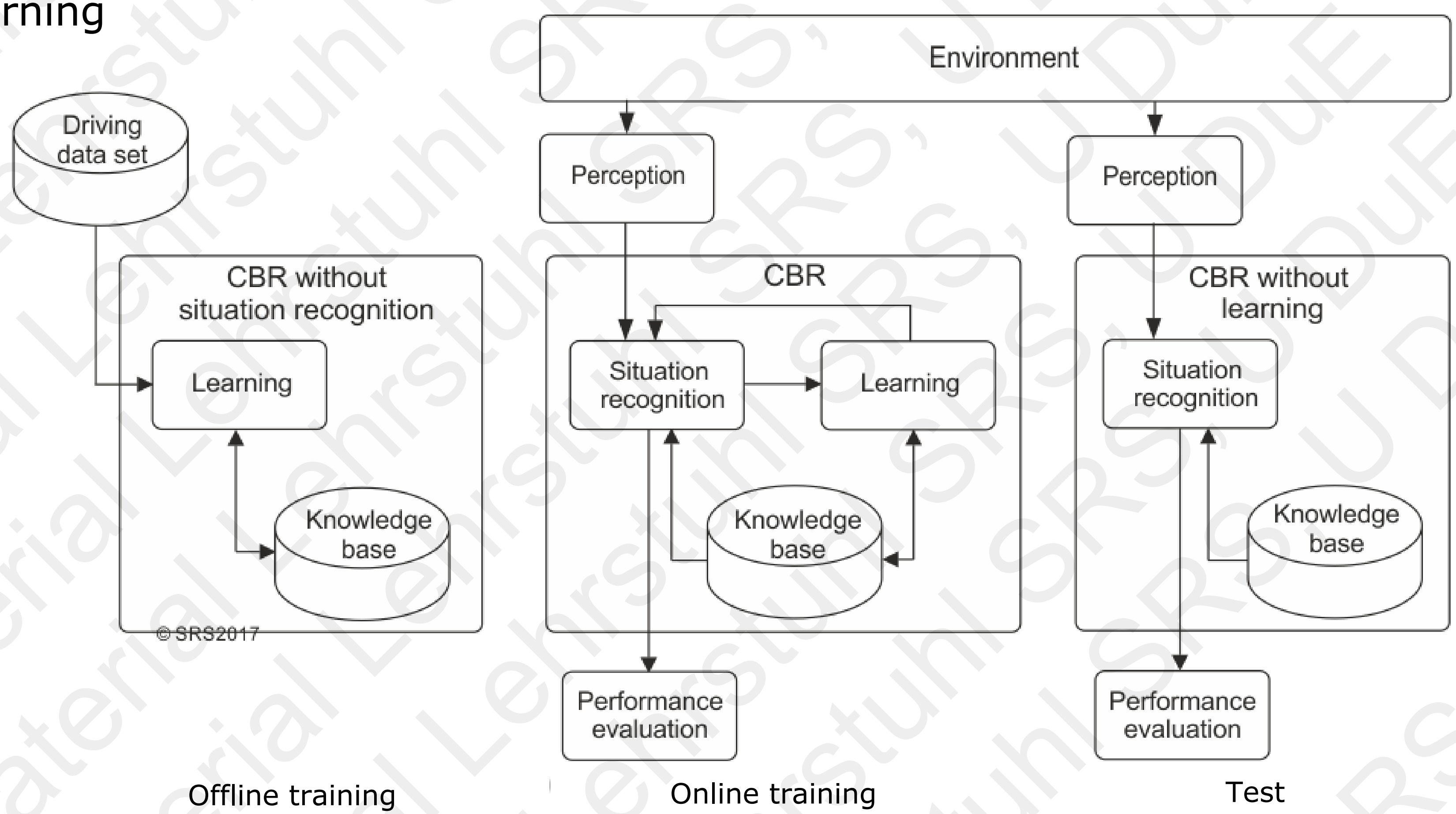

* Sarkheyli-Hägele, A.; Söffker, D.: Fuzzy SOM-based Case-Based Reasoning for individualized situation recognition applied to supervision of human operators. Journal of Knowledge-Based Systems, 2017, pp. 1-12.

* Sarkheyli-Hägele, A.; Söffker, D.: Online learning for an individualized lane-change situation recognition applied to driving assistance system. IEEE Conference on Cognitive and Computational Aspects of Situation Management (CogSIMA 2017), SAVANNAH, GA, March 27-31, 2017, pp. 1-6.

Situation recognition using SOM-based CBR VI

Experimental results: different lane-change behaviors

- Using around 340 lane-change maneuvers done by the drivers #1,#2,…,#6
- Clustering the behaviors based on average distance, velocity, and time to collision (TTC) to the vehicles in front or right behind in the points P_1, P_2, P_3
- Clustering the drivers based on maximum number of experience in each behavior cluster

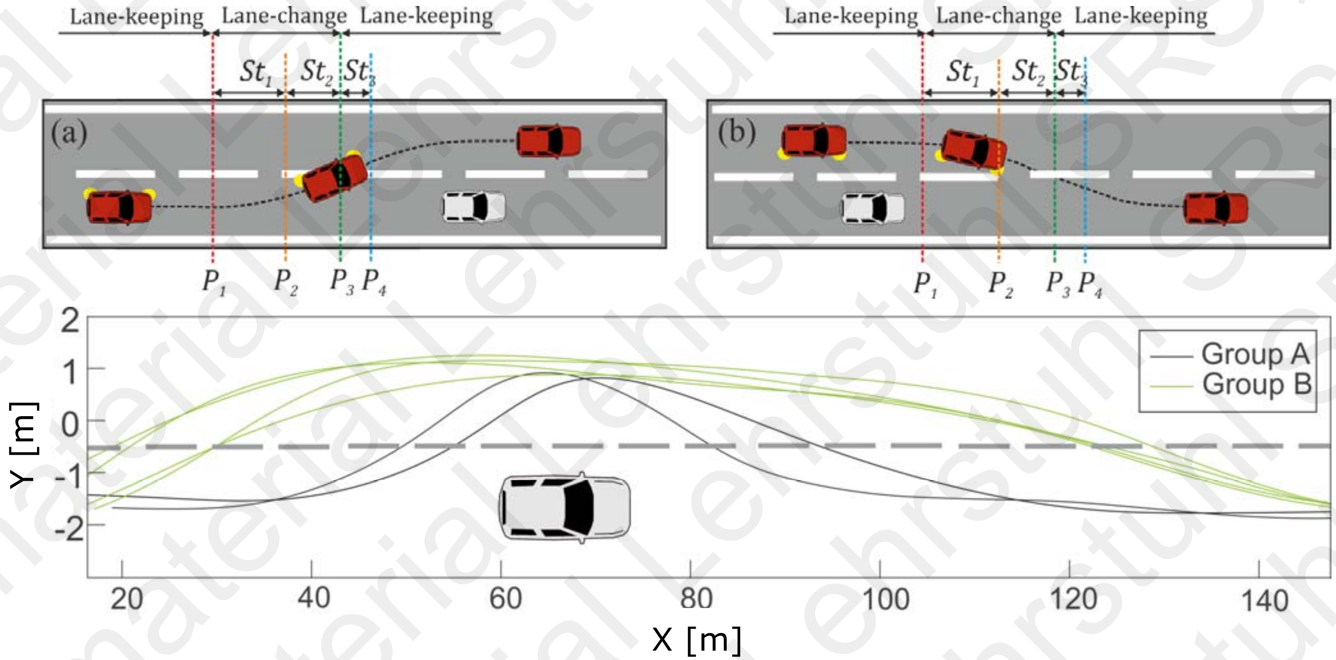

Related lane-change points:

P_1: approximate start point
P_2: approximate middle point
P_3: exact point
P_4: approximate end point

2-dimensional representation of ego-vehicle trajectories samples during lane-change maneuvers done by drivers

→ Two groups of drivers (A: drivers #1,#2,#5, B: drivers #3,#4,#6)

Situation recognition using SOM-based CBR VII

Performance evaluation
based on the experiments

- Feature selection approach
- 10-Fold cross validation
  - Evaluation independent of the data
  - Generalizability of the approach
- Evaluation of learning process
- Evaluation of individualized recognition

Driver No.	No. of lane-change experiences		Driving duration time [m:s]	
	To left	To right	Online learning	Offline test
#1	34	33	31:30	56:19
#2	30	28	28:15	38:44
#3	25	26	30:41	45:21
#4	20	22	30:33	42:17
#5	35	33	29:20	52:11
#6	28	29	32:21	39:22

Experiments

Performance evaluation metrics

- Recognition/Learning elapsed time
- Detection rate $= \frac{TP}{TP+FN}$
- False alarm rate $= \frac{FP}{TN+FP}$
- Accuracy $= \frac{TP+TN}{TP+TN+FP+FN}$

Metric	Number of lane change situations which are
TP	Correctly recognized
FN	Not correctly not recognized
TN	Correctly not recognized
FP	Not correctly recognized

Evaluation metrics

Situation recognition using SOM-based CBR VIII

Evaluation: Situation recognition before and after online learning

- Training using offline learning
- Evaluation before and after online learning

Driver No.	Offline learning		After online learning	
	Detection rate	False alarm rate	Detection rate	False alarm rate
#1	0.9522	0.0760	0.9794	0.0143
#2	0.9678	0.0465	0.9756	0.0129
#3	0.9714	0.0371	0.9646	0.0179
#4	0.9683	0.0335	0.9886	0.0074
#5	0.6551	0.0563	0.9654	0.0175
#6	0.9755	0.0335	0.9671	0.0147

Highlights

- Improvement of detection rate in most of the tests
- Reduction of false alarm for all the tests to less than 2%

➔ Acceptable improvement of situation recognition by online learning application

Situation recognition using SOM-based CBR IX

Results: Situation recognition performance during online learning

- Training using offline learning
- Evaluation of online learning every 5 seconds
- Recognition elapsed time: 0.04 sec in average
- Learning elapsed time: 0.3 sec in average

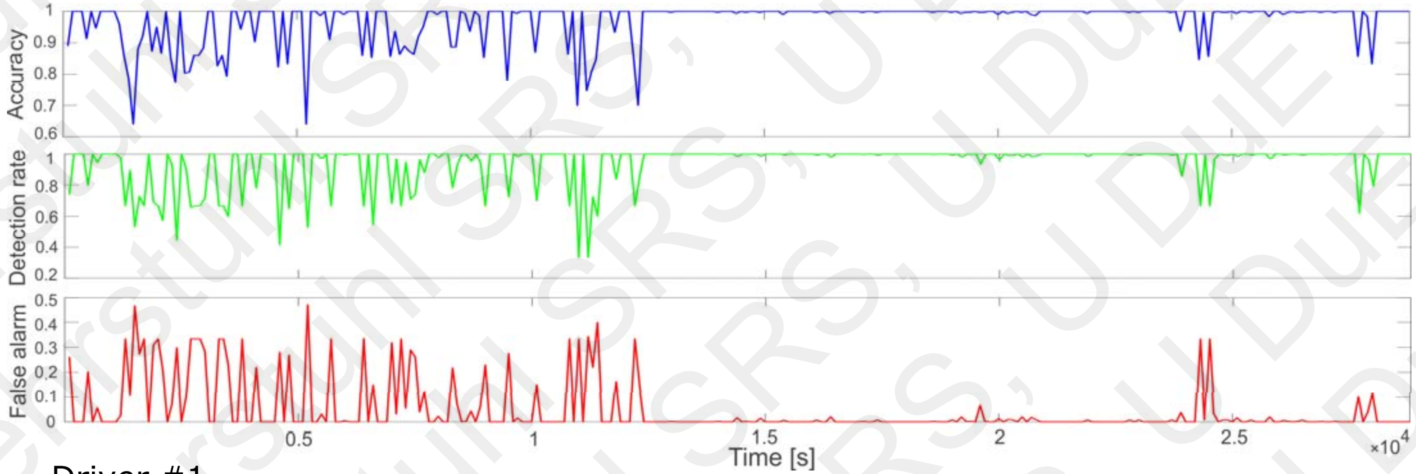

Driver #1

Highlights

- Learning frequently done in the first minutes
- Considerable changes in situation recognition accuracy
- Effectiveness of online learning of new cases

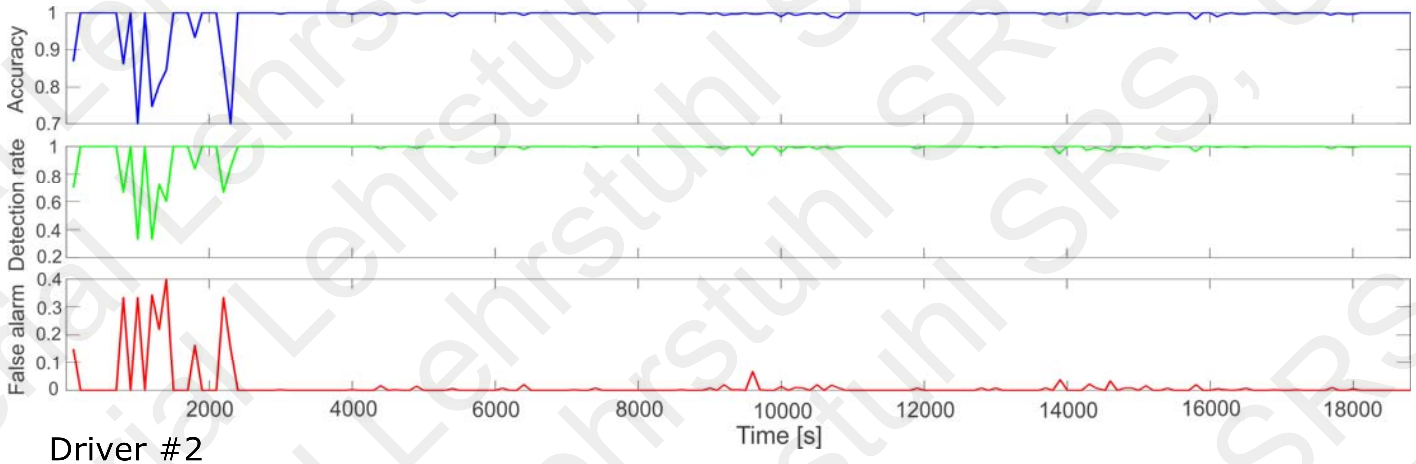

Driver #2

➔ Effectiveness and importance of online learning for situation recognition is illustrated.

Situation recognition using SOM-based CBR X

Effectiveness of using individual and non-individual knowledge base (KB)

- Application of different trainers and users
- Evaluation through online learning

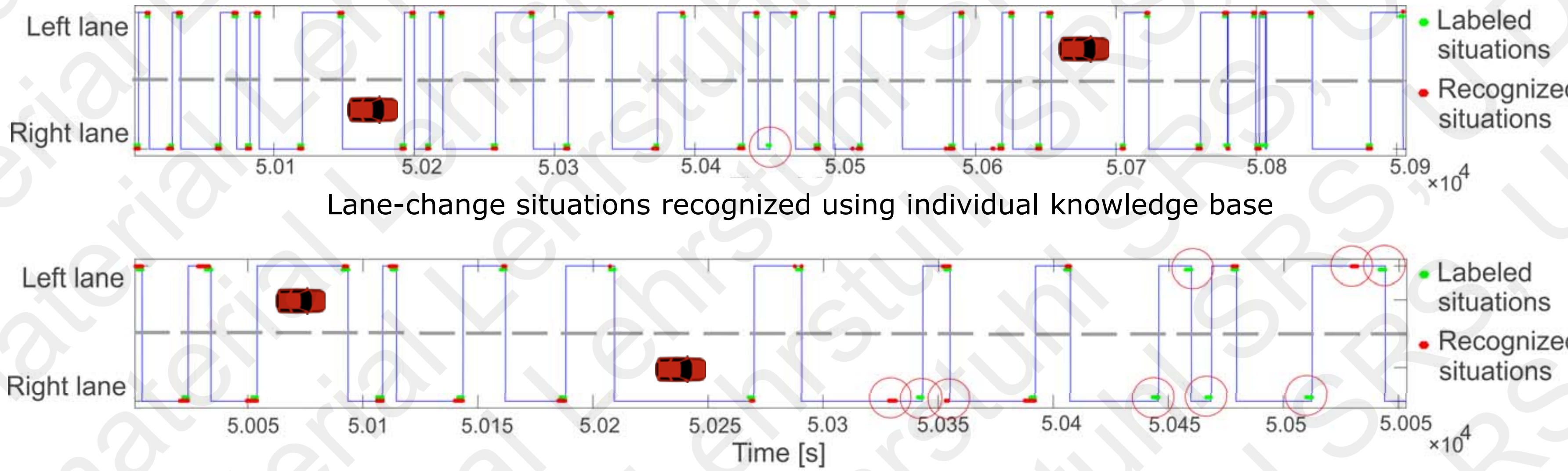

Lane-change situations recognized using not-individual knowledge base

Highlights

- Individualized KB: recognized situations nearly overlap the labeled situations
- Non-individualized KB: inconsistency between the recognized and labeled situations

➔ Considering individual driver behavior strongly affects the recognition properties.

Intention prediction using FL-HMM I

Concept using a prefilter-based (FL) multi-HMM approach *

- Data processing
- Driving behaviors prediction
- Optimization

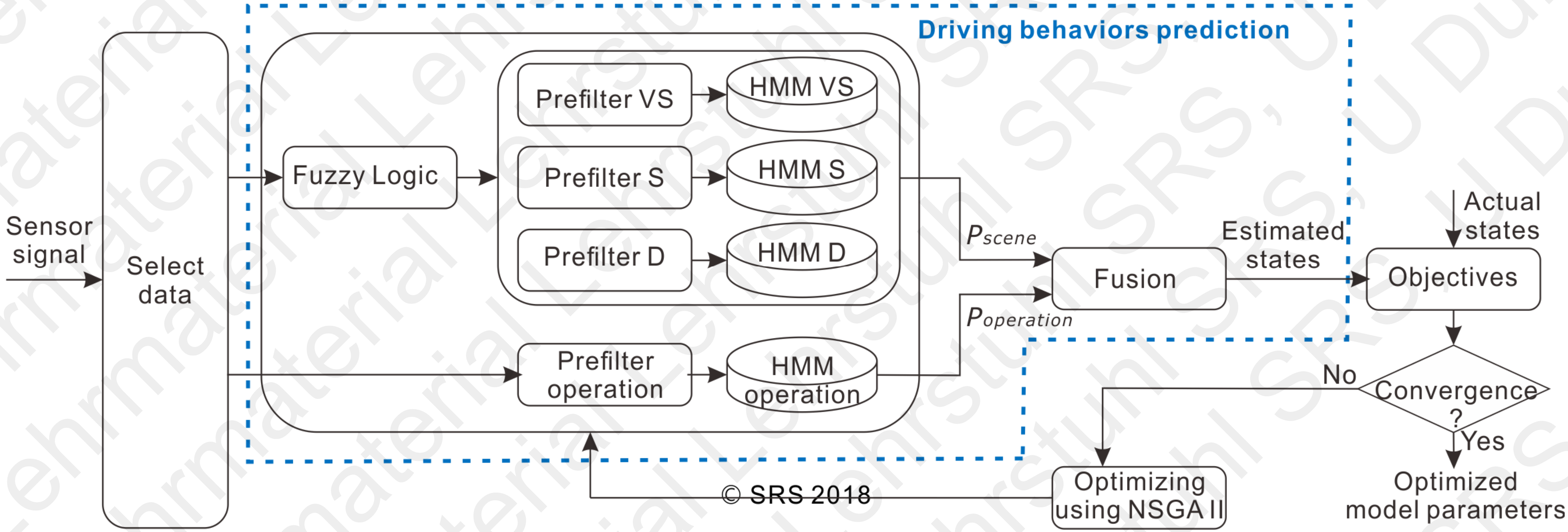

* Deng, Q.; Söffker, D.: Improved dring behaviors prediction based on Fuzzy Logic-Hidden Markov Model (FL-HMM). IEEE Intelligent Vehicles Symposium, Changshu, Suzhou, China, 2018, pp. 2003-2008.

Intention prediction using FL-HMM II

Predicting behaviors: FL-HMM based on driving scenes

- VS-, S-, and D-scenes distinguished by FL using d_f and TTC_f
- Establishment of a corresponding HMM (HMM VS/S/D) for each scene
- Applying a prefilter for each HMM
  to process and combine observation variables
- Observation variables: TTC values
- Output: probability of driving behaviors P_{scene}

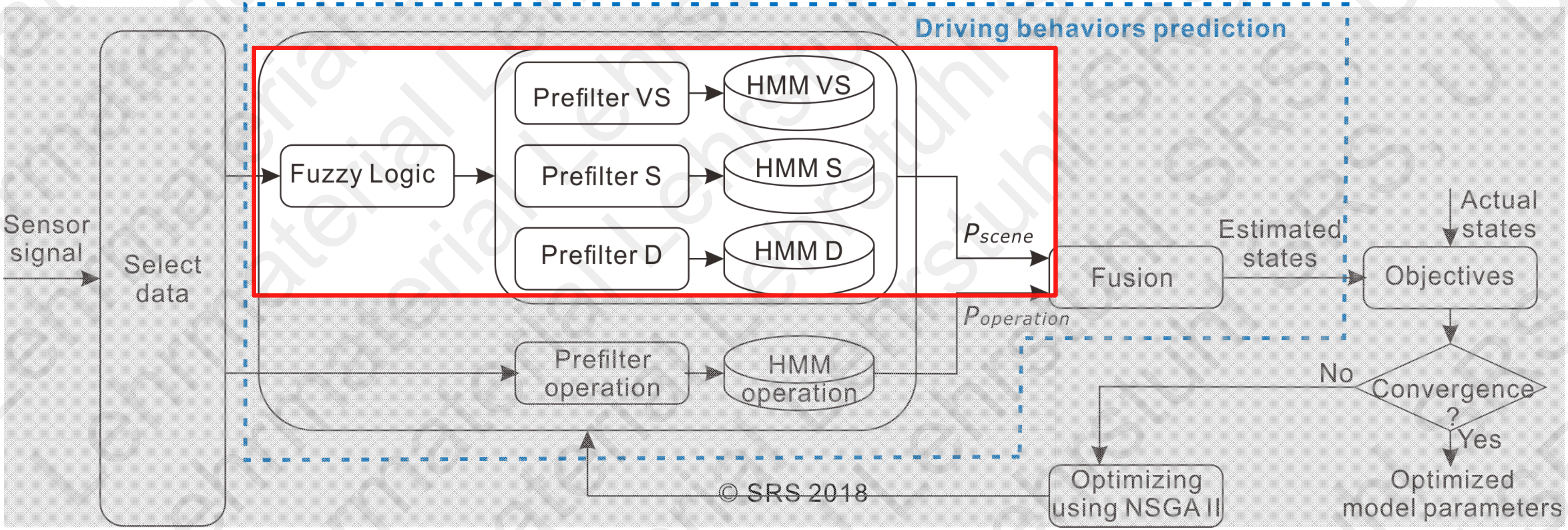

Intention prediction using FL-HMM III

Predicting behaviors II: HMM based on drivers operation

- As a supplement to the model, another HMM established based on drivers operation signals
- Applying a prefilter to process and combine observation variables
- Observation variables: Accelerator/brake pedal signal, steering wheel angle, etc.
- Output: probability of driving behaviors $P_{operation}$

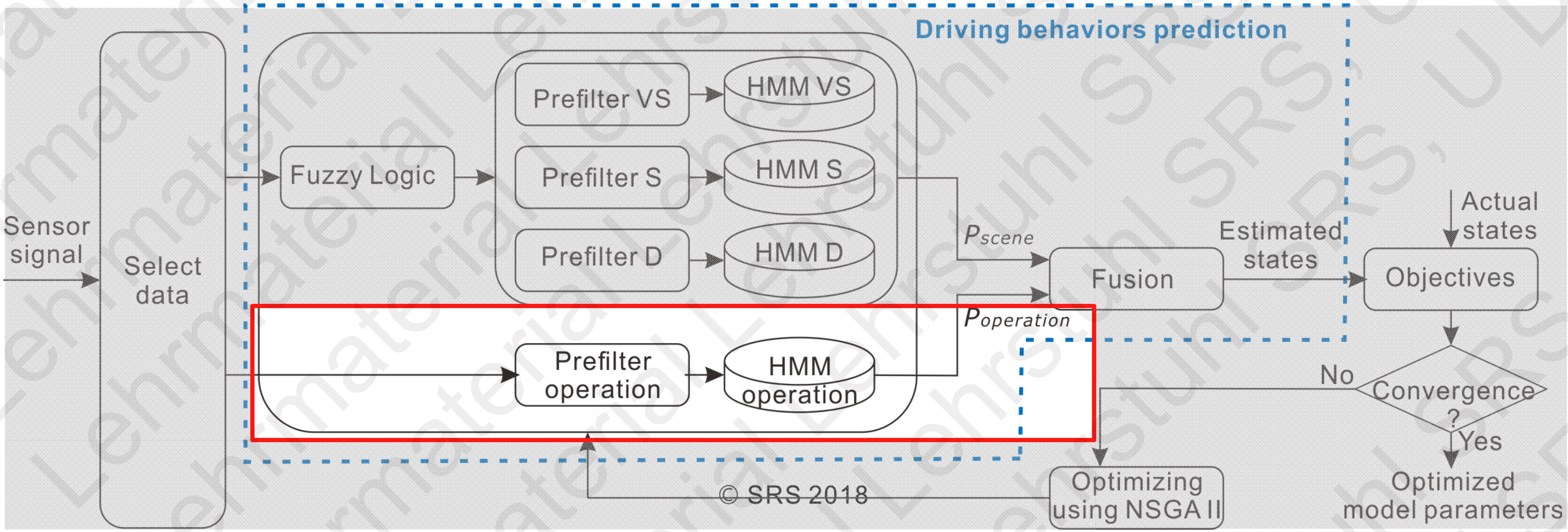

Intention prediction using FL-HMM IV

Predicting behaviors III: Fusion

- Calculating the probabilities of FL-HMM (driving scene) P_{scene} and HMM (operation) $P_{operation}$ separately
- Final probability of the next driving behaviors fused using a weight w as
  $P = w * P_{scene} + (1 - w) * P_{operation}, \quad w \in [0,1]$
- Output: the highest final probability defines the predicted driving behaviors.

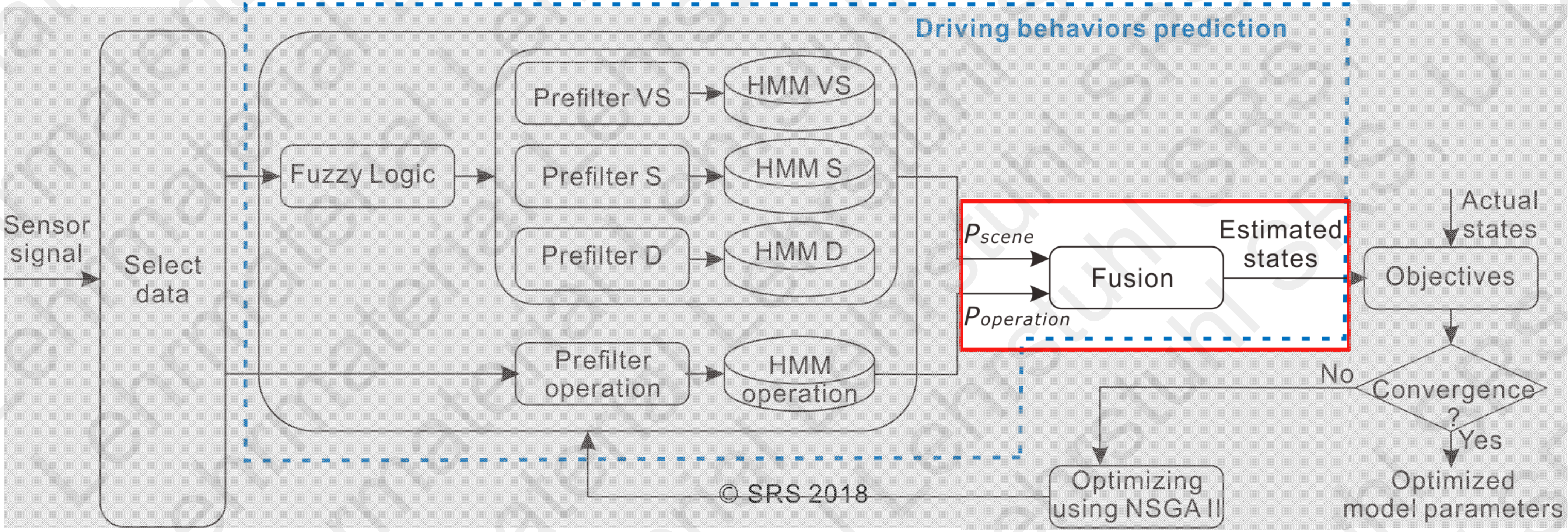

Intention prediction using FL-HMM V

Optimization I: Design parameters

- Optimization achieved by finding the most suitable design parameters
- Design parameters are defined as parameters affecting the model prediction capability.
  - FL thresholds (prediction of driving scene, selecting HMM and prefilter)
  - Prefilter thresholds of HMMs (defining observation sequence)
  - Weight w (affecting driving scene prediction)

Approach	Input	Definition	Design parameters
FL	d_f	Distance to vehicle in front	$[x_{df1}...x_{df4}]$
	TTC_f	TTC to vehicle in front	$[x_{ttc1}...x_{ttc4}]$
HMM (scene)	TTC_f	TTC to vehicle in front	$[ttc_{f1}...ttc_{f5}]$
	TTC_{fl}	TTC to vehicle in left-front	$[ttc_{fl1}...ttc_{fl5}]$
	TTC_{fr}	TTC to vehicle in right-front	$[ttc_{fr1}...ttc_{fr5}]$
	TTC_{bl}	TTC to vehicle left-behind	$[ttc_{bl1}...ttc_{bl5}]$
	TTC_{br}	TTC to vehicle right-behind	$[ttc_{br1}...ttc_{br5}]$
	TTC_b	TTC to vehicle behind	$[ttc_{b1}...ttc_{b5}]$
HMM (operation)	I	Indicator	$[I_1...I_3]$
	S	Steering wheel angle	$[S_1...S_3]$
	P_a	Accelerator pedal position	$[P_{a1}...P_{a3}]$
	P_b	Brake pedal pressure	$[P_{b1}...P_{b3}]$
Fusion	w	Weight	$[w]$

Descriptions of observation variables and design parameters

→ Optimization of design parameters is important to improve the performance of driving behaviors prediction.

Optimization II: Minimizing objective functions

- Selecting optimal design parameters by using Non-dominated Sorting Genetic Algorithm II (NSGA-II)
- Objective functions in terms of
max. accuracy (ACC), max. detection rate (DR), and min. false alarm rate (FAR):
$f_{1-3} = (1 - ACC_{1-3}) + (1 - DR_{1-3}) + FAR_{1-3}$
$f_4 = abs(estimated\ maneuvers - actual\ maneuvers)$

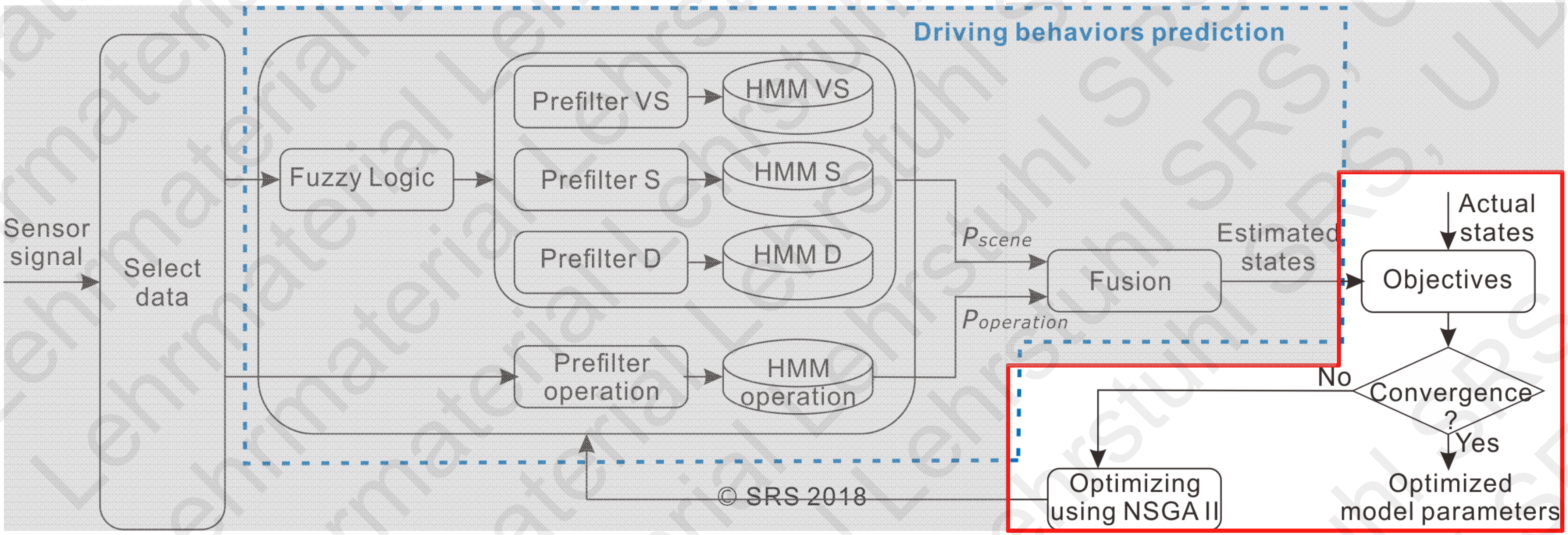

Experimental results: Experimental setup

Realization of the experiments

Driving simulator (SCANeR Studio)

Design of the experiment

- Driving scenario
  - Highway (4 lanes, two directions)
  - Traffic environment
- 7 test drivers
  - Age: 25 to 38
  - Driving license required
- Training/test data
  - Training data (about 40 min. driving)
  - Test data (10 min. driving)

Intention prediction using FL-HMM VII

Training phase

- Goal
  Determination of optimal design parameters and model
  - FL thresholds
  - Prefilter thresholds
  - Weight w
- Input (training data)
  - Measured driving behaviors
  - Measured observation variables

Test phase

- Goal
  Calculation of driving behaviors
- Input (test data)
  Measured observation variables
- Comparison
  - Measured driving behaviors
  - Computed driving behaviors

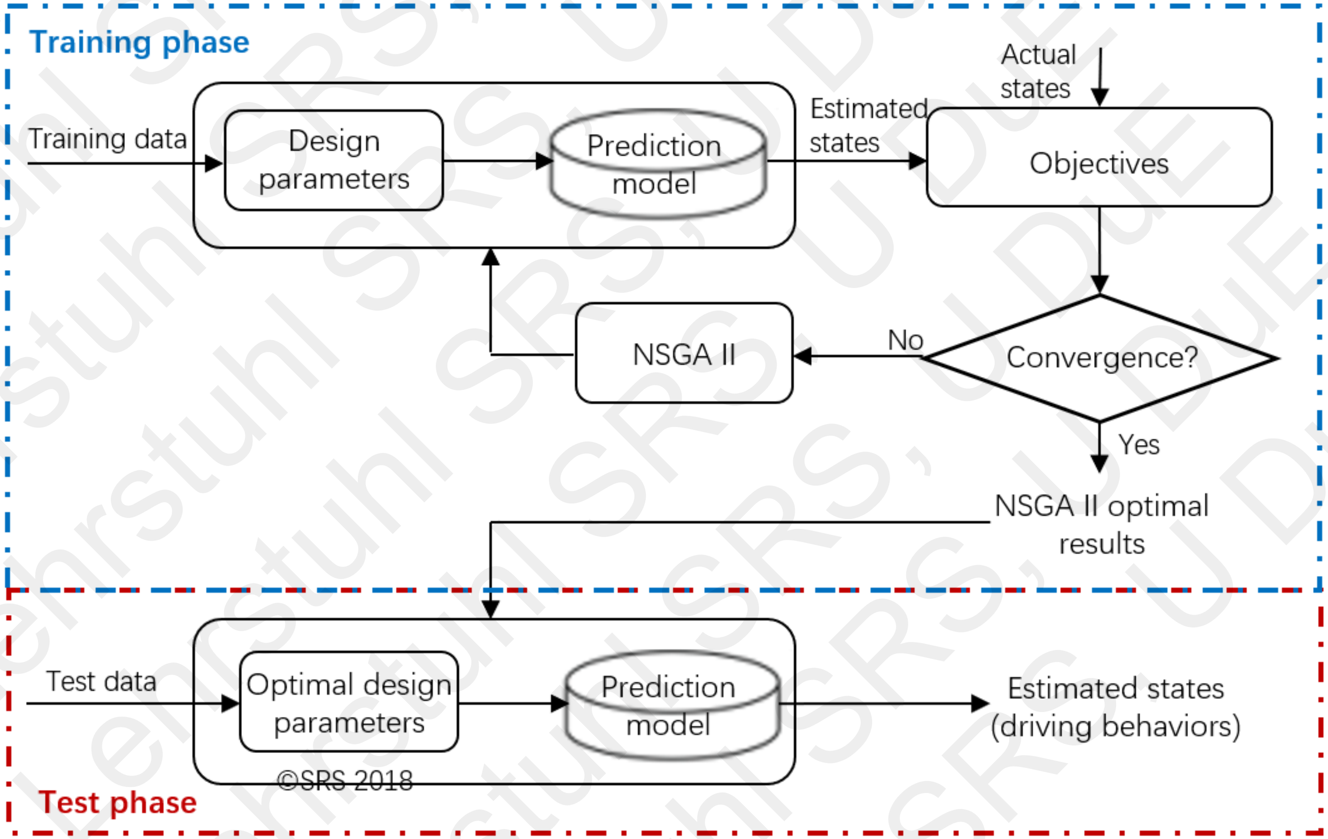

Intention prediction using FL-HMM VIII

Prediction results of the optimal FL-HMM for test data set #2

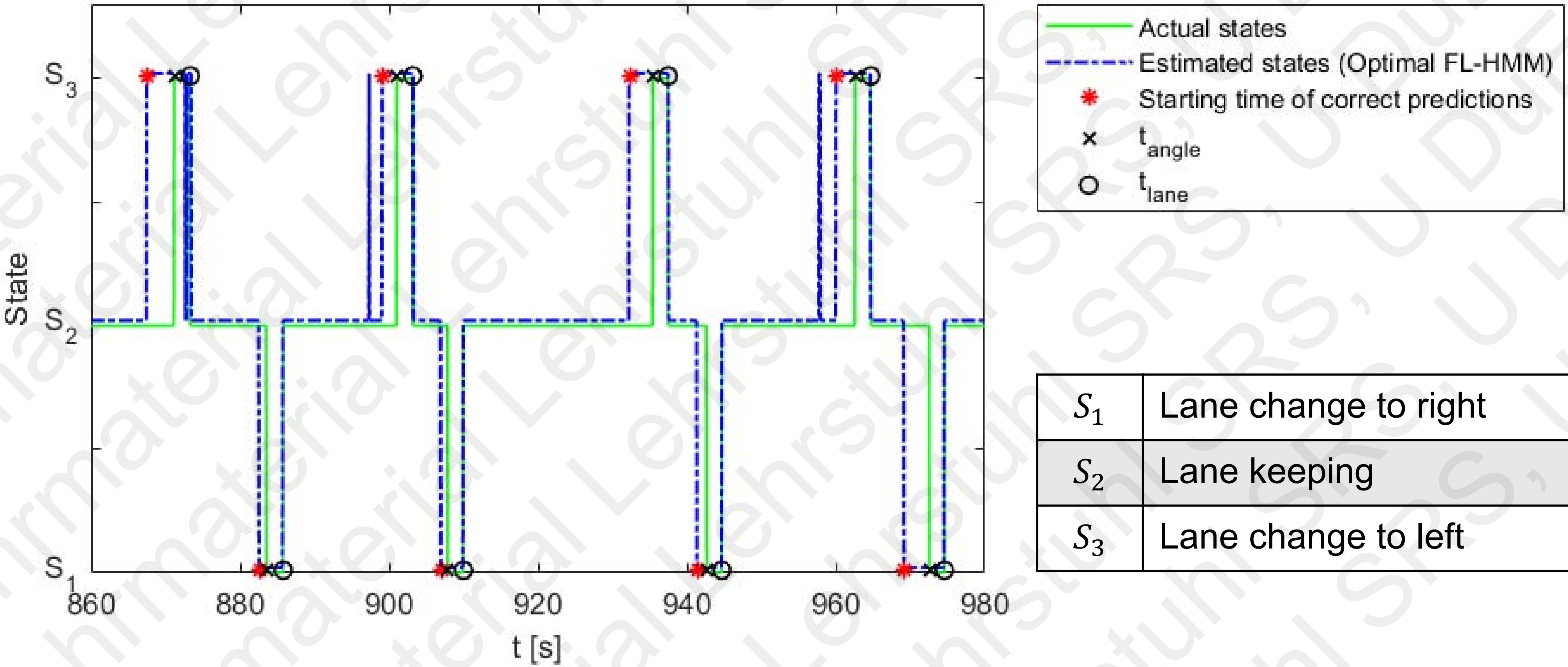

S_1	Lane change to right
S_2	Lane keeping
S_3	Lane change to left

➔ Successful prediction of driving behaviors

➔ Average prediction time for dataset #2:

- 1.8±0.7s before t_{angle}
- 3.9±0.8s before t_{lane}

Intention prediction using FL-HMM IX

Evaluation: average ACC, DR, and FAR achieved by different models for 7 test

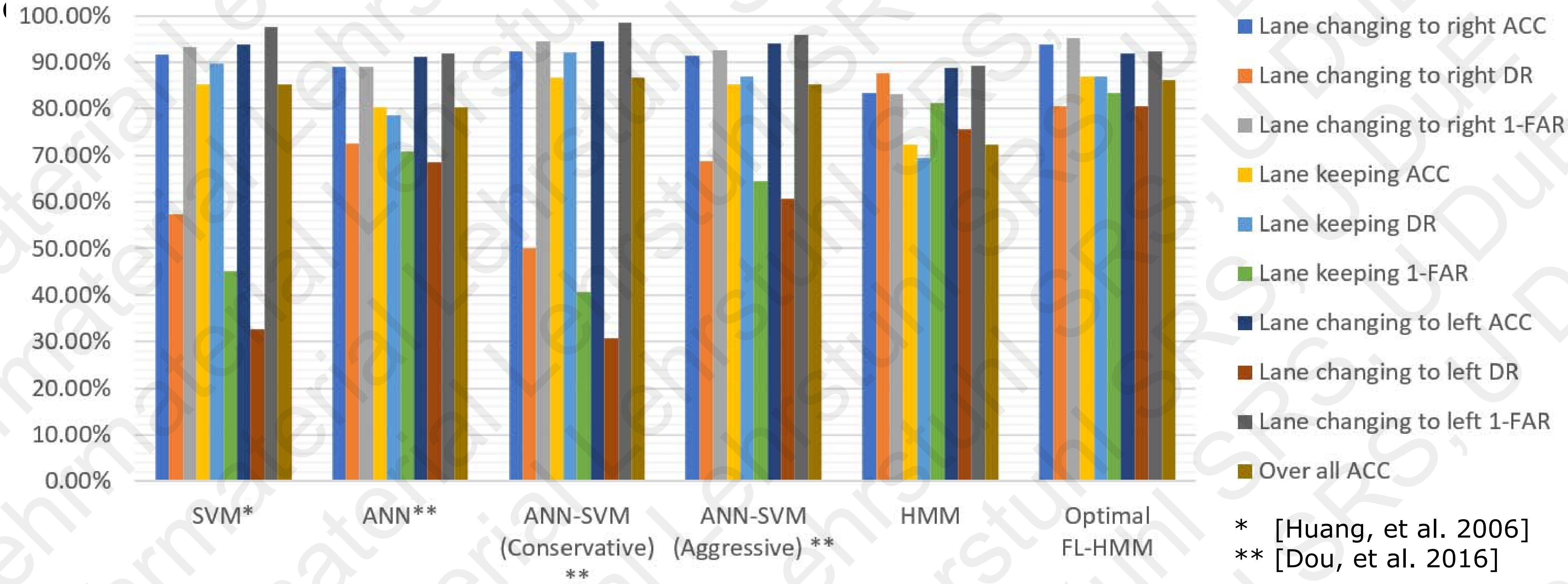

* [Huang, et al. 2006]
** [Dou, et al. 2016]

➔ Comparison to Artificial Neural Networks (ANN), Support Vector Machines (SVM), and combined ANN and SVM
- All ACC, DR, and (1-FAR) values are higher than 80 %
- A high ACC and DR in combination with a very low FAR can be achieved using optimal FL-HMM.

Intention prediction using FL-HMM X

Receiver Operating Characteristic (ROC) graph for different models

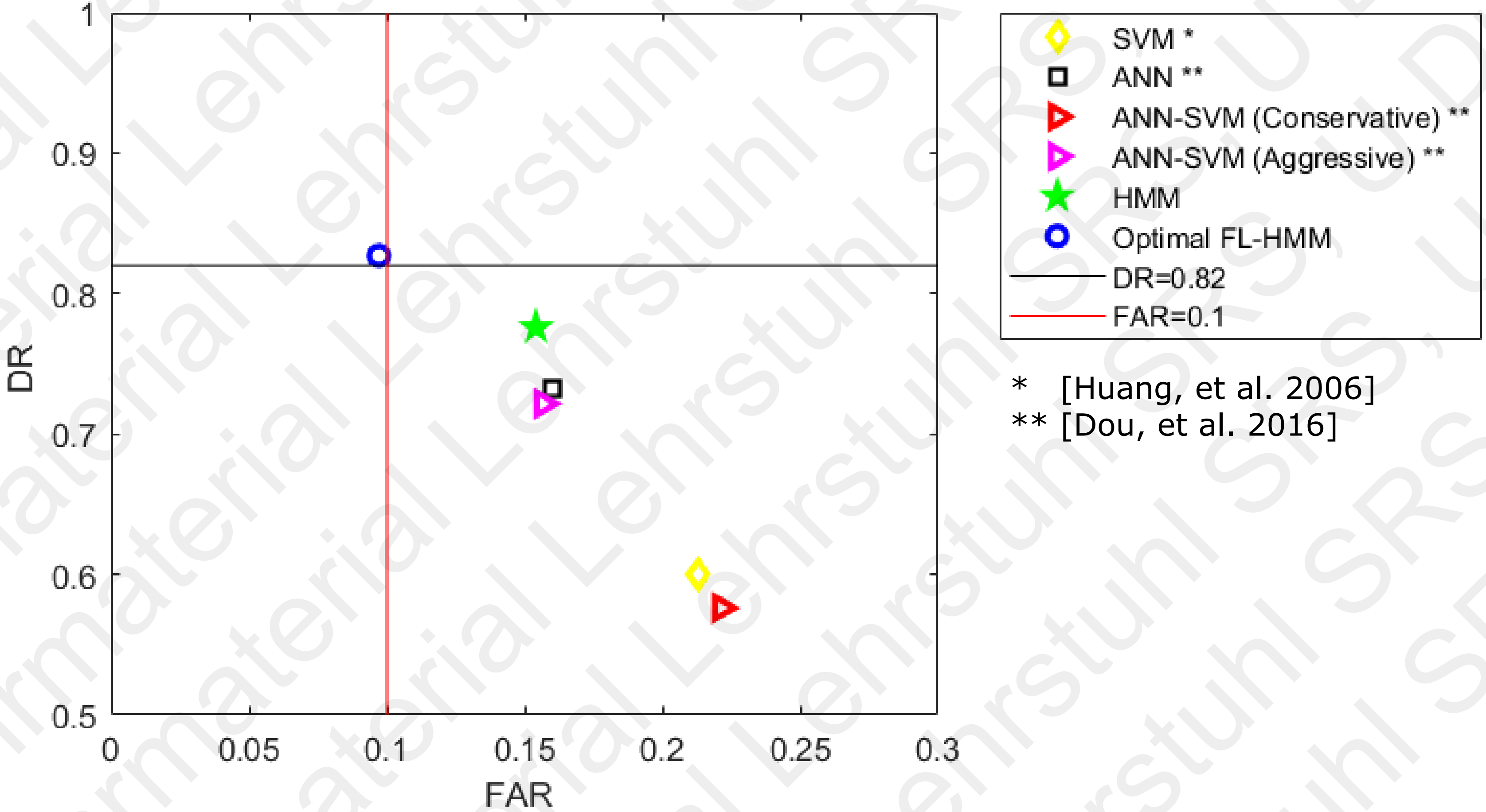

* [Huang, et al. 2006]
** [Dou, et al. 2016]

➔ Highest DR (> 82 %) and lowest FAR (< 10 %)

➔ Optimal FL-HMM shows the best prediction performance in terms of DR and FAR of all models

Next step: closing the loop

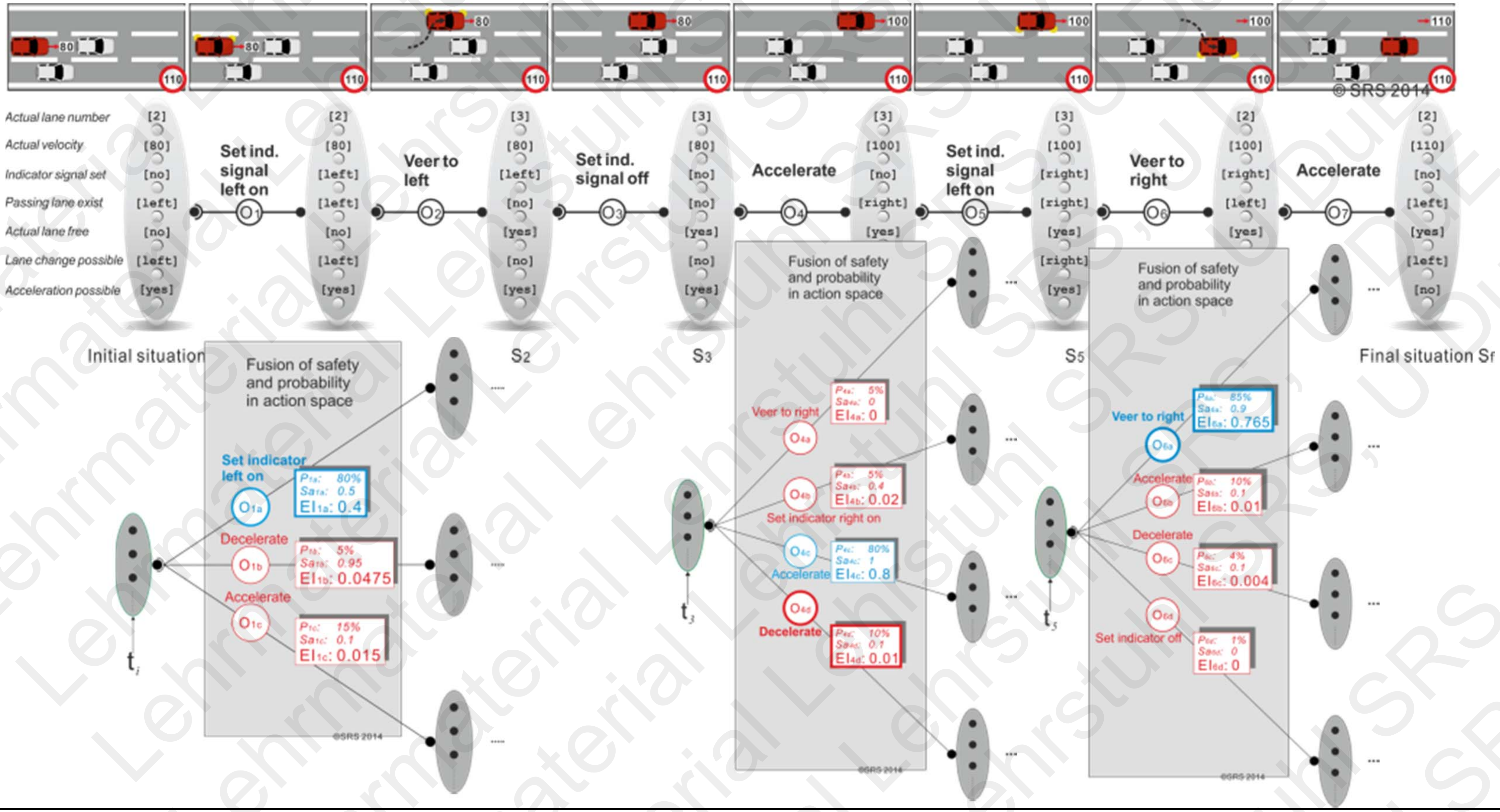

Summary and outlook

Summary

- Introduction to SOM-approach used for
  - event-discrete modeling of interaction (of driver-vehicle or operator-machine systems)
  - action space generation including optional actions
- Realization of CBR-based situation recognition
  - Understand the SOM-triple as case
  - Learning the CBR-data base > model of behaviors
  - Online-learning to update the data base for individualization
  - Experimental results show high DR and low FAR
- First realization of FL-HMM-based intention prediction
  - Continuous evaluation of real scenes for classification of intended behaviors
  - Introduced approach shows best performance in comparison to standard approaches
  - Results must be improved to be used for practical application

Outlook

- Combining action space generation, safety evaluation, and prediction estimation to determine and display interaction conflicts *
- Improving computation load of CBR-based approaches

* Wang, J.; Söffker, D.: Bridging gaps among human, assisted, and automated driving with DVIs: a conceptional experimental study. IEEE Transactions on Intelligent Transportation Systems, 2018, accepted.

Intention and option:
modeling and recognition of human driver behavior

Dirk Söffker

Chair of Dynamics and Control (SRS)
University of Duisburg-Essen

soeffker@uni-due.de
www.srs.uni-due.de